LUCE BAYOU INTERBASIN TRANSFER PROJECT
WATER QUALITY ASSESSMENT AND HYDRODYNAMICS STUDY
Technical Memorandum - DRAFT

Prepared for:

AECOM
5757 Woodway, 101 West
Houston, TX 77057
Tel 713.267.2849
Fax 713.267.3110

By:

Espey Consultants, Inc.
4801 Southwest Parkway
Parkway 2, Suite 150
Austin, Texas 78735

T (512) 326-5659
F (512) 326-5723

www.espeyconsultants.com

EC Project No. 5081.01

2/8/2010

TABLE OF CONTENTS

1.0 EXECUTIVE SUMMARY

As a subconsultant to AECOM, Inc., Espey Consultants, Inc. (EC) was retained to perform a water quality study of the interbasin transfer of water from the Trinity River to Lake Houston for the Coastal Water Authority (CWA). The purpose of this study is to assess the impact on water circulation and water quality in Lake Houston as a result of transferring raw Trinity River water into the lake as part of the Luce Bayou Interbasin Transfer Project. More specifically, this study investigates the changes in water quality and treatability parameters of the blended Lake Houston water at the Northeast Water Purification Plant (NEWPP) intake as a result of the transfer.

The study involved an extensive compilation of water quality and environmental data from multiple sources. Statistical regression was performed on the data using the United States Geological Survey's (USGS's) Load Estimator model (LOADEST) to determine the daily loadings of nutrients (such as dissolved oxygen, ammonia, nitrate and phosphate) and other constituents (alkality and magnesium) from the contributing watershed into Lake Houston. A lake-specific hydrodynamic model was built using EPA's Environmental Fluid Dynamics Code (EFDC) model to simulate water circulation and mixing under different hydrologic conditions and reservoir management scenarios. Finally, a water quality model was developed using EPA's Water Quality Analysis Simulation Program WASP model to incorporate loads and flows estimated by the previous two models to simulate nutrient fate and transport within the lake.

A flow analysis was performed to evaluate the historical inflow patterns in the lake. From the analysis, the frequency and duration of high, normal and low-flow conditions were determined. The year 2000 was found to represent the low-flow conditions. The year 2004 represents the high-flow conditions, and the year 2008 represents the normal-flow conditions. Both the EFDC and WASP models were calibrated and then validated to these years to ensure their robustness under different hydrologic regimes.

The calibrated model was used to simulate several different scenarios pertaining to the diversion of the Trinity River water and to various degrees of lake drawdown determined by reservoir management. The resulting hydraulic and water quality conditions were evaluated.

Based on the evaluation of hydraulic conditions, it was projected that for approximately 90% of the inflows to Lake Houston, water diverted from the Trinity River through Luce Bayou will mix completely with flows from the San Jacinto Basin before reaching the NEWPP intake. Thus, an improvement in water quality over current conditions is expected. During high inflows from the Lake Houston watershed, the mixing zone may extend past the NEWPP intake potentially causing the plant to receive incompletely mixed flows. Such flows would most likely consist of runoff from the western portion of the San Jacinto watershed. Currently, the large inflows from the San Jacinto watershed are causing treatability issues for the NEWPP.

Based on the water quality simulation, it was found that the imported Trinity River water would improve dissolved oxygen concentrations in the lake more than other water quality parameters. Implementing the diversion increases the dissolved oxygen in the lower model layer and reduces the occurrence of hypoxic events. For most other nutrient parameters, concentrations are not found to change appreciably with the diversion.

Drawdowns on lake levels are found to have a deteriorating effect on the water quality because nutrient loads and benthic effects (such as sediment oxygen demand, benthic ammonia flux, and benthic phosphate flux) are exerted on smaller volumes of water. Among the various water quality parameters, drawdowns have the greatest impact on dissolved oxygen. For all flow conditions simulated, each additional one foot of drawdown caused an average drop of 0.2 mg/L in dissolved oxygen.

To evaluate treatability of the mixed water, a mass balance analysis was performed for alkalinity and magnesium. Alkalinity was found to increase by 31% with the diversion from the Trinity River. Magnesium was found to increase by 10% with the diversion. The increase in alkalinity improves the treatability of the water. However, the increase in magnesium also increases the hardness of the water to be treated.

Two primary recommendations are made for improving the Lake Houston model in future work. First, use of a physically-based watershed model, such as Texas A&M University's Soil and Water Assessment Tool (SWAT), is recommended to better characterize nutrient and sediment loads from the San Jacinto watershed. Second, use of an advanced sediment transport module within EFDC or WASP is recommended to estimate the wind-induced resuspension of total suspended solids in the lake. To support the sediment transport modeling, site-specific sediment erosion rates would need to be obtained by collecting several sediment cores in the lake and measuring erosion rates using apparatus such as the sedflume (Lick, 2008).

2.0 INTRODUCTION

As a subconsultant to AECOM, Inc., Espey Consultants, Inc. (EC) was retained to perform a water quality study of the interbasin transfer of water from the Trinity River to Lake Houston for the Coastal Water Authority (CWA). The purpose of the Luce Bayou Interbasin Transfer Project is to provide additional water supply into Lake Houston from the Trinity River in order to meet the growing demand for water in unincorporated north and west Harris County, the City of Houston, and Montgomery County for the next 50 years. The total permitted water from the Trinity River that can be diverted at the Luce Bayou diversion point is 450,000 acre-feet per annum or an average of about 400 million gallons per day (MGD).

The purpose of this study is to investigate the impact of the transferred Trinity River water on circulation and water quality. More specifically, the goal of this study is to assess the treatability of the blended Lake Houston water at the intake of the Northeast Water Purification Plant (NEWPP).

This study builds upon a preliminary water quality study undertaken by EC in 2006 (EC, 2006). In the earlier study, EC staff compiled an extensive amount of water quality and GIS data of the San Jacinto basin from 1990 to 2005 into a database. A mass balance analysis was performed on the data to preliminarily determine the significance of imported Trinity River water on the quality of water to be treated at the NEWPP. Results from the preliminary study indicated overall improvement in water quality in the lake due to the better water quality of the Trinity River compared to other tributaries of the San Jacinto watershed. Nonetheless, the earlier study recommended developing a lake-specific hydrodynamic model to confirm the estimated improvement. The model would simulate the circulation and mixing of the water in Lake Houston based on incoming tributary flow, the imported Trinity River water flow, pumping activities and dam operations. Using the circulation and mixing patterns, the model would account for the fate and transport of constituents and other water quality parameters of interest.

This study carries out the in-depth investigation recommended in the earlier study and contains the following components:

- Evaluation of inflows and nutrient loads into Lake Houston,
- Development of a hydrodynamic model for Lake Houston to determine impacts on water levels and water movement for treatment plant operational issues,
- Development of a water quality model to be linked with the hydrodynamic model to evaluate impact on nutrients and chemical constituents within Lake Houston (e.g. alkalinity, iron and magnesium), and
- Use of the lake models to evaluate impacts on water circulation and water quality under the following contamination scenarios:
    - Diversion of 400 MGD of Trinity River,
    - Historical high, average and low-flow conditons in the San Jacinto Basin, and
    - Drops in water surface elevations caused by hydrologic conditions or operations at the Lake Houston dam.

2.1 BACKGROUND

Lake Houston is a reservoir located on the San Jacinto River and is located east of the City of Houston. The drainage basin for Lake Houston is 2,800 sq. miles (USGS, 2000). The reservoir's main body of water is approximately 8.5 miles long and 1.5 miles wide located between the dam and confluence of the West and East Forks of the San Jacinto River (TWDB, 2003). The lake is formed by a dam that consists of two earth-fill embankment sections and a 3,160-ft-long uncontrolled concrete spillway midway between the embankment sections for a total length of 12,100 ft. The elevation of the spillway crest is 44.5 ft above mean sea level (NGVD 29). The dam contains two tainter gates (18 ft. wide by 20.5 ft high)

with a sill elevation of 27.3 ft. Also located east of the spillway are two flashboard-type gates (18ft wide by 6 ft high). The sill elevation for the flashboard-type gates is 38.8 ft (TWDB, 2003). The storage capacity at this level is 146,700 acre-ft with a surface area of 12,240 acres. The mean depth of Lake Houston is 12 ft with a maximum depth of about 50 ft near the dam (USGS, 2000).

The theoretical residence time of the lake varies with flow conditions. The maximum is about 400 days during extreme low flows – when the only withdrawals are by the City of Houston (COH). The minimum is about 0.5 day during extreme high flows. Theoretical residence time for average flow conditions is about 40 days (USGS, 2000).

Seven major tributaries flow into Lake Houston as shown in Figure 2.1. These tributaries include: Cypress Creek, Spring Creek, West Fork of San Jacinto River (West Fork), Caney Creek, Peach Creek, East Fork of San Jacinto River (East Fork) and Luce Bayou.

The Trinity River is located approximately 20 miles east of Lake Houston and flows south towards the Gulf of Mexico. At its closest point to Lake Houston, the river passes within 3 mi from the upstream end of Luce Bayou. Thus, this study investigates the impact on water quantity, quality and hydrodynamics in Lake Houston resulting from interbasin transfer of water from Trinity River to Lake Houston using Luce Bayou as the diversion route. The total permitted water from the Trinity River that can be diverted at the Luce Bayou diversion point is 450,000 acre-feet per annum or an average of about 400 million gallons per day (MGD).

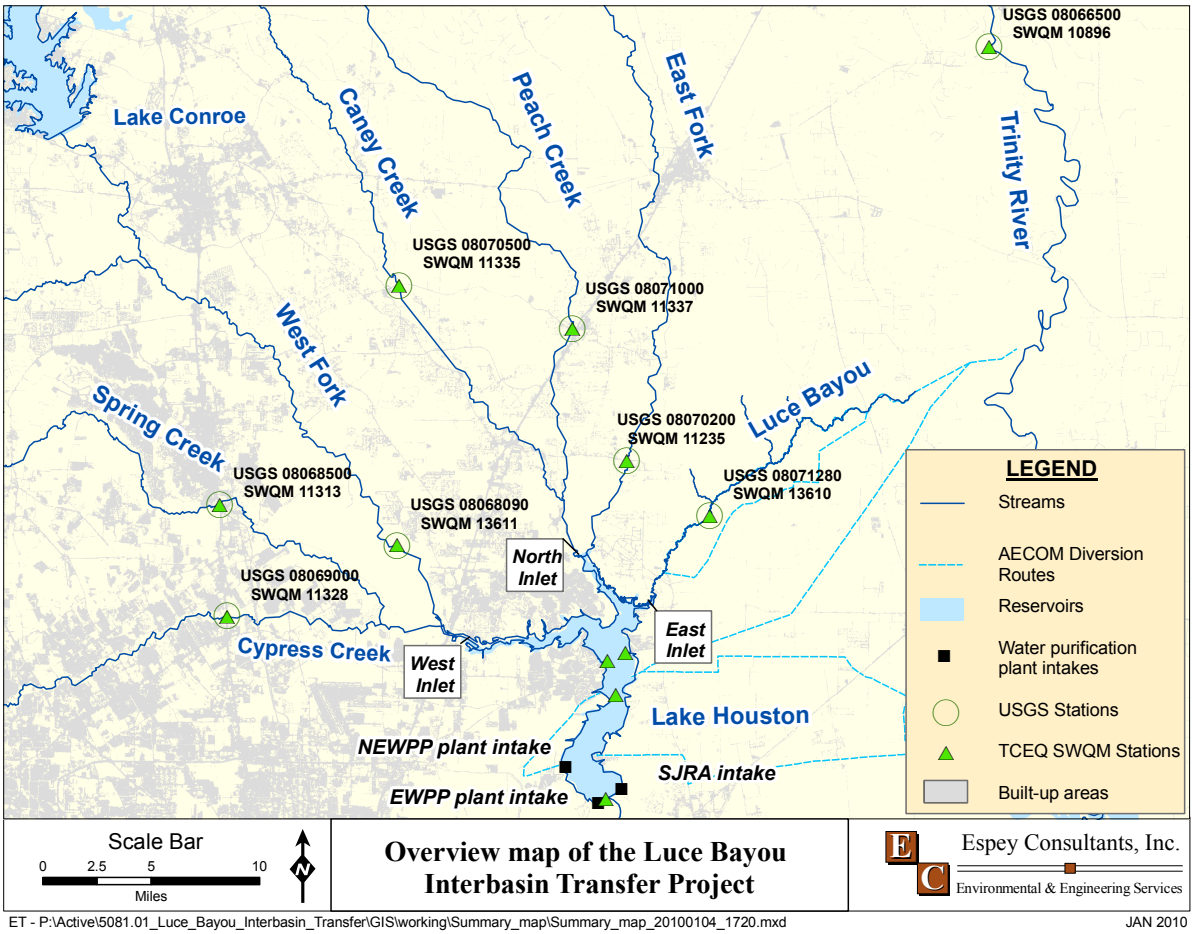

Figure 2.1 Overview map of the Luce Bayou Interbasin Transfer Project.

2.1.1 Inflows into Lake Houston

The seven major tributaries mentioned in the previous section enter Lake Houston at three inlets:

1. Cypress Creek, Spring Creek and the West Fork of San Jacinto River enter via the **West Inlet**. These tributaries drain an urbanized area of the City of Houston and also the western portion of the San Jacinto watershed.
2. Caney Creek, Peach Creek, and the East Fork of San Jacinto River enter via the **North Inlet**. These creeks drain the eastern portion of the San Jacinto watershed, which is less urbanized and more rural than the western portion.
3. Luce Bayou, which would convey the diverted Trinity River water, enters the lake via the **East Inlet**.

Based on the 1984 to 2005 data (EC, 2006), the West Inlet receives an average of 64% of the total flow entering Lake Houston. The North Inlet receives 26% while the East Inlet receives 10% of the total flow. The average total flow from 1984 to 2005 entering the lake is about 2,000 cfs (~1,300 MGD). With the 400 MGD diversion, the total flow entering the lake increases to about 2,600 cfs (~1,700 MGD). The diversion leads to a 30% increase in the total flow into Lake Houston and 300% increase in the flow received by the East Inlet.

2.1.2 Outflows from Lake Houston

Outflows from Lake Houston consist of 1) overflows from the spillway, 2) release flows from the dam gates and 3) pump withdrawals by the NEWPP, East Water Purification Plant (EWPP) and the San Jacinto River Authority (SJRA). The location of the SJRA, NEWPP and EWPP intakes are also shown in Figure 2.1.

Overflows from the spillway are dependent on lake elevation which is, in turn, related to the amount of precipitation in the San Jacinto watershed and other inflows and diversions. Rating curves that relate water surface elevation to flow rates have been developed by the USGS and the Texas Water Development Board (TWDB).

Release flows from the dam gates are dependent on reservoir management and maintenance. For example, the City of Houston (COH) lowered the lake level by 2 feet in October 2004 for contractors to repair cracks on the dam. In September 2005, COH lowered the lake level to around 42.5 ft in preparation for Hurricane Rita.

For pump withdrawals, the EWPP withdraws an average of 87 cfs (56 MGD) based on 2000 to 2008 data (COH, 2009). The NEWPP started operation in January 2006 and draws and average of 45 cfs (29 MGD) based on 2006 to 2008 data (COH, 2009). Finally, the SJRA draws an average of 78 cfs (or 50 MGD) based on 2000 to 2008 data (SJRA, 2009).

2.1.3 General approach and organization of report

The following describes the approach adopted by this study to investigate the impact of the diverted Trinity River water on lake circulation and water quality. The subsequent sections of this report are organized around the sequence of steps below.

1. An extensive data collection was performed to update and augment the database assembled in the 2006 study. The data collected include:
    a. streamflow and water quality data for both the lake and its tributaries;
    b. reservoir storage, stage heights, pump withdrawals and operation records; and,
    c. meteorological data such as wind, precipitation and evaporation.
2. Statistical regressions were used to analyze the relationship between water quality parameters and streamflow from the Lake Houston watershed. Rating curves were developed to estimate the time series of nutrient loads into Lake Houston from the watershed.
3. A statistical analysis of historical inflow patterns was performed. The frequencies and durations of high-flow, low-flow and normal-flow conditions and their impacts on lake water surface elevations were evaluated. Three separate years were selected to represent high-flow, low-flow and normal-flow years for model simulation.
4. A hydrodynamic model for Lake Houston was developed and calibrated. The model estimates water circulation and mixing by taking into account the physical forces caused by inflows, outflows, wind, precipitation and evaporation.
5. A tracer simulation was performed using the hydrodynamic model to evaluate the mixing of tributary inflows in the lake under different flow conditions. The location of the NEWPP intake was evaluated based on the predicted mixing patterns.
6. A water quality model was developed and calibrated to the low-flow, high-flow and normal flow years. This model links to the hydrodynamic model and use the water circulation patterns to evaluate the fate and transport of water quality parameters.
7. The hydrodynamic and water quality models are used to evaluate impacts on water circulation and water quality under the following contamination scenarios:
    a. Diversion of 400 MGD of Trinity River.

b. Historical high, average and low-flow conditons in the San Jacinto Basin.
c. Drops in water surface elevations caused by operations at the Lake Houston dam.

3.0 DATA COLLECTION AND SOURCES

The period from 1/1/2000 to 1/1/2009 was selected as the historical period for this study to provide a sizable dataset that is also descriptive of the current state of the watershed. Data collection and modeling efforts were directed towards this nine-year timeframe.

This study augmented the database compiled in the previous 2006 study by updating the existing data sets with more recent, post-2005 data and incorporating other relevant data from additional sources. The 2006 study gathered spatial and temporal data that are relevant to the San Jacinto watershed from many sources. These spatial data included basemaps of political boundaries, road maps, sub-basins, monitoring locations, river flowlines, bathymetry and other pertinent data for a water quality database (EC, 2006). The temporal data included time series of streamflow and water quality parameters, such as dissolved oxygen and nutrients. This new study added the following information:

- Post-2005 streamflow and water quality data from the seven major tributaries to Lake Houston and Trinity River above the diversion point;
- Post-2005 water quality data from Lake Houston collected by the Texas Commission on Environmental Quality (TCEQ)'s surface water quality monitoring program (SWQM) and USGS, including provisional data from the USGS's discrete sampling program in the lake that were available only through request;
- Intake water quality data collected by the City of Houston at the Duessen Park Marina location (near the NEWPP intake location);
- Post-2005 Lake Houston water surface elevation and storage data collected by USGS;
- Diversion rates from NEWPP, EWPP, and the San Jacinto River Authority; and,
- Meteorological data for the Lake Houston area.

3.1 STREAMFLOW DATA

Daily flow data from the USGS were acquired for the seven major tributaries into Lake Houston (Cypress Creek, Spring Creek, West Fork, Caney Creek, Peach Creek, East Fork and Luce Bayou), as well as for Trinity River above the diversion point. This flow data was downloaded from the USGS website at http://waterdata.usgs.gov/tx/nwis/dv/?referred_module=sw. A list of the USGS streamflow stations is provided in Table 3.1. A map of these stations is given in Figure 2.1.

3.2 WATER QUALITY DATA

3.2.1 Water quality data for tributaries

Water quality data for the seven tributaries and Trinity River were obtained from the TCEQ. The data were measured at TCEQ surface water quality monitoring (SWQM) stations that are located at the same sites as the USGS streamflow stations mentioned in the previous section. Having water quality data that are concurrent and collocated with streamflow data permits the calculation of nutrient loads and the estimation of relationships between flow and concentration at each tributary.

Table 3.1 List of relevant USGS and TCEQ SWQM stations in tributaries to Lake Houston.

Waterbody	Agency	Station	Location
Caney Creek	USGS	08070500	Caney Ck nr Splendora
	SWQM	11335	
Cypress Creek	USGS	08069000	Cypress Ck nr Westfield
	SWQM	11328	
East Fork San Jacinto	USGS	08070200	E Fk San Jacinto Rv nr New Caney
	SWQM	11235	
Luce Bayou	USGS	08071280	Luce Bayou abv Lk Houston nr Huffman
	SWQM	13610	
Peach Creek	USGS	08071000	Peach Ck nr Splendora
	SWQM	11337	
Spring Creek	USGS	08068500	Spring Ck nr Spring
	SWQM	11313	
Trinity River	USGS	08066500	Trinity Rv at Romayor
	SWQM	10896	
West Fork San Jacinto	USGS	08068090	W Fk San Jacinto Rv abv Lk Houston nr Porter
	SWQM	13611	

3.2.2 Water quality data for Lake Houston

Water quality data within Lake Houston are collected at four SWQM stations and five USGS stations. They are listed in Table 3.2 and mapped in Figure 3.1. The data collected at these stations were used to calibrate both the Lake Houston hydrodynamic and water quality models.

Table 3.2 List of relevant USGS and TCEQ SWQM stations in Lake Houston

Waterbody	Agency	Station	Location
Lake Houston	USGS	08072000	USGS Lake Houston Reservoir Storage Data
	SWQM	11204	LAKE HOUSTON NEAR DAM
	SWQM	11208	LAKE HOUSTON AT RR BRIDGE
	SWQM	11211	LAKE HOUSTON AT FM 1960 WEST
	SWQM	11212	LAKE HOUSTON AT FM 1960 EAST
	USGS	295435095082201	Lk Houston at CWA Structure nr Houston, TX
	USGS	295510095084801	Lk Houston Site C nr Deussen Pk nr Houston, TX
	USGS	295554095093401	Lk Houston at mouth of Jack's Ditch nr Houston, TX
	USGS	295724095092301	Lk Houston Site A nr Alcoa oil field nr Houston, TX
	USGS	295826095082200	Lk Houston S Union Pacific RR Bridge nr Houston,TX

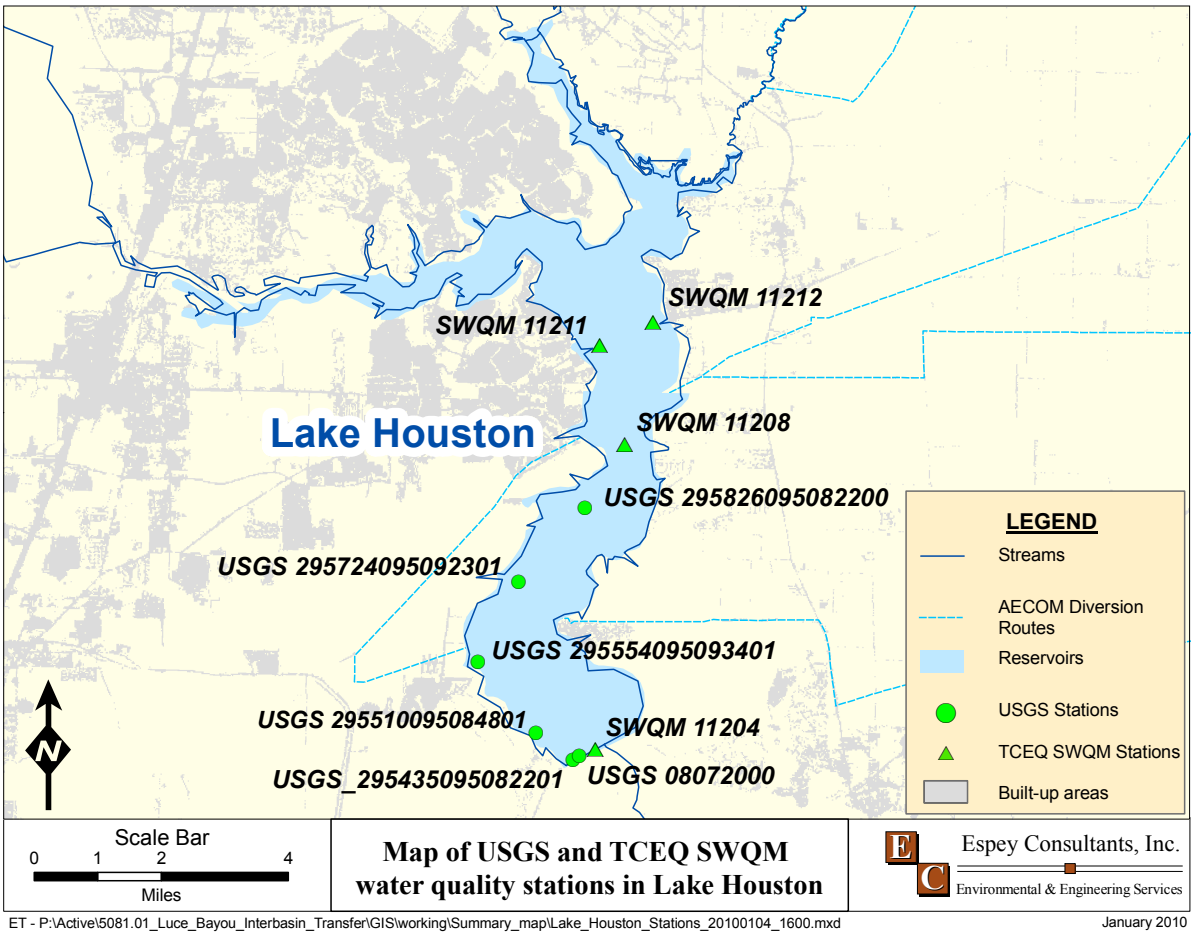

Figure 3.1 Map of USGS and TCEQ SWQM water quality stations in Lake Houston.

3.2.3 List of relevant water quality data for Lake Houston

A list of the water quality parameters relevant to the project was created (Table 3.3) to organize the assembled water quality data. Water quality data were consolidated into a Microsoft Access database to support the modeling work in this project. The parameters in the database include the following:

- physical parameters, i.e., temperature and secchi depth;
- nutrient-related parameters, i.e., dissolved oxygen, biochemical oxygen demand (BOD), pH, nitrogen species (i.e., ammonia, total Kjeldahl nitrogen, and nitrate), phosphorus species (i.e. phosphate, total phosphorus) and chlorophyll-a; and,
- water-treatment-related parameters, i.e., alkalinity, magnesium and iron.

Because some parameters can be measured in different ways (e.g. nitrate can be measured filtered versus unfiltered). Results maybe stored under different EPA storet codes and with different units. An extensive effort was made to ensure all storet codes that pertain to each parameter were captured in the database. Conversions were carried out to ensure that the units were consistent before the data were entered into the database.

Table 3.3 List of relevant water quality parameters and associated USGS/EPA Storet Codes.

Parameter	Storet Code	Explanation
Temperature	10	Temperature water (degrees Celsius)
Secchi Depth	78	Transparency water in situ Secchi disc (meters)
Specific Conductance	95	Specific conductance water unfiltered (µS/cm at 25 degrees Celsius)
Dissolved oxygen	300	Dissolved oxygen water unfiltered (mg/L)
BOD	310	Biochemical oxygen demand water unfiltered 5 day at 20 degrees C (mg/L)
pH	400	pH water unfiltered field
	403	pH water unfiltered lab
Alkalinity	39036	Alkalinity water filtered fixed endpoint (pH 4.5) titration field (mg/L as calcium carbonate)
	39086	Alkalinity water filtered inflection-point titration method (incremental titration method) field (mg/L as calcium)
Total Suspended Solids	530	Residue total nonfilterable (mg/L)
	80154	Suspended sediment concentration (mg/L)
Ammonia	608	Ammonia water filtered (mg/L as N)
	610	Ammonia water unfiltered (mg/L as N)
	71846	Ammonia water filtered (mg/L)
Total Kjeldahl Nitrogen (TKN)	623	TKN - Ammonia + org-N water filtered (mg/L as N)
	625	TKN - Ammonia plus organic N water unfiltered (mg/L as N)
Nitrate	618	Nitrate water filtered (mg/L as N)
	620	Nitrate water unfiltered (mg/L as N)
	71851	Nitrate water filtered (mg/L)
Orthophosphate	671	Orthophosphate water filtered (mg/L)
	660	Orthophosphate water filtered (mg/L as PO_4)
	70507	Orthophosphate water unfiltered (mg/L)
Total Phosphorus	666	Phosphorus water filtered (mg/L as P)
	665	Phosphorus water unfiltered (mg/L as P)
Magnesium	925	Magnesium water filtered (mg/L)
Iron	1046	Iron water filtered (µg/L)
Phytoplankton Chlorophyll - a	32211	Chlorophyll a phytoplankton spectrophotometric acid method (µg/L)
	70953	Chlorophyll a phytoplankton chromatographic-fluorometric method (µg/L)

3.3 RESERVOIR WATER SURFACE ELEVATION AND STORAGE DATA

Reservoir storage data were obtained from the USGS Lake Houston gage station 08072000. This site provided data for both gage height as well as reservoir storage. This data was obtained for the time period January 2000 through September 2009.

3.4 METEOROLOGICAL DATA

Meteorological data were obtained, to the extent available, from the National Climatic Data Center (NCDC), National Solar Radiation Database (NSRDB), United States Naval Observatory and TWDB for

the period beginning 2000 through September 2009. These include a variety of parameters including air temperature, daily precipitation, wind speed and relative humidity. A list of the sources of data is shown in Table 3.4.

Table 3.4 Sources of meteorological data

Meteorological data	Source	Web link (if available)	Period of data
Average Daily Temperature (deg F)	NCDC (Houston Intercontinental Airport)	http://www.ncdc.noaa.gov/oa/ncdc.html	2000-2009
Maximum Daily Temperature (deg F)	NCDC (Houston Intercontinental Airport)	http://www.ncdc.noaa.gov/oa/ncdc.html	2000-2009
Minimum Daily Temperature (deg F)	NCDC (Houston Intercontinental Airport)	http://www.ncdc.noaa.gov/oa/ncdc.html	2000-2009
Average Daily Wind Speed	NCDC (Houston Intercontinental Airport)	http://www.ncdc.noaa.gov/oa/ncdc.html	2000-2009
Resultant Wind Direction	NCDC (Houston Intercontinental Airport)	http://www.ncdc.noaa.gov/oa/ncdc.html	2000-2009
Resultant Wind Speed	NCDC (Houston Intercontinental Airport)	http://www.ncdc.noaa.gov/oa/ncdc.html	2000-2009
Average Relative Humidity	NCDC (Houston Intercontinental Airport)	http://www.ncdc.noaa.gov/oa/ncdc.html	2000-2009
Maximum Relative Humidity	NCDC (Houston Intercontinental Airport)	http://www.ncdc.noaa.gov/oa/ncdc.html	2000-2009
Minimum Relative Humidity	NCDC (Houston Intercontinental Airport)	http://www.ncdc.noaa.gov/oa/ncdc.html	2000-2009
Solar Radiation (W/m^2)	National Solar Radiation Database (NSRDB)	http://www.ncdc.noaa.gov/oa/ncdc.html	2000-2005
Day Length	United States Naval Observatory	http://aa.usno.navy.mil/data/docs/RS_OneYear.php	2000-2009
Lake surface evaporation	Texas Water Development Board (TWDB)	http://midgewater.twdb.state.tx.us/Evaporation/evap.html	2000-2007
Precipitation	Texas Water Development Board (TWDB)	http://midgewater.twdb.state.tx.us/Evaporation/evap.html	2000-2007
Pan evaporation	Texas A & M AgriLIFE Research Center at Beaumont, Texas.	http://beaumont.tamu.edu/ClimaticData	2000-2009
Precipitation	Texas A & M AgriLIFE Research Center at Beaumont, Texas.	http://beaumont.tamu.edu/ClimaticData	2000-2009

3.5 DIVERSION DATA

The pumpage rates from 2000 to 2009 and the locations of the NEWPP and EWPP intakes on Lake Houston were acquired from the COH. Pumpage rates and intake location of the SJRA pump station from 2000 to 2009 were obtained from SJRA.

3.6 RESERVOIR OPERATIONS RECORDS

Normal dam release flows for the regular maintenance of the dam and the management of the reservoir are generally insignificant compared to spillway flows. In addition, the reservoir rating curves themselves take into account the dam release flows because the curves are created from regressions between the lake elevation and the total flow downstream of the dam (which includes both spillway and dam release flows). Seldom do dam release flows become significant in relation to the spillway flow. Despite this, to identify these unusual events, EC contacted the COH and obtained operation logs of the dam from 2005 to 2009 (Operation logs prior to 2005 were not available). Through communication with COH staff, EC learned about two significant dam release events from 2004 to 2009:

1. In October 2004, the lake level was lowered to around 42.7 ft in October 2004 for contractors to repair cracks on the dam. Lake level was back to 44.52 ft on November 2nd, 2004.
2. In September 2005, the lake level was lowered to around 42.5 ft in preparation for Hurricane Rita. Lake level was back to 44.45 ft on October 7th, 2005.

The amount of dam release flows for these two events are calculated based on the change in volume over the time of drawdown. The dam release flows are incorporated into the hydrodynamic model.

4.0 EVALUATION OF INFLOWS AND CONCENTRATIONS

Nutrient concentrations in the Lake Houston watershed are monitored by TCEQ on a quarterly basis, at best. Because of the sparseness of the data, it is necessary to establish mathematical functions that correlate nutrient concentrations to more abundant data, e.g. daily flow data. The mathematical functions allow the generation of more complete time series of the external loads so that the lake model can be better characterized.

4.1 APPLICATION OF USGS LOADEST MODEL

The USGS Load Estimator model LOADEST is a statistical regression program that can calculate nutrient concentrations as functions of time and/or flow (USGS, 2008). These functions are referred to as water quality rating curves. LOADEST was used to estimate rating curves for all seven tributaries and Trinity River using the concurrent flow and concentration data collected at the collocated USGS and SWQM stations.

The ability of LOADEST to generate reasonable results is highly dependent on the correlation between the concentration of a parameter (e.g. Total Suspended Solids) and the dependent variable (e.g. flow). Therefore before using LOADEST, the degree of correlation with flow was evaluated for each parameter. LOADEST was only applied to develop rating curves for parameters that are strongly correlated with flow. When LOADEST could not be used based on these correlations, the mean of measured concentrations from the available datasets were used as parameter concentrations. Mean concentrations were also used for parameters not having sufficient data for analysis.

An example of such analysis is shown in Figure 4.1. In this figure, parameter values of temperature, specific conductance, dissolved oxygen, BOD, pH and alkalinity collected at SWQM gage 11328 are plotted against the concurrent streamflow measured at USGS 0806900. For each plot, the Pearson's correlation coefficient is computed for the log-transformed flow and the log-transformed concentration. As a simple rule of thumb, parameters that have coefficients that have an absolute value greater than 0.5 are considered strongly correlated with the flow.

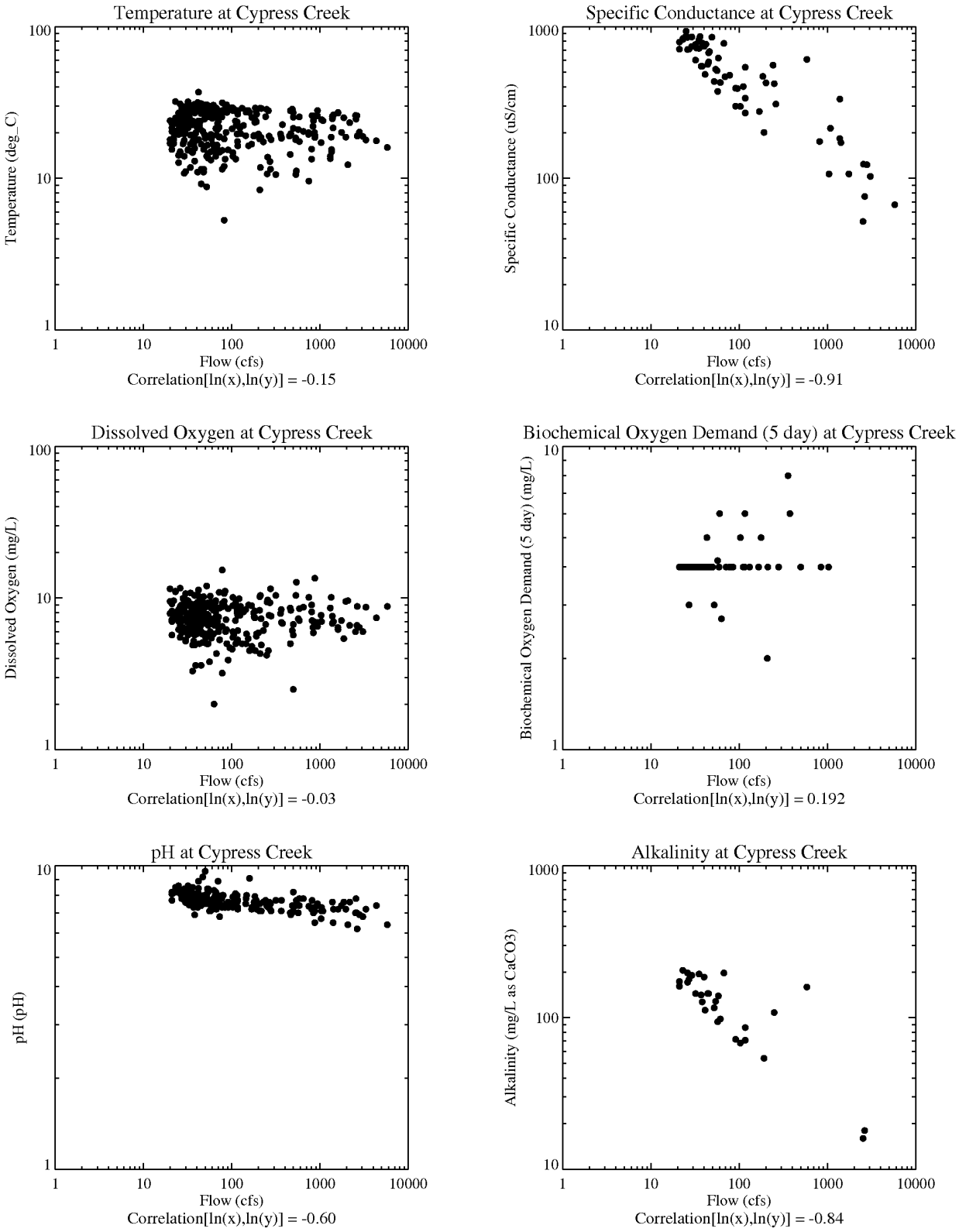

Figure 4.1 Flow vs. concentration plots for the west for of the San Jacinto River.

In Figure 4.1, conductivity, pH, and alkalinity were found to have strong negative correlations that have a magnitude greater than 0.5. For these parameters, LOADEST was applied. Despite having weak correlations with flows, temperature and dissolved oxygen are found to follow seasonal patterns and are thus highly correlated with time. For these two parameters, LOADEST was applied but in a different manner. The concentration was regressed against both time and flow. BOD_5 was found to have weak correlation with both flow and time and a constant average concentration was used as the time series.

The analysis was applied to all seven tributaries and Trinity River. The plots of flow versus concentration for all the tributaries are available in Appendix A. A summary of the correlation coefficients for each combination of tributary and parameter is shown in Table 4.1. The numbers that are enlarged and in bold indicate strong correlations where LOADEST was applied. The remaining cells are considered weak correlations and a constant average concentration was applied. For many of the parameters at Peach Creek, the data were insufficient for estimation either with using LOADEST or by calculating the average concentration. Therefore, due to the similar nature of the two creeks, average concentrations from Caney Creek were applied to Peach Creek. The reason for choosing Caney Creek is because the Caney Creek watershed is adjacent to the Peach Creek watershed and exhibits similar landuse properties and is approximately the same size (~110 sq mi).

Table 4.1 Summary of correlation coefficients between log-streamflow and log-concentrations for water quality parameters at each tributary of Lake Houston

	Caney Creek	Cypress Creek	East Fork San Jacinto	Luce Bayou	Peach Creek	Spring Creek	Trinity River	West Fork San Jacinto
Conductivity	**0.51**	**-0.91**	**-0.55**	**-0.77**	Limited or No Data	**-0.93**	-0.31	**-0.89**
BOD_5	0.18	0.19	-0.04	Limited or No Data	Limited or No Data	Limited or No Data	-0.49	Limited or No Data
pH	-0.41	**-0.60**	-0.28	0.23	0.18	**-0.61**	-0.45	**-0.62**
Alk	**0.68**	**-0.84**	-0.27	**-0.86**	Limited or No Data	**-0.92**	Limited or No Data	**-0.76**
TSS	0.34	**0.73**	**0.60**	Limited or No Data	Limited or No Data	**0.66**	**0.60**	Limited or No Data
NH3	**0.54**	-0.10	0.03	0.15	0.49	-0.09	-0.01	0.01
TKN	**0.71**	0.00	**0.71**	0.23	Limited or No Data	-0.15	0.04	0.35
NO3	Limited or No Data	**-0.64**	-0.47	Limited or No Data	Limited or No Data	**-0.81**	**0.69**	Limited or No Data
PO4	0.45	**-0.66**	Limited or No Data	-0.26	Limited or No Data	**-0.62**	0.14	**-0.77**
TP	0.47	**-0.89**	0.16	-0.17	Limited or No Data	**-0.78**	0.21	**-0.77**
Mg	**0.56**	**-0.91**	**-0.65**	**-0.77**	Limited or No Data	Limited or No Data	-0.45	Limited or No Data
Fe	0.28	0.43	0.31	0.42	Limited or No Data	0.27	0.06	**0.61**
Chl-a	0.25	0.00	0.02	Limited or No Data	Limited or No Data	Limited or No Data	-0.43	Limited or No Data

After application of the appropriate concentration estimation method, the estimated time series of the water quality parameter concentration were plotted. An example of these plots is shown in Figure 4.2. In

this figure, the estimated concentrations are represented by blue dots. The observed data are represented by the black dots. The mean of the data are represented by the horizontal dashed line. Finally, the standard deviation around the mean is represented by the yellow shaded area.

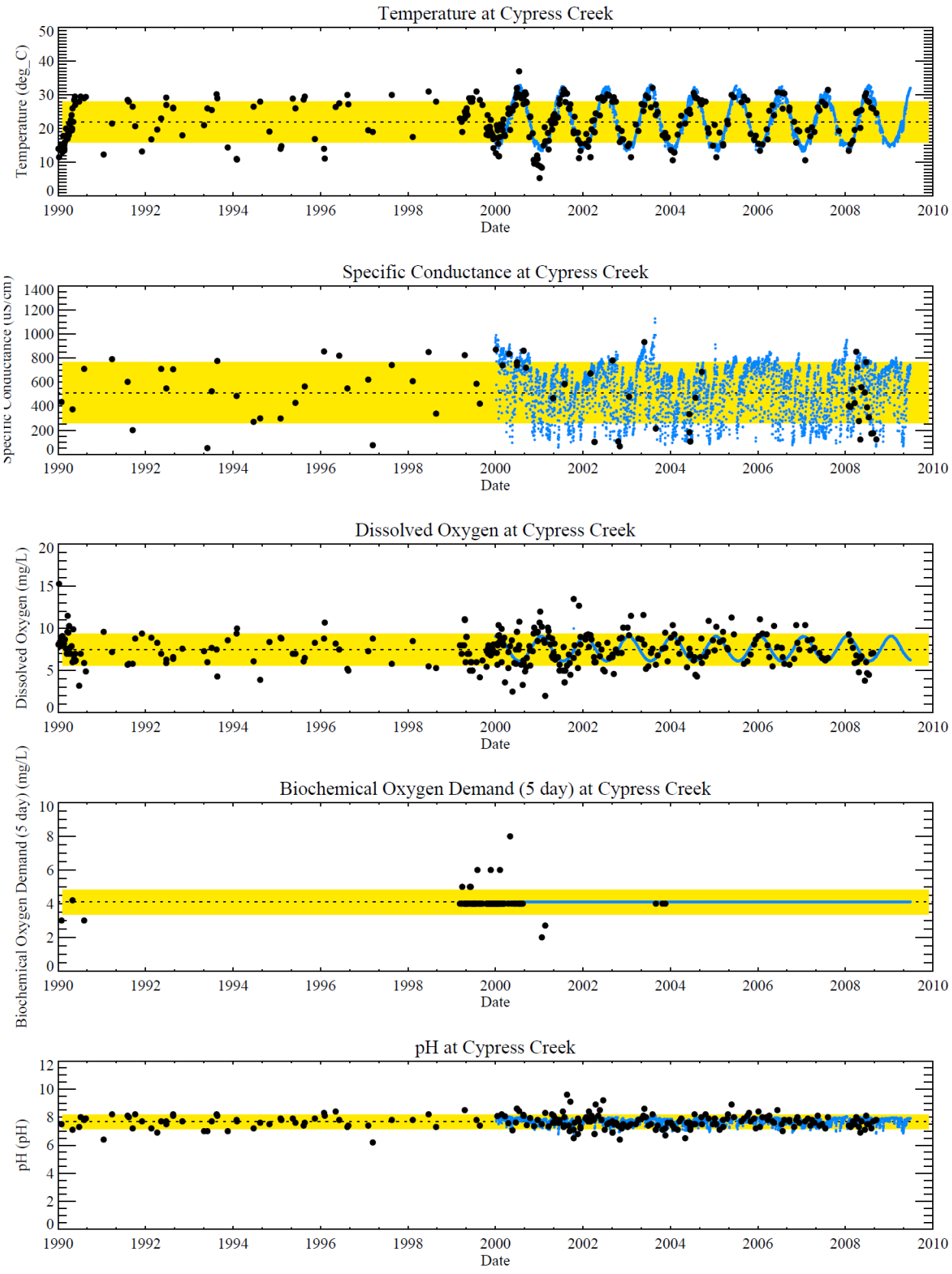

Figure 4.2 Time series of concentration of water quality parameters at Cypress Creek.

From these plots it can be seen that temperature and dissolved oxygen concentrations follow seasonal patterns that are reasonably described by LOADEST. LOADEST also provides reasonable estimation of the specific conductance and pH, which are highly correlated with flow. For BOD5, LOADEST was not used because of weak correlation but the average concentration provides a reasonable estimate. The plots for the remaining tributaries and parameters can be found in Appendix B.

4.2 PRORATION OF FLOWS AND CONCENTRATIONS

Tributary gages are located some distance upstream from Lake Houston (Figure 1.1). To account for additional runoff received in the stream sections located between the gages and the lake inlets, flows were prorated on the basis of catchment area. Catchment areas at the gages, stream confluences and the lake inlets are presented in Table 4.2.

Table 4.2 Summary of correlation coefficients between log-streamflow and log-concentrations for water quality parameters at each tributary of Lake Houston

Inlet to Lake Houston	Catchment	Catchment Area	Units
North Inlet	Caney Creek (USGS 08070500)	105	sq mi
	Caney Creek (USGS 08070500) to Caney-Peach Confluence	80	sq mi
	Peach Creek (USGS_08071000)	117	sq mi
	Peach Creek (USGS_08071000) to Caney-Peach Confluence	40	sq mi
	Caney-Peach Confluence to Lake Houston (North Inlet)	30	sq mi
	East Fork (USGS 08070200)	388	sq mi
	East Fork (USGS 08070200) to Lake Houston (North Inlet)	15	sq mi
West Inlet	Cypress Creek (USGS 08069000)	285	sq mi
	Cypress Creek (USGS 08069000) to Cypress-Spring Confluence	434	sq mi
	Spring Creek (USGS 08068500)	409	sq mi
	Spring Creek (USGS 08068500) to Cypress-Spring Confluence	29	sq mi
	Cypress-Spring Confluence to Cypress-West Fork Confluence	6	sq mi
	West Fork (USGS 08068090)	962	sq mi
	West Fork (USGS 08068090) to Cypress-West Fork Confluence	20	sq mi
	Cypress-West Fork Confluence to Lake Houston (West Inlet)	5	sq mi
East Inlet	Luce Bayou (USGS 08071280)	218	sq mi
	Luce Bayou (USGS 08071280) to Lake Houston (East Inlet)	15	sq mi

The derived proration ratios are shown in the following three equations. Proration ratios are multipliers applied to the measured flow at each tributary before it is summed into the total inlet flow.

[Flow into West Inlet] = 1.17* [Flow at Cypress Creek (USGS 08069000)]
+1.08* [Flow at Spring Creek USGS 08068500]
+1.02* [Flow at West Fork USGS 08068090] Equation 4.1

[Flow at North Inlet] = 1.92*[Flow at Caney Creek (USGS 08070500)]
+ 1.46 * [Flow at Peach Creek (USGS 08071000)]
+1.04*[Flow at East Fork (USGS 08070200)] Equation 4.2

[Flow at East Inlet] = 1.07*([Flow at Luce Bayou (USGS_08071280)]
+ diverted flow from Trinity River Equation 4.3

The same ratios can also be applied to calculate the loads into Lake Houston at the three inlets (see Equations 4.4 to 4.6).

[Load into West Inlet] = 1.17* [Load at Cypress Creek (USGS 08069000)]
+1.08* [Load at Spring Creek USGS 08068500]
+1.02* [Load at West Fork USGS 08068090] Equation 4.4

[Load at North Inlet] = 1.92*[Load at Caney Creek (USGS 08070500)]
+ 1.46 * [Load at Peach Creek (USGS 08071000)]
+1.04*[Load at East Fork (USGS 08070200)] Equation 4.5

[Load at East Inlet] = 1.07*([Load at Luce Bayou (USGS_08071280)]
+ diverted Load from Trinity River Equation 4.6

Concentrations of water quality parameters at the three inlets are calculated by dividing the load and the flow at each inlet (see Equations 4.7 to 4.9).

[Concentration of West Inlet] = [Load into West Inlet]/ [Flow into West Inlet] Equation 4.7

[Concentration of North Inlet] = [Load into North Inlet]/ [Flow into North Inlet] Equation 4.8

[Concentration of East Inlet] = [Load into East Inlet]/ [Flow into East Inlet] Equation 4.9

4.3 CONCENTRATIONS OF WATER QUALITY PARAMETERS AT WEST INLET

At the West Inlet, the concentrations of each water quality parameter are calculated using Equations 4.1, 4.4 and 4.7. The time series of each parameter from 1/1/2000 to 1/1/2009 are plotted in Figures 4.3, 4.4 and 4.5.

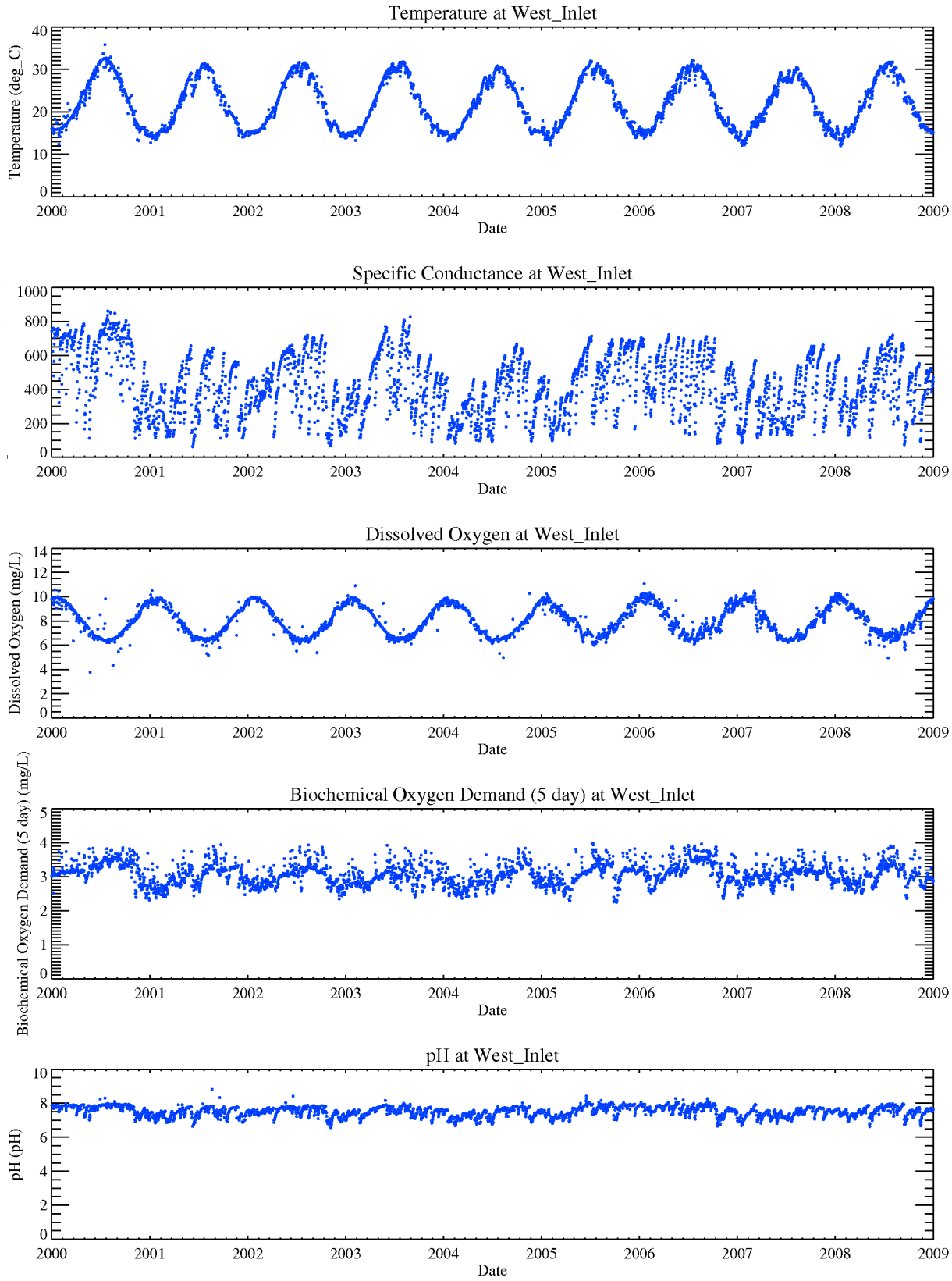

Figure 4.3 Calculated time series of temperature, specific conductance, dissolved oxygen, BOD_5 and pH at West Inlet from 1/1/2000 to 1/1/2009.

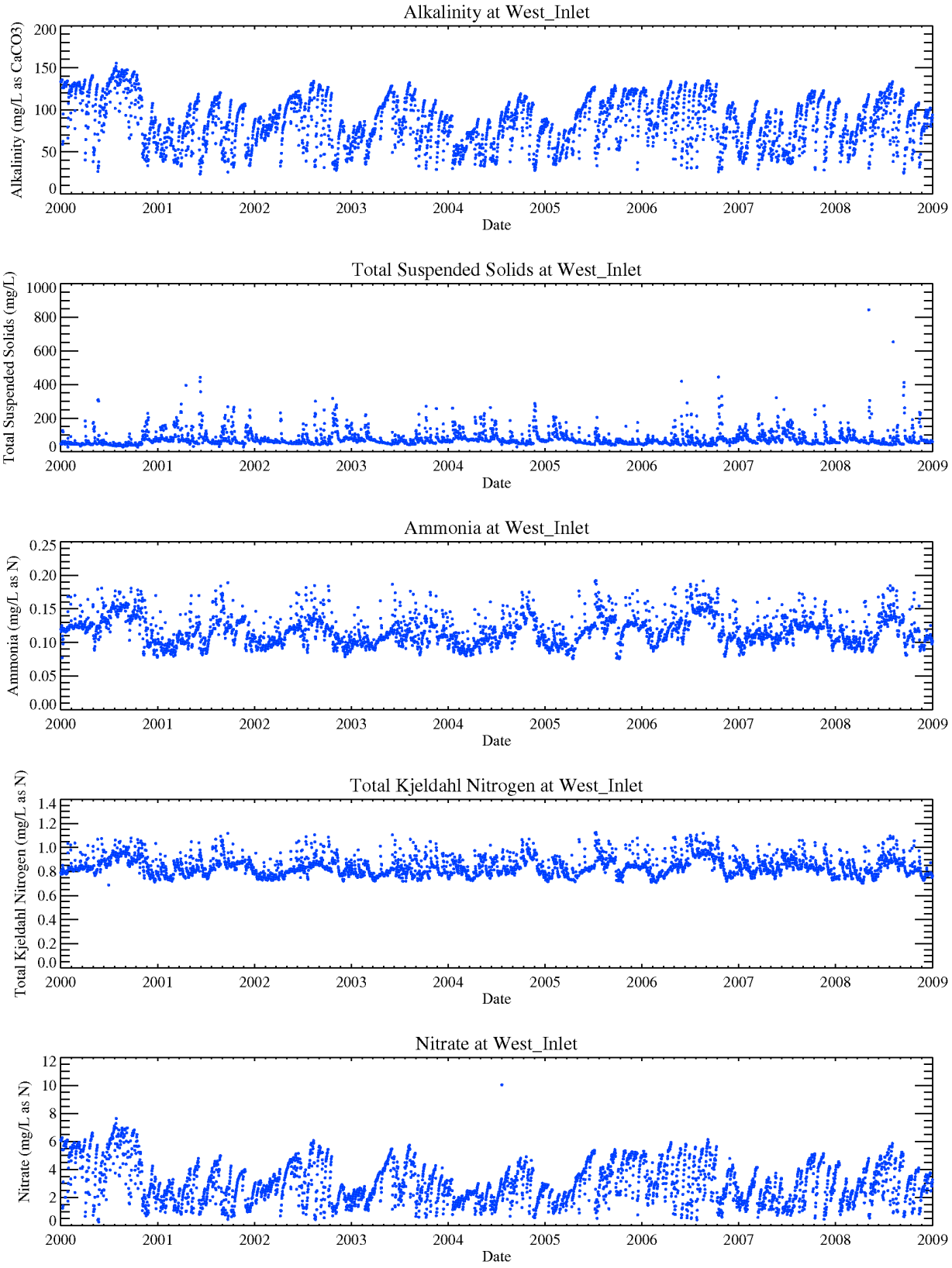

Figure 4.4 Calculated time series of alkalinity, total suspended solids, dissolved oxygen, ammonia, total kjeldahl nitrogen and nitrate concentrations at West Inlet from 1/1/2000 to 1/1/2009.

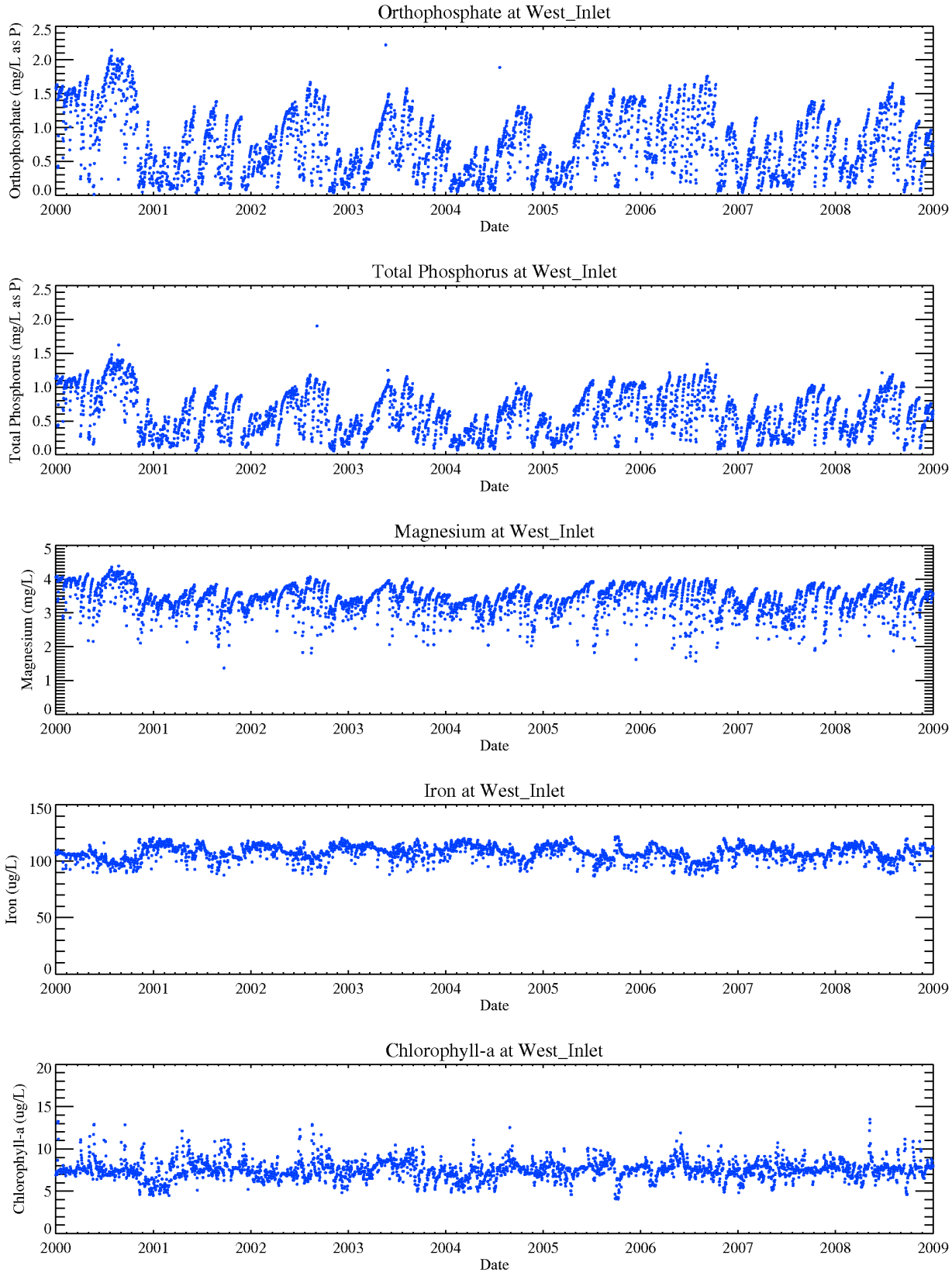

Figure 4.5 Calculated time series of orthophosphate, total phosphorus, magnesium, iron, chlorophyll-a concentrations at West Inlet from 1/1/2000 to 1/1/2009.

4.4 CONCENTRATIONS OF WATER QUALITY PARAMETERS AT NORTH INLET

At the North Inlet, the concentrations of each water quality parameter are calculated using Equations 4.2, 4.5 and 4.8. The time series of each parameter from 1/1/2000 to 1/1/2009 are plotted in Figures 4.6, 4.7 and 4.8.

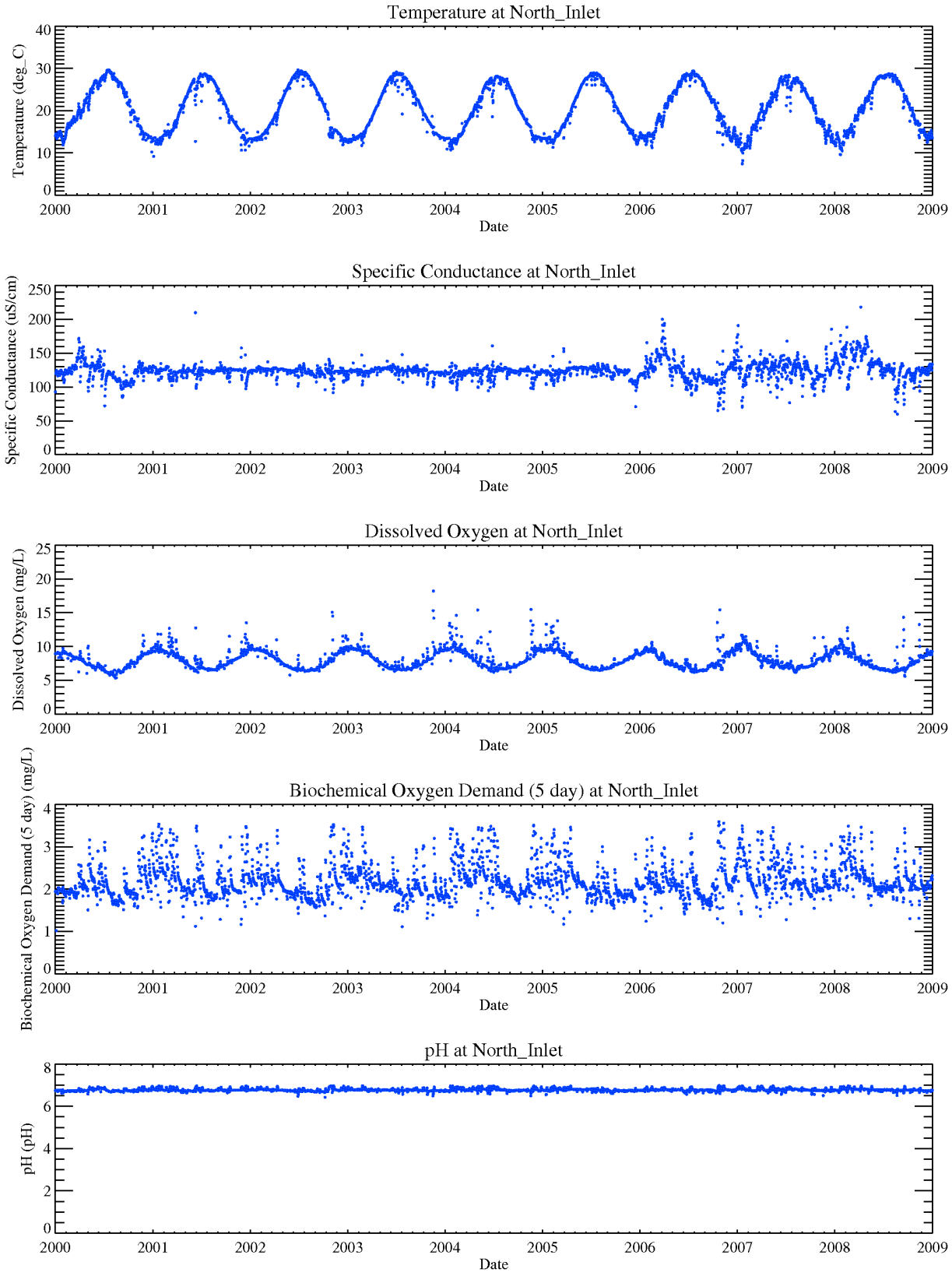

Figure 4.6 Calculated time series of temperature, specific conductance, dissolved oxygen, BOD_5 and pH at North Inlet from 1/1/2000 to 1/1/2009.

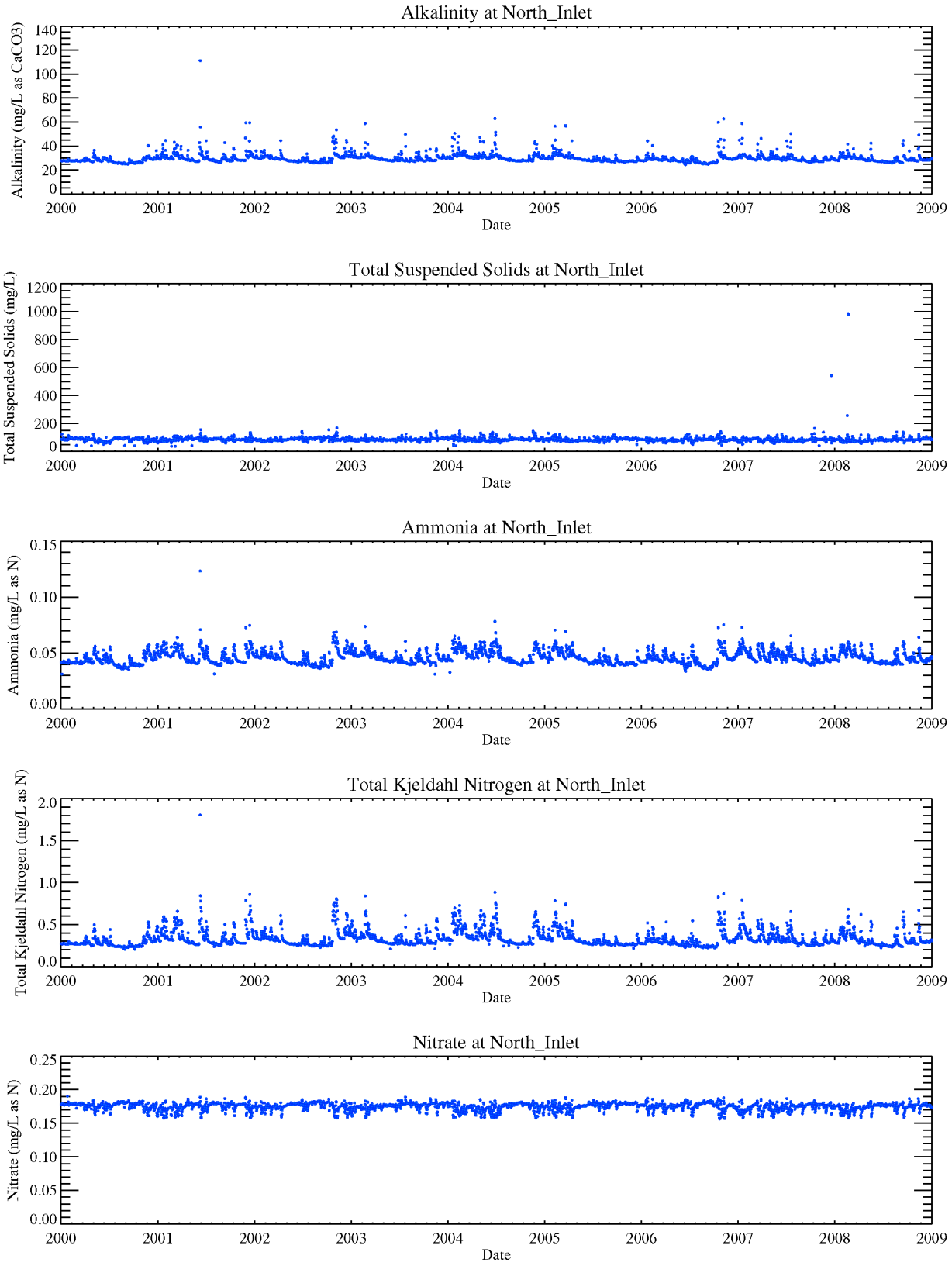

Figure 4.7 Calculated time series of alkalinity, total suspended solids, dissolved oxygen, ammonia, total kjeldahl nitrogen and nitrate concentrations at North_Inlet from 1/1/2000 to 1/1/2009.

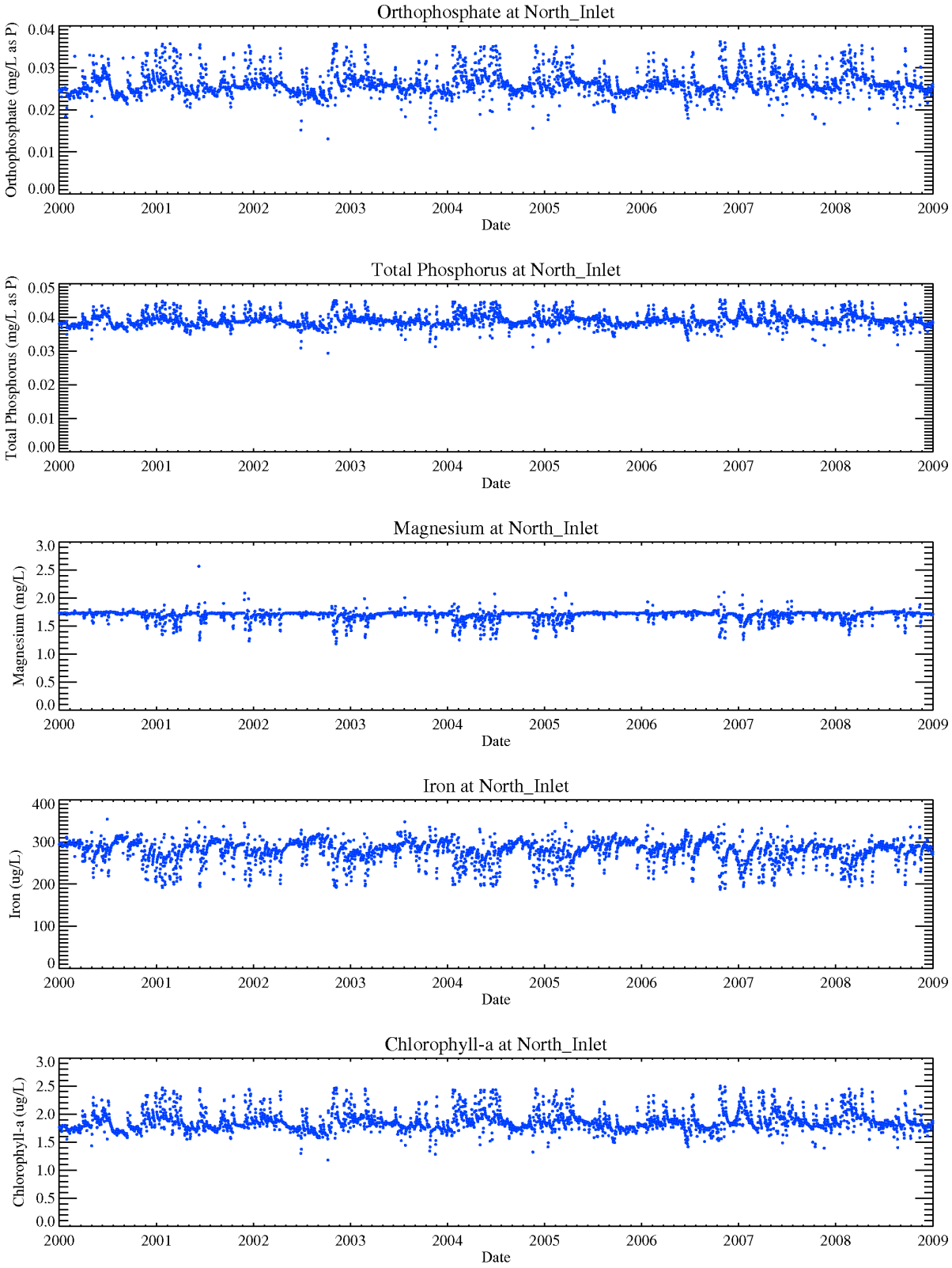

Figure 4.8 Calculated time series of orthophosphate, total phosphorus, magnesium, iron, chlorophyll-a concentrations at North Inlet from 1/1/2000 to 1/1/2009.

4.5 CONCENTRATIONS OF WATER QUALITY PARAMETERS AT EAST INLET (NO DIVERSION)

At the East Inlet, the concentrations of each water quality parameter are calculated using Equations 4.3 (without diverted Trinity water), 4.6 (without diverted Trinity water) and 4.9. The time series of each parameter from 1/1/2000 to 1/1/2009 are plotted in Figures 4.9, 4.10 and 4.11.

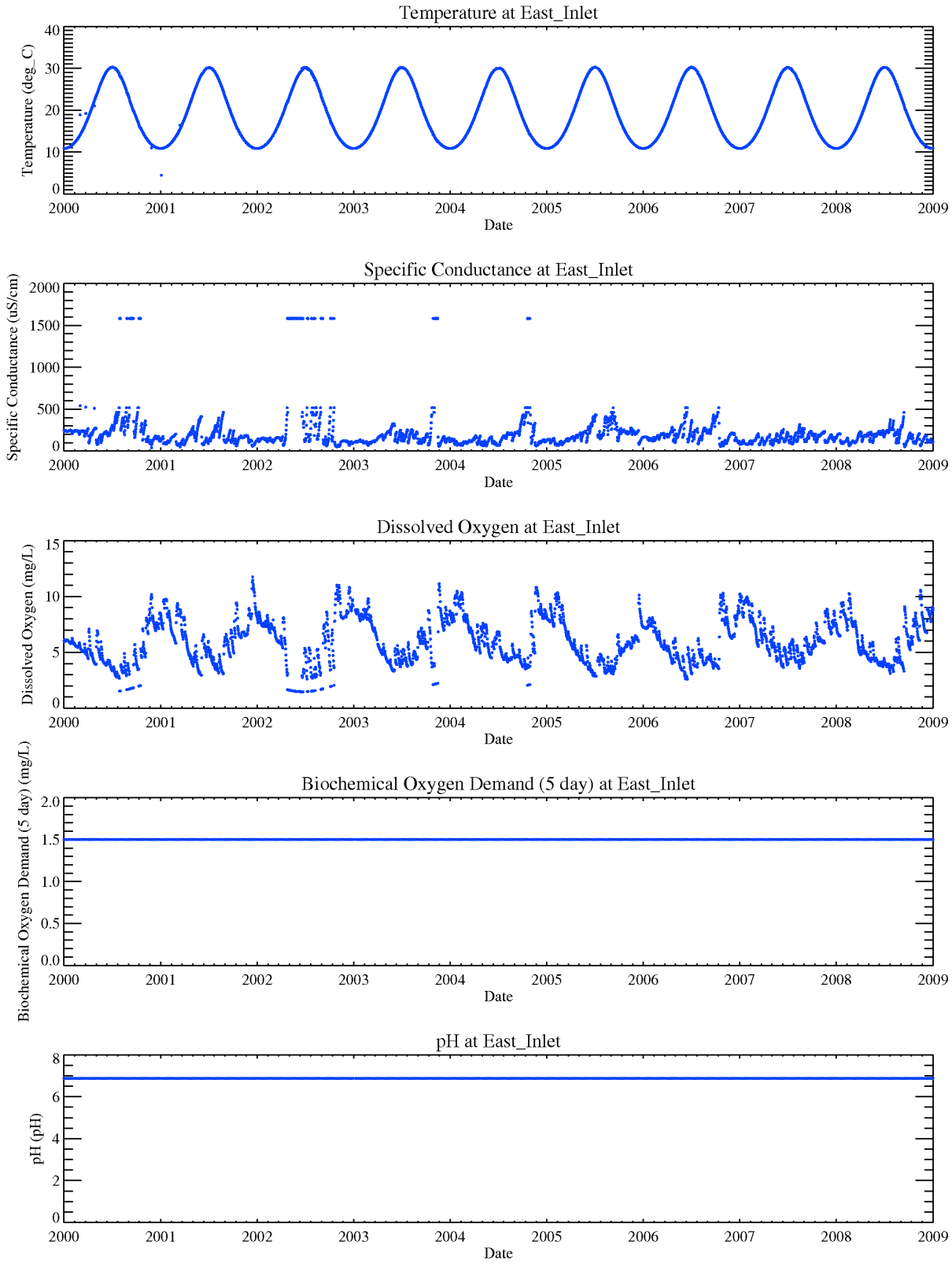

Figure 4.9 Calculated time series of temperature, specific conductance, dissolved oxygen, BOD_5 and pH at East Inlet (no diversion) from 1/1/2000 to 1/1/2009.

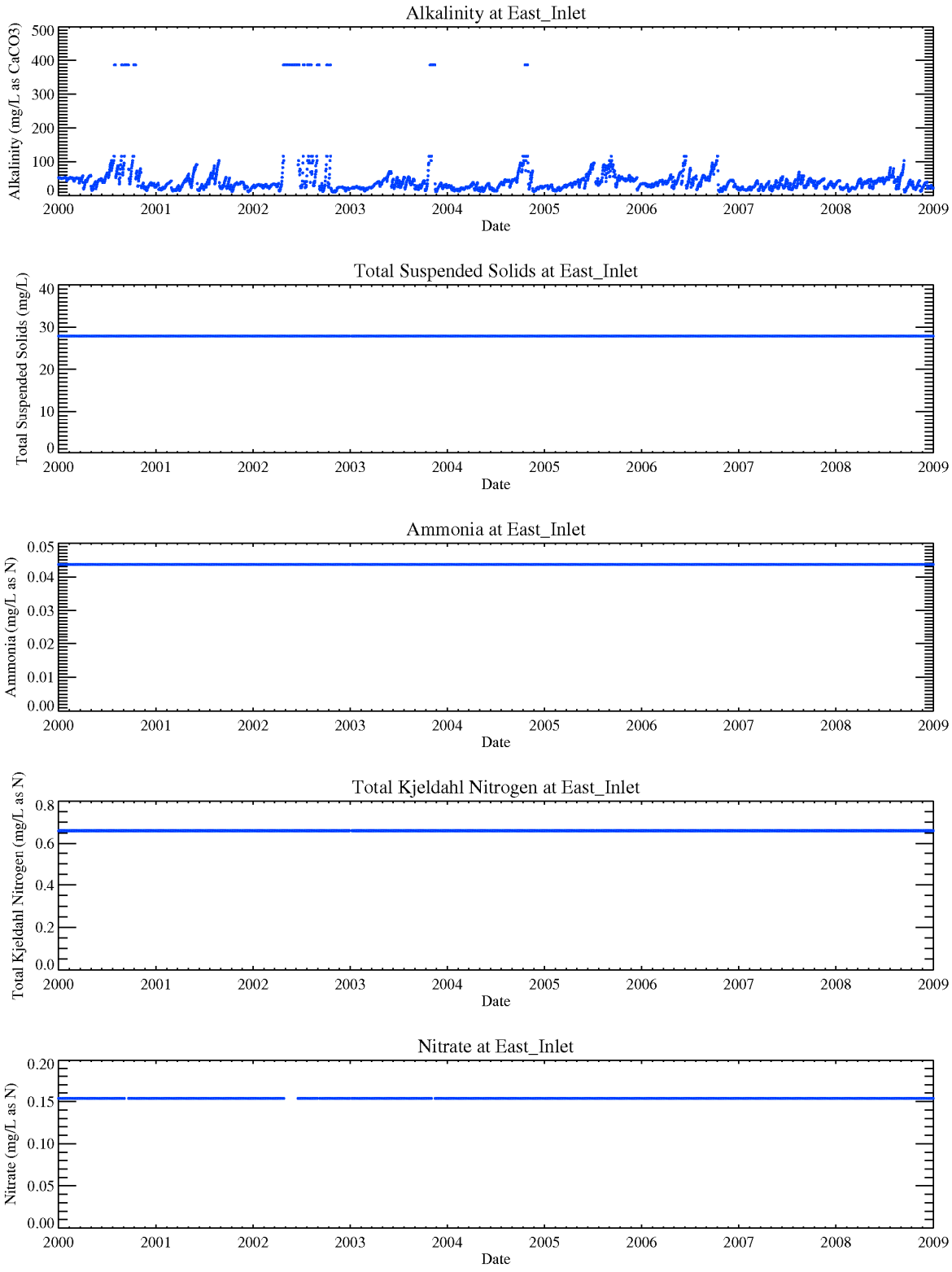

Figure 4.10 Calculated time series of alkalinity, total suspended solids, dissolved oxygen, ammonia, total kjeldahl nitrogen and nitrate concentrations at East Inlet (no diversion) from 1/1/2000 to 1/1/2009.

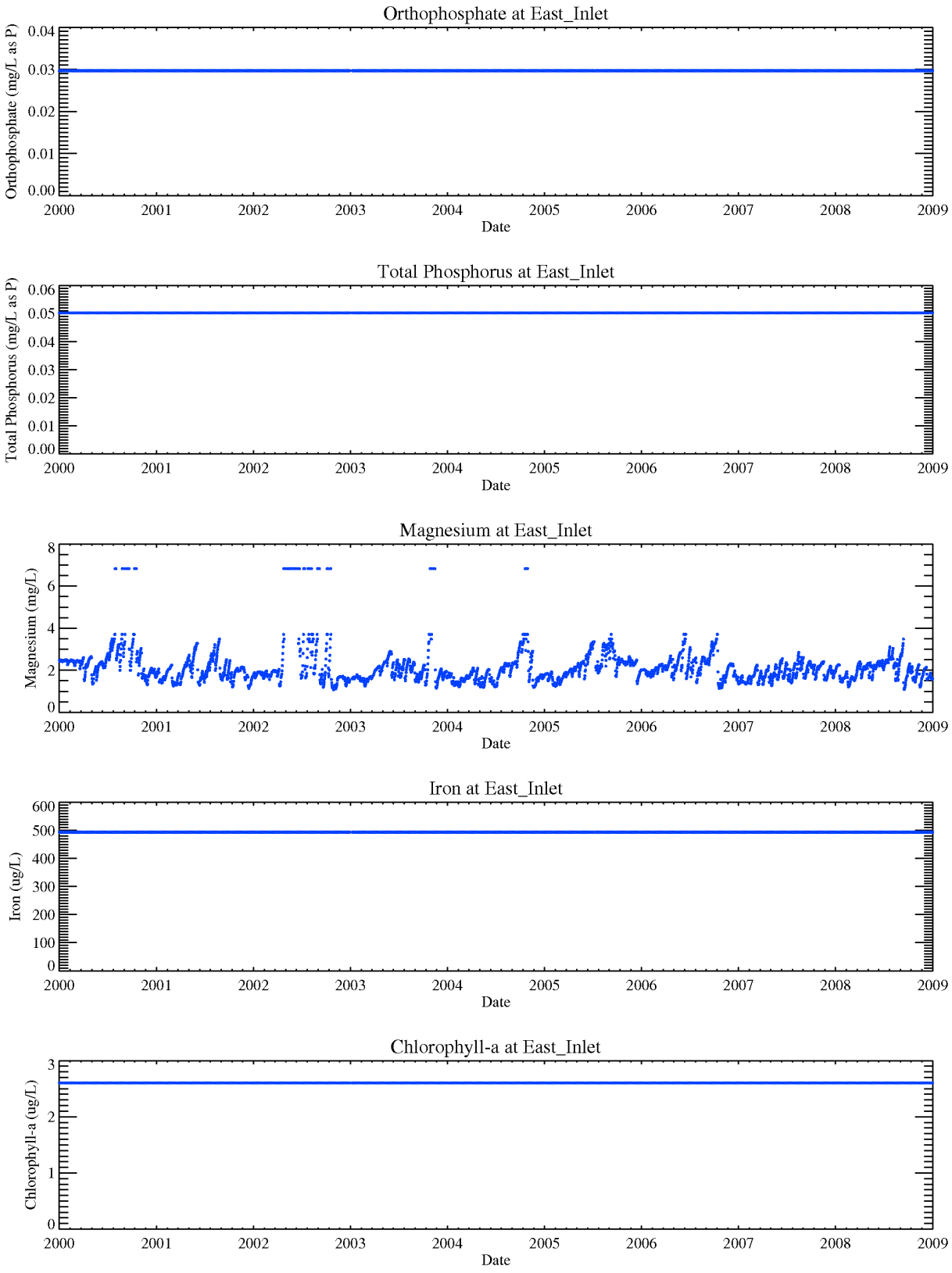

Figure 4.11 Calculated time series of orthophosphate, total phosphorus, magnesium, iron, chlorophyll-a concentrations at East Inlet (no diversion) from 1/1/2000 to 1/1/2009.

4.6 CONCENTRATIONS OF WATER QUALITY PARAMETERS AT EAST INLET (WITH 400 MGD DIVERSION)

At the East Inlet, the concentrations of each water quality parameter are calculated using Equations 4.3 (with 400 MGD of diverted Trinity River water), 4.6 (with 400 MGD of diverted Trinity River water) and 4.9. Because of the high Trinity diversion flow rate compared to the natural Luce Bayou flow rate, the water quality at the East Inlet is heavily influenced by the Trinity River. The time series of each parameter from 1/1/2000 to 1/1/2009 are plotted in Figures 4.12, 4.13 and 4.14.

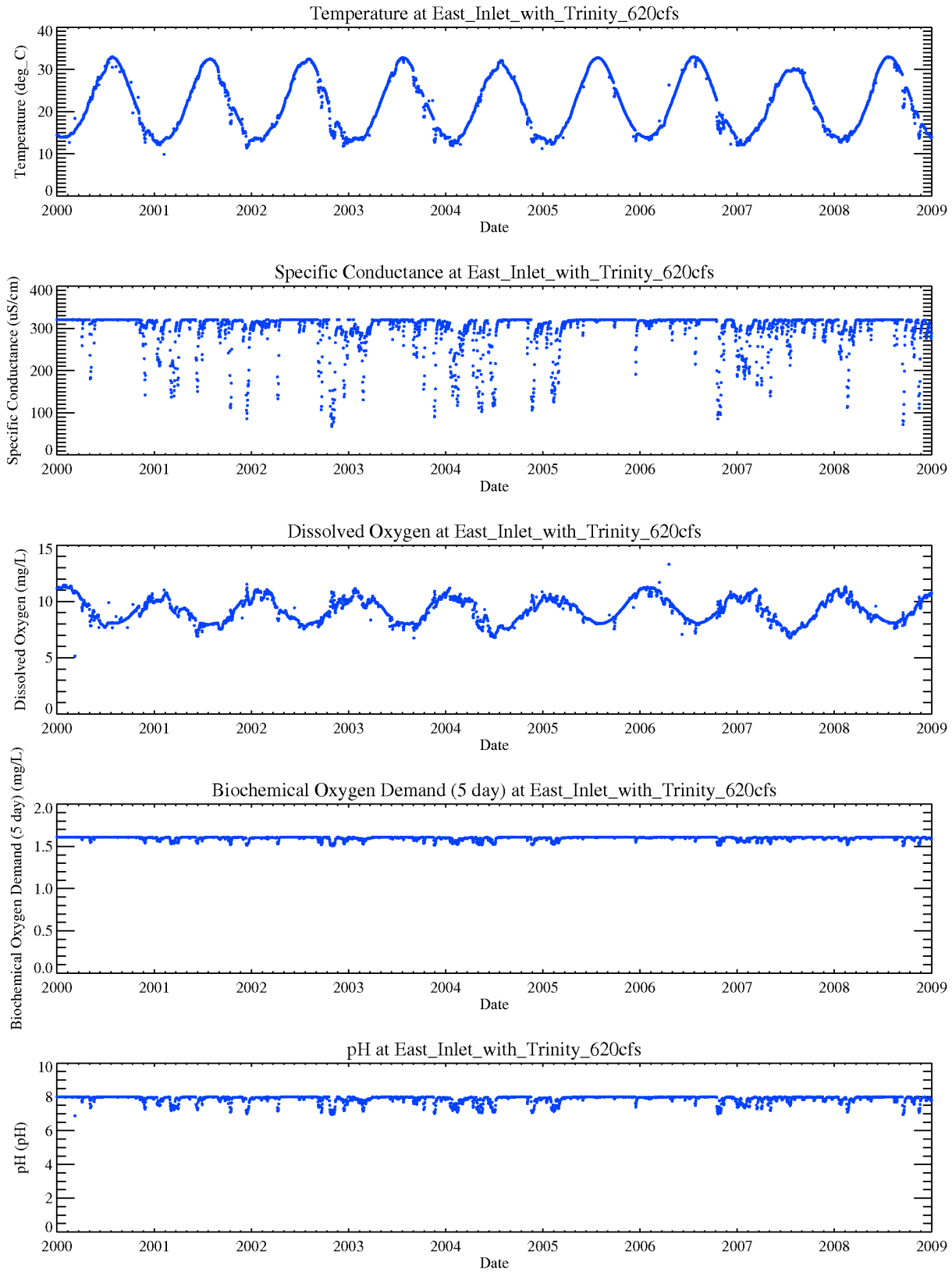

Figure 4.12 Calculated time series of temperature, specific conductance, dissolved oxygen, BOD_5 and pH at East Inlet (400MGD diversion) from 1/1/2000 to 1/1/2009.

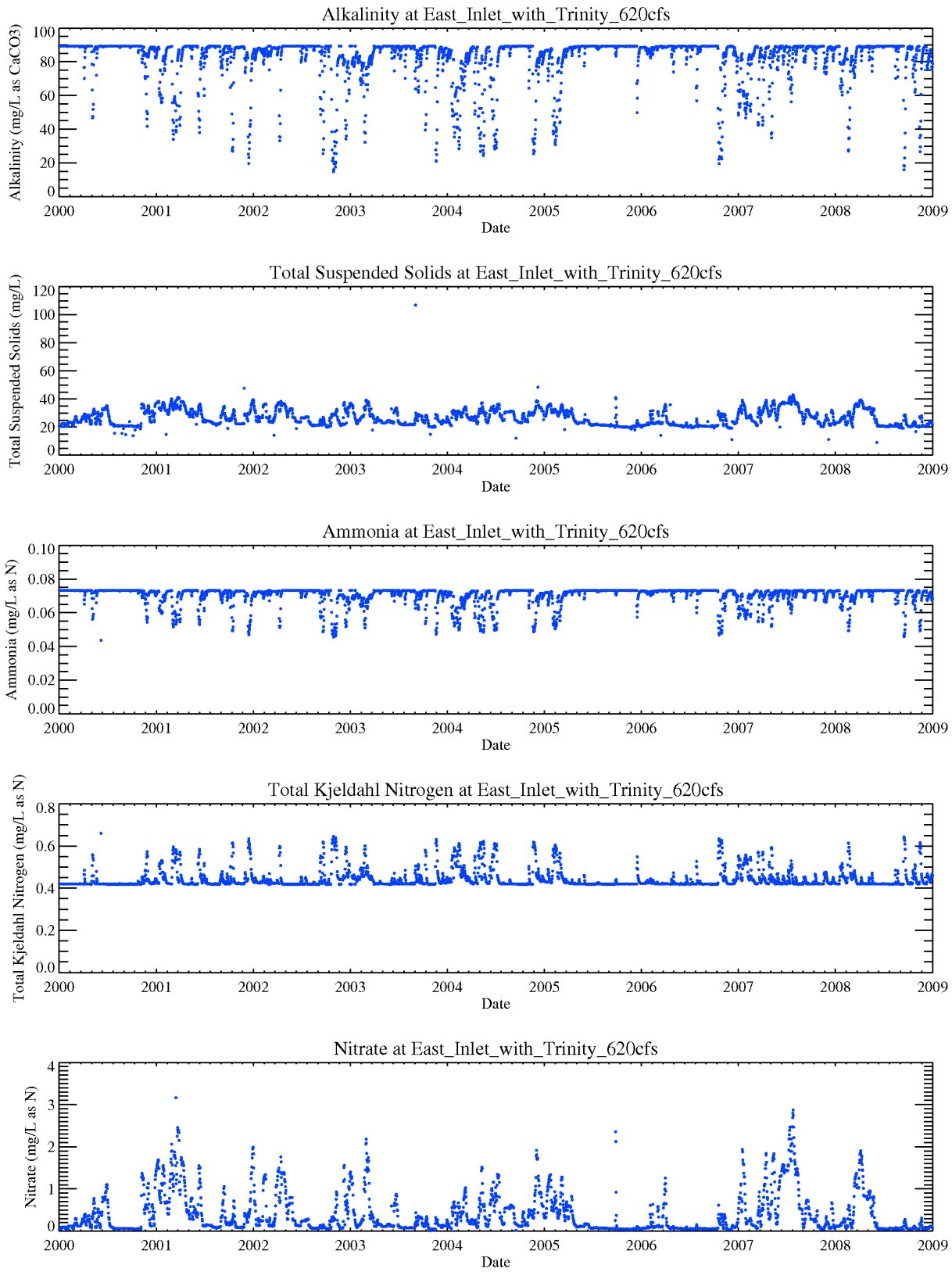

Figure 4.13 Calculated time series of alkalinity, total suspended solids, dissolved oxygen, ammonia, total kjeldahl nitrogen and nitrate concentrations at East Inlet (400MGD diversion) from 1/1/2000 to 1/1/2009.

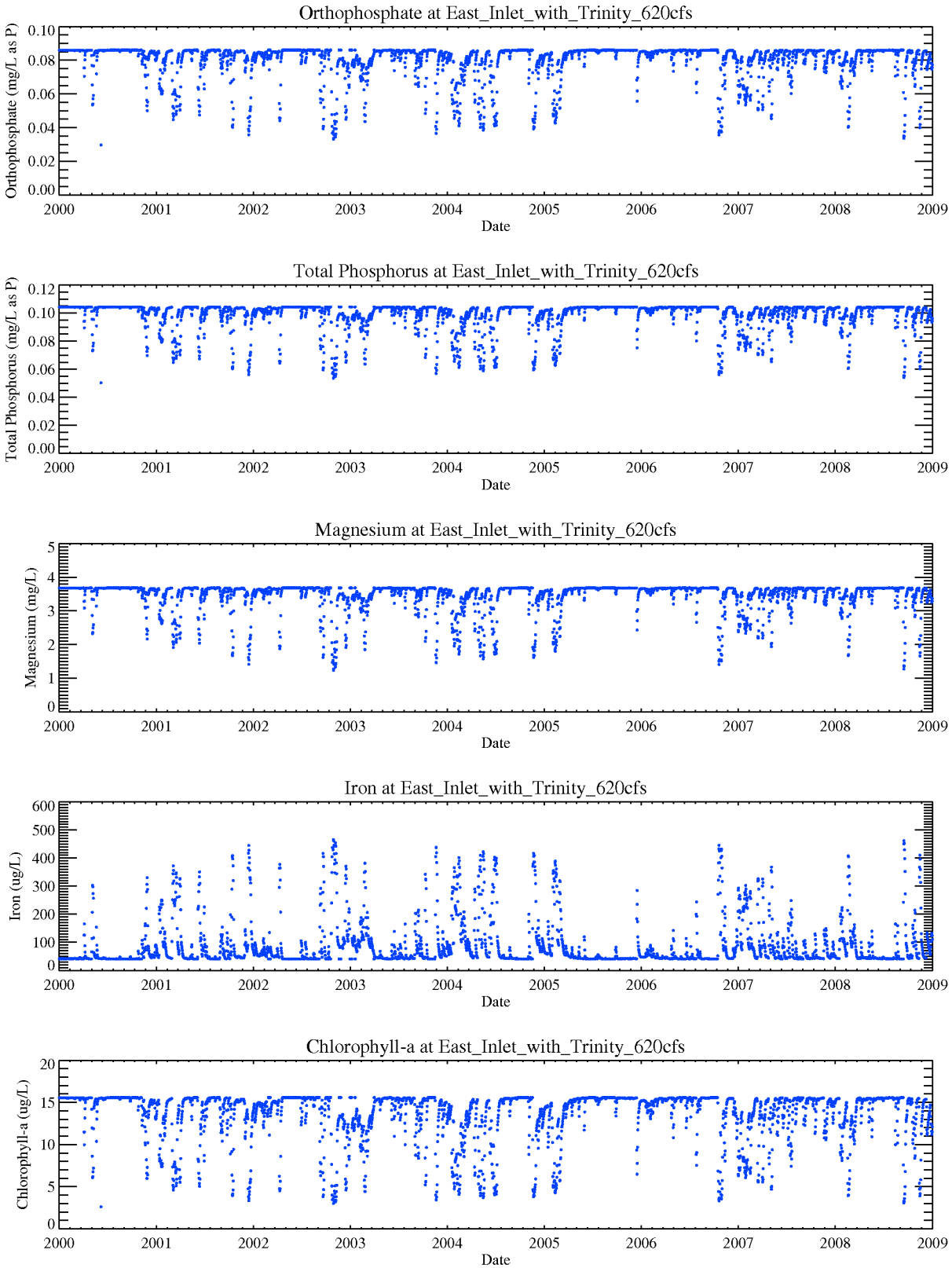

Figure 4.14 Calculated time series of orthophosphate, total phosphorus, magnesium, iron, chlorophyll-a concentrations at East Inlet (400MGD diversion) from 1/1/2000 to 1/1/2009.

5.0 EVALUATION OF HISTORICAL INFLOW PATTERNS AND IMPACTS TO THE LAKE

5.1 HISTORICAL INFLOW PATTERN WITHIN STUDY PERIOD

To understand the flow patterns within this period, a cumulative distribution of the total daily flow entering Lake Houston is plotted (see Figure 5.1). The total flow is calculated by summing the flows from the North, West and East inlets. These inlet flows are calculated by utilizing USGS streamflow data in Equations 4.1 to 4.3. The data are from the period between 1/1/2000 and 1/1/2009.

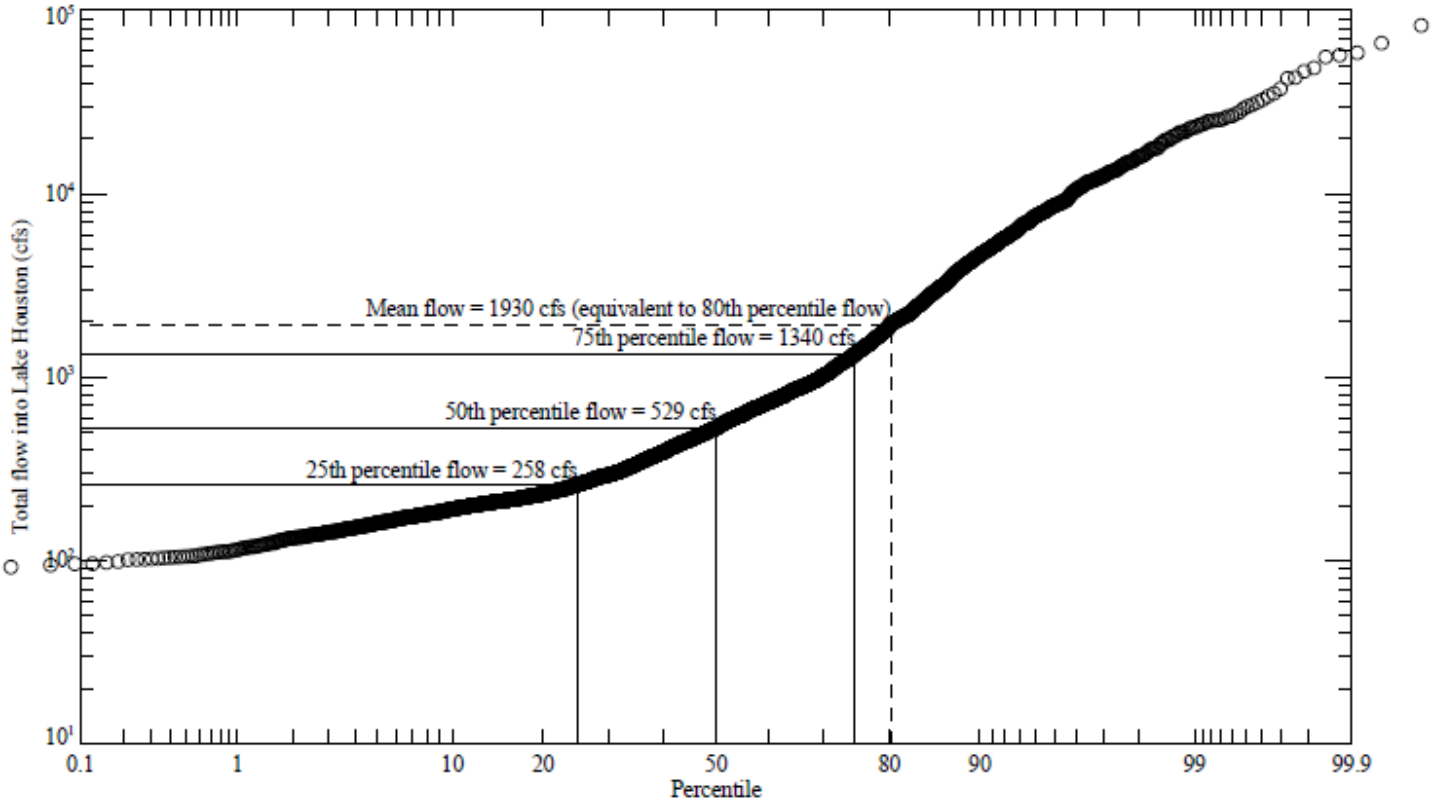

Figure 5.1 Frequency distribution of total daily flows entering Lake Houston (based on data from 1/1/2000 to 1/1/2009).

The highest daily flow into Lake Houston is 83,000 cfs (on 6/9/2001) and the lowest flow is 92 cfs (on 9/8/2000). The mean flow is 1,930 cfs and the median flow is 529 cfs. The 25th percentile flow is 258 cfs and the 75th percentile flow is 1,340 cfs. The distribution of the total flow spans a wide range with the maximum flow being three orders of magnitude greater than the minimum. The distribution is also positively skewed with most of the flows being significantly less than the mean.

To study the duration and frequency of hydraulic impacts, the following categories are used to classify the flows:

- Low flows are flows less than the 25th percentile flow; i.e., flows < 258 cfs;
- Normal flows are flows between the 25th percentile and the 75th percentile flows; i.e., 259 cfs ≤ flows < 1,340 cfs; and
- High flows are flows greater than or equal to the 75th percentile flows; i.e., flows ≥ 1,340 cfs.

Using the above definition, low flows are experienced 25% of the time over the entire study period, normal flows are experienced 50% of the time and high flows are experienced 25% of the time.

However, this distribution does not apply evenly to all the years. Predominantly high flow or low-flow conditons can occur in some years. This will be discussed in further detail in the next section.

5.2 DURATION AND FREQUENCY OF FLOW CONDITIONS

Figure 5.2 and 5.3 show the usage of above three classifications to show the duration and frequency of hydraulic impacts (or flow conditions). Figure 5.2 depicts the time series of total flow into Lake Houston. Due to the large range in flow values, the y-axis is in logarithmic scale and ranges from 100 to 100,000 cfs. The thresholds for the 25th percentile and 75th percentile flows are marked in red and blue, respectively.

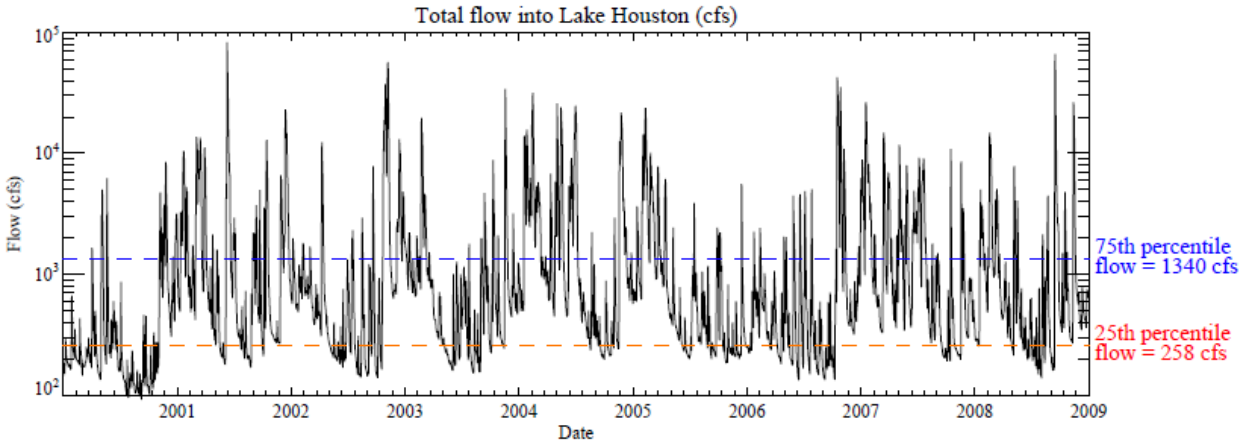

Figure 5.2 Time series of flows entering Lake Houston.

Figure 5.3 shows the classification of total flow into high, normal and low conditions. Blue bands show the days where the flow is high, green bands indicate normal flows and orange bands indicate low flows. Consecutive days of similar flow conditions are grouped into periods which are then analyzed. The following describes the statistics of these periods.

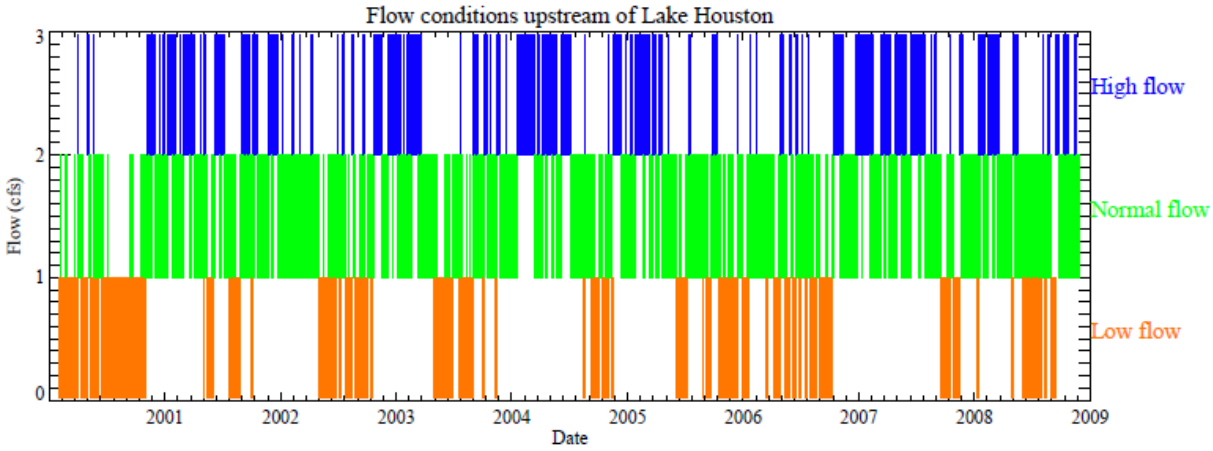

Figure 5.3. Time series of flow conditions entering Lake Houston

The total number of high-flow periods between 1/1/2000 and 1/1/2009 is 116. The average length of a high-flow period is 7.1 days. The longest period of high flow is 55 days (from 1/17/2004 to 3/11/2004) during which the average flow was 7,400 cfs.

The total number of normal-flow periods is 204. The average length of a normal-flow period is 7.9 days. The longest period of normal flow is 45 days (from 11/28/2007 to 1/11/2008) during which the average flow experienced was 505 cfs.

The total number of low-flow periods is 100. The average length of a low-flow period is 8.1 days. The longest period of low flow is 69 days (from 7/6/2000 to 9/12/2000) during which the average flow experienced was 130 cfs.

The annual count of the number of days in each flow condition is shown in Table 5.1. The highest number of low-flow days (234 days) occurred in 2000. The highest number of high-flow days (147 and 144 days) occurred in 2004 and 2007, respectively. The highest number of normal-flow days (220 and 214) occurred in 2003 and 2008, respectively.

Table 5.1 Number of low, high and normal-flow days for the years 2000 to 2008.

Year	Count of high-flow days	Count of low-flow days	Count of normal-flow days
2000	38	234	94
2001	129	45	191
2002	79	99	187
2003	66	79	220
2004	147	38	181
2005	77	93	195
2006	56	118	191
2007	144	41	180
2008	86	65	214

Based on this analysis, similar flow conditions typically last for an average of 7 days before shifting to a different condition. Low-flow conditions are known to last as long as 69 days while high-flow conditons are known to last as long as 55 days. Thus, flow conditions can vary significantly from year to year.

5.3 IMPACT OF INFLOW HISTORICAL PATTERNS ON WATER SURFACE ELEVATION

The effects of the flow conditions on lake levels from 2000 to 2008 are shown in Figure 5.4. The lake levels are measured at USGS gage 08072000 (Lake Houston near Sheldon, TX) and have units of feet above mean sea level. The horizontal dashed line indicates the spillway elevation of 44.5 ft above mean sea level.

From the figure, it can be seen that prolonged periods of low-flow conditions have the highest and the most persistent impacts on water surface elevation. In 2000, low-flow conditons led to extended periods of low lake levels throughout the spring and the fall. At the lowest point, water surface elevation dropped to 41 feet above mean sea level (or 3.5 feet below the spillway). Note that sharp drops and rises in lake levels are experienced in October 2004 and September 2005. These are not caused by hydrological conditions but by dam release flows directed by the COH for reasons explained in Section 3 of this report.

The impacts of high-flow conditions on lake levels are much shorter than that of low-flow conditions. The highest lake level recorded is 48.7 ft (4.2ft above spillway) on June 10th, 2001. The corresponding total flow was 58,700 cfs on the same day and 83,000 cfs on the preceding day. High-flow conditons tend not to have as drastic and long-term effect on lake levels because the spillway allows excess flows to

pass over the dam and that preventive measures such as drawdowns are implemented by the COH in anticipation of high flow events to prevent flooding.

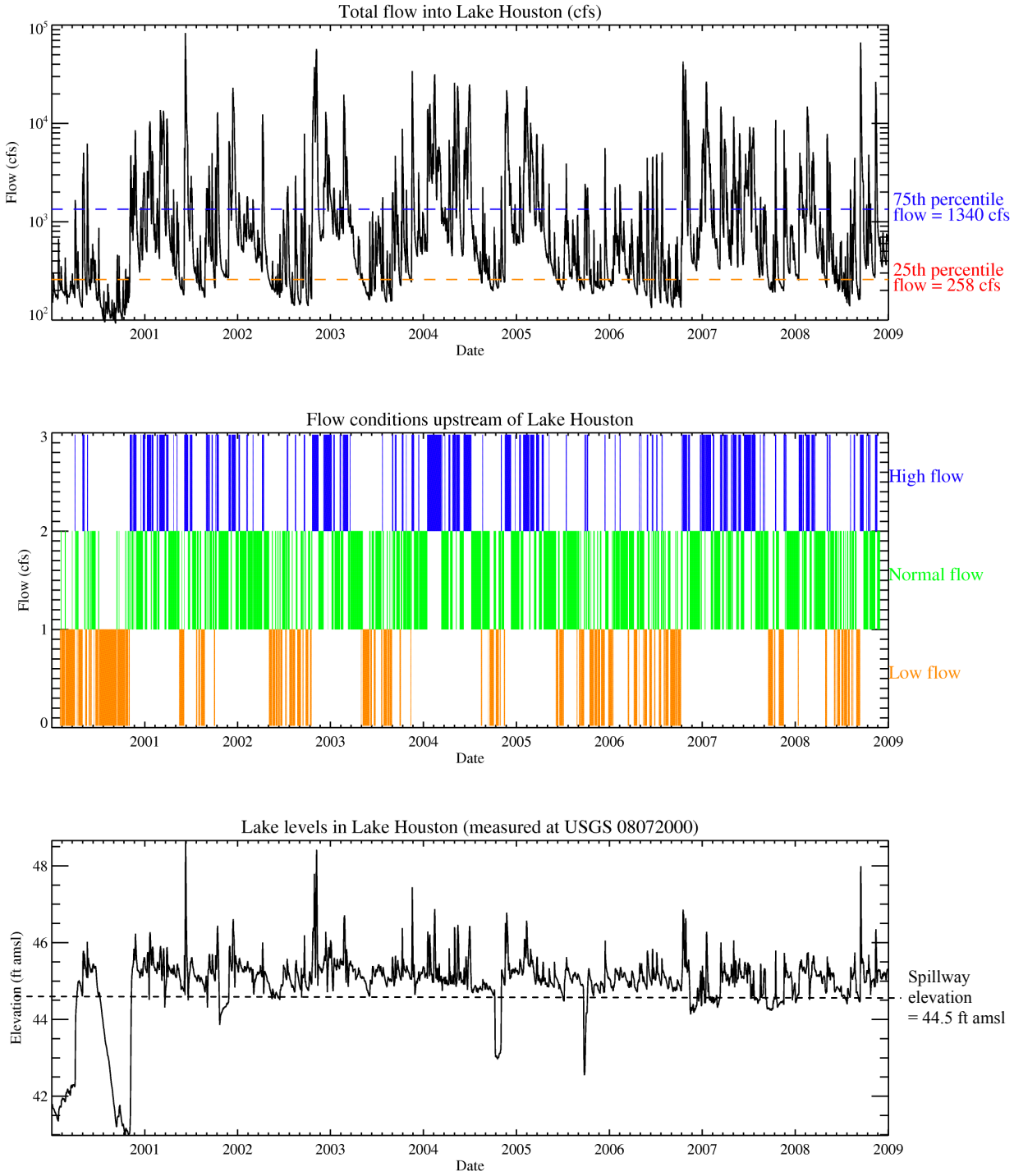

Figure 5.4 Duration and frequency of high, normal and low flows and their impact on lake levels.

6.0 MODELING APPROACH

The modeling utilized in this project includes the Environmental Fluid Dynamics Code (EFDC) to characterize the hydrodynamics of the lake coupled with the Water Analysis Simulation Program (WASP) to model the interactions of water quality constituents with the environment.

Environmental Fluid Dynamics Code (EFDC)

The Environmental Fluid Dynamics Code (Tetra Tech, 2002; Hamrick, 1992), also known as EFDC–Hydro, is a state-of-the-art hydrodynamic model that can be used to simulate the circulation and transport of material in complex aquatic systems in one, two, and three dimensions. The model has evolved over the past two decades to become one of the most widely used and technically defensible hydrodynamic models in the world. The physics of the EFDC model and many aspects of the computational scheme are equivalent to the widely used Blumberg-Mellor model and U. S. Army Corps of Engineers' Chesapeake Bay model. The hydrodynamic model is based on the three-dimensional shallow water approximation of the Navier-Stokes equation and includes dynamically coupled salinity and temperature transport. EFDC uses stretched, or sigma, vertical coordinates and either Cartesian or curvilinear, orthogonal horizontal coordinates to represent the physical characteristics of a water body. EFDC solves three-dimensional, vertically hydrostatic, free surface, turbulent-averaged equations of motion for a variable-density fluid. Dynamically-coupled transport equations for turbulent kinetic energy, turbulent length scale, salinity and temperature are also solved. The EFDC model allows for drying and wetting in shallow areas by a mass conservation scheme.

In the Lake Houston study, EFDC was used to simulate (1) water surface elevation (m); (2) velocity (m/s); (3) velocity direction; (4) flow rate (m^3/s crossing a cell-to-cell boundary); and (5) temperature. EFDC outputs were used as inputs to WASP.

Water Analysis Simulation Program (WASP)

The Water Quality Analysis Simulation Program (WASP7) is an enhancement of the original WASP (Di Toro et al., 1983; Connolly and Winfield, 1984; Ambrose, R.B. et al., 1988). This model helps users interpret and predict water quality responses to natural phenomena and manmade pollution for various pollution management decisions. WASP is a dynamic compartment-modeling program for aquatic systems, including both the water column and the underlying benthos. WASP allows the user to investigate 1, 2, and 3 dimensional systems, and a variety of pollutant types. The time varying processes of advection, dispersion, point and diffuse mass loading and boundary exchange are represented in the model. WASP also can be linked with hydrodynamic and sediment transport models that can provide flows, depths, velocities, temperature, salinity and sediment fluxes.

WASP has been used to examine eutrophication of Tampa Bay, FL; phosphorus loading to Lake Okeechobee, FL; eutrophication of the Neuse River Estuary, NC; eutrophication Coosa River and Reservoirs, AL; PCB pollution of the Great Lakes, eutrophication of the Potomac Estuary, kepone pollution of the James River Estuary, volatile organic pollution of the Delaware Estuary, heavy metal pollution of the Deep River, North Carolina, and mercury in the Savannah River, GA.

In the Lake Houston study, WASP was used to simulate water quality parameters such as (1) DO (mg/L); (2) nitrogen species concentration (mg/L); (3) phosphorus species concentration (mg/L); (4) TSS concentration (mg/L); and (5) CBOD (mg/L).

6.1 SELECTION OF SIMULATION PERIODS

Because EFDC and WASP model complex physical processes, the computational time required to complete a simulation can often be long. Estimation of one year of water quality conditions in Lake Houston requires a total of almost 20 hours of computation time – in which 8 to 10 hours are used to simulate hydrodynamic conditions, and another 8 to 10 hours are used to simulate water quality conditions. Therefore, it is impractical to run the model for the entire nine-year study period and evaluate different management scenarios. Instead, three one-year periods characterized by predominately low-flow, high-flow or normal-flow days were selected to evaluate the lake behavior under different flow conditions. The three periods selected are listed below:

1) 1/1/2000 to 1/1/2001– low-flow conditons;
2) 1/1/2004 to 1/1/2005 – high-flow conditons; and,
3) 1/1/2008 to 1/1/2008 – normal-flow conditons.

6.2 CALIBRATION AND VALIDATION APPROACH

The WASP and EFDC models were calibrated under 2000, 2004 and 2008 conditions to test the robustness of the models under low, high and normal-flow conditons. After validation, the models were run under different diversion and drawdown scenarios to evaluate water quality impacts caused by the Luce Bayou Interbasin Transfer Project.

6.2.1 EFDC calibration approach

The EFDC hydrodynamic model was calibrated in the following manner:

1. The model was calibrated to measured water surface elevation data. Fitting the water surface elevation ensures proper accounting of the water budget and inclusion of all major sinks and sources to the lake.
2. The model was calibrated to the temperature data. Fitting the model to temperature ensures that the mixing of intrinsic properties of the water is simulated properly.

Ideally, the model calibration would be completed by fitting the model to measured current velocities in the lake. However, current velocities were not monitored in Lake Houston and no tracer studies are known to have been conducted. EFDC calibration therefore focused on improving model simulation of temperature and water surface elevations. The EFDC calibration process and the EFDC model parameters adjusted during calibration are discussed further in Section 7 of this report.

6.2.2 WASP calibration approach

The WASP water quality model was calibrated following the sequence outlined in published WASP materials (USEPA, 2009):

1. Dissolved oxygen and ultimate carbonaceous biological oxygen demand (CBOD) parameters were calibrated to ensure that basic oxygen mechanisms were properly described.
2. Ammonia, nitrate and organic nitrogen parameters were calibrated to ensure that the basic eutrophication and nitrification processes were adequately defined.
3. Third, organic phosphorus and phytoplankton phosphorus parameters were adjusted to ensure that more complicated eutrophication processes and algal interactions were properly accounted.
4. Finally, algal growth, death, respiration, and settling rates were adjusted to fit the phytoplankton data.

The WASP calibration process and model parameters that are adjusted during the calibration are discussed in further detail in Section 7 of this report.

7.0 HYDRAULIC/HYDRODYNAMIC MODEL DEVELOPMENT

7.1 MODEL GRID DESIGN

A Cartesian grid was developed for the EFDC and WASP models to represent Lake Houston. The grid consists of more then 500 cells divided into two vertical layers. The two vertical layers allow the evaluation of deep and shallow water quality. The grid is designed to adequately represent the complex underlying bathymetry of Lake Houston while achieving economy in computer run time. Because Lake Houston is an in-channel impoundment (USGS, 2000) the lake bottom consists of deep areas along the original river channel and shallower areas on the inundated parts of the original banks. To capture this variation in the lake cross-section at least six cells span the width of the lake in the main body. Lake geometry in the northern portion of the lake is complex because the three inlets merge into the main body of the lake. To capture the complexity, higher grid resolution is appropriated to the northern portion than the southern portion. The grid is curved slightly to follow the bend of the lake, but a fully curvilinear, orthogonal grid matched exactly to the lake shoreline was not created for this project. Development of a more detailed grid for further refinement may be beneficial in future work.

Elevation and depth values were assigned to the cells of the Lake Houston model grid using bathymetry data collected by the TWDB (TWDB 2003). A map of the grid is shown in Figure 7.1.

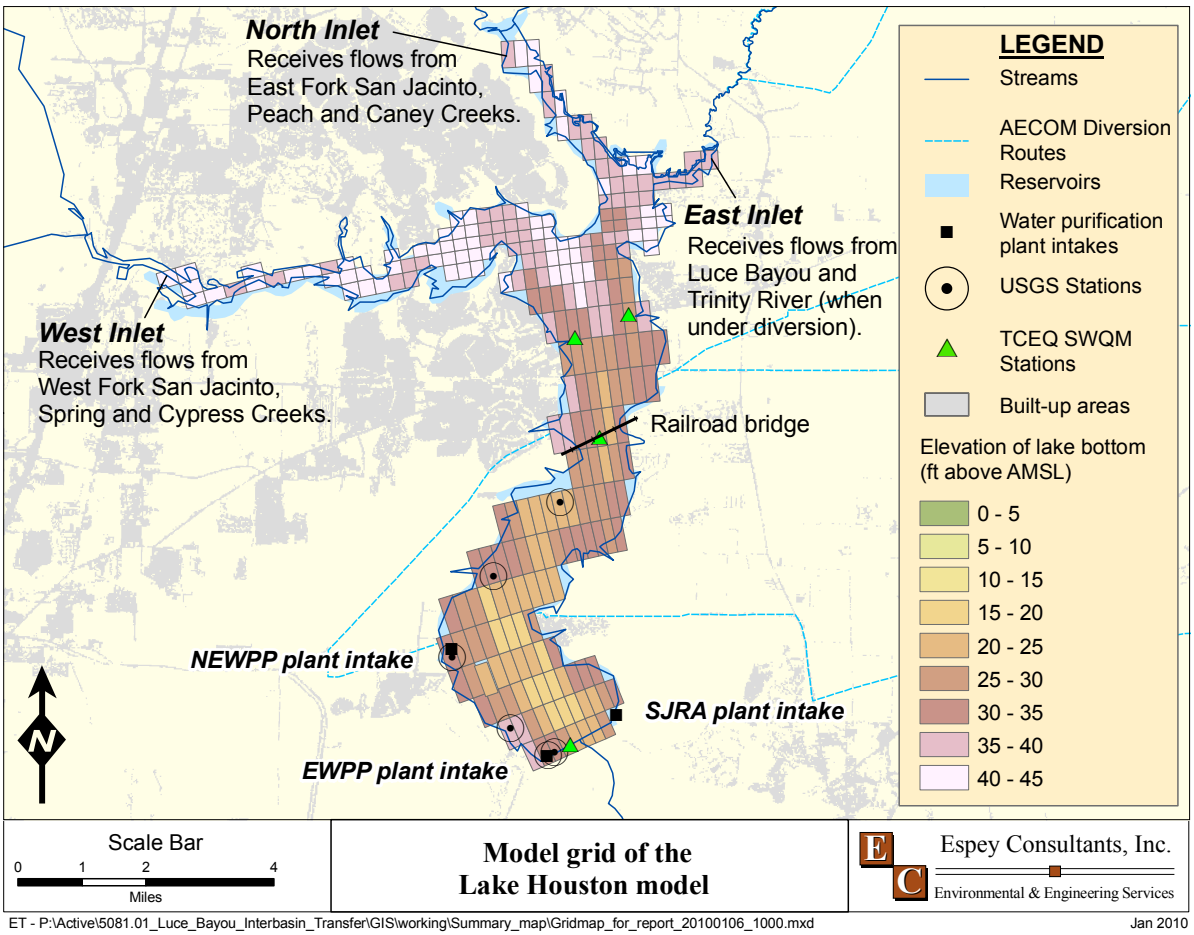

Figure 7.1 Model grid of the Lake Houston model.

7.2 EFDC INPUT DATA

Table 7.1 lists the specific input data for the Lake Houston model and respective units.

Table 7.1 List of EFDC Model Inputs

EFDC Model Inputs	Units
Bathymetry	m
Inflows	m^3/s
Pumpage	m^3/s
Water Surface Elevation	m
Wind Speed and Direction	m/s and degree
Temperature	°C
Precipitation	m/s
Evaporation	m/s
Solar Radiation	W/m^2
Rating Curves at Control Structures	m^3/s per m

Inflows into the lake were calculated using the methodology outlined in Section 5.1 and applied to the cells relating to the West, North and East Inlets (see Figure 7.1). Pumpage rates obtained from the NEWPP, EWPP and SJRA plants were applied to the cells closest to their intakes. Spillway flows from the Lake Houston dam are calculated using rating equations obtained from Dr. Ruben Solis of the TWDB (see Equations 7.1 and 7.2). For lake elevation greater than 44.8 ft above mean sea level amsl, spillway discharge was calculated using Equation 7.1.

$$Q(y) = a(y - 44.5)^2 + b(y - 44.5), \quad y>44.8 \text{ ft amsl} \qquad \text{Equation 7.1}$$

where
Q = spillway discharge, ft^3/sec,
y = lake elevation, ft amsl (NGVD 29)
a = 5418.31 ft/sec, and
b = -1336.29 ft^2/sec.

Below elevation of 44.8 ft amsl, spillway discharge was calculated using Equation 7.2.

$$Q(y) = c\,(y - 44.5), \quad 44.5 < y < 44.8 \text{ ft amsl} \qquad \text{Equation 7.2}$$

where
Q = spillway discharge, ft^3/sec,
y = lake elevation, ft,
c = 86.76 ft^2/sec

The rating equations were used to calculate outflows through the middle five cells on the southern boundary of the model grid. Each cell produced 1/5 of the total discharge, Q(y), over the spillway.

Atmospheric forces such as wind, precipitation, evaporation and solar radiation were obtained from the meteorological data sources mentioned in Section 3.4 and applied uniformly over the model grid.

7.3 CALIBRATION OF EFDC MODEL

7.3.1 Calibration parameters

The EFDC model was calibrated using data collected from 2005. The model was first calibrated to water surface elevations measured at USGS gage 08072000, located closest to the spillway. The model was then calibrated to temperature data measured at SWQM stations 11211, 11212, 11208 and 11204.

The EFDC model parameters that affect temperature and water budget are identified in Table 7.2. These model parameters are internal constants used in the equations that estimate water budget, circulation and mixing. Most values are obtained from the literature since values specific to Lake Houston are not available. These values were adjusted during calibration within the common range of values reported to fit the model results to observed data. Table 7.2 provides the common range of values for each parameter and the final value used.

Table 7.2 EFDC model parameters for Lake Houston

EFDC Model Parameters	Units	Common range of values	Value used in EFDC model
Dispersion Coefficient	m^2/sec	0.01 to 2	1
Fast Scale Solar Radiation Attenuation Coefficient	1/m	1 to 7	7
Slow Scale Solar Radiation Attenuation Coefficient	1/m	0 to 1	0
Fraction of Fast Scale Solar Radiation Attenuated	NA	0 to 1	1
Convective Heat Coefficient between Bed and Bottom Water Layer	NA	0 to 1.0E-6	5.0E-07
Heat Transfer Coefficient between Bed and Bottom Water Layer	m/sec	1.0E-9 to 1.0E-6	9.0E-07
Depth or Thickness of active bed temperature layer	m	1 to 5,000	1,000

7.3.2 Calibration results

For the EFDC model, a test calibration was performed first on the 2005 data and then the calibrated parameters were applied to the three simulation years for validation. Figure 7.2 shows the results of the water surface elevation calibration for 2005. The simulated water surface elevations from the model grid cell nearest the spillway are plotted with water surface elevations measured at USGS gage 08072000. The model results compare well to the measured elevations. The rises and falls in measured lake levels are closely mimicked by the model within a margin of ± 0.2 m (0.7 ft).

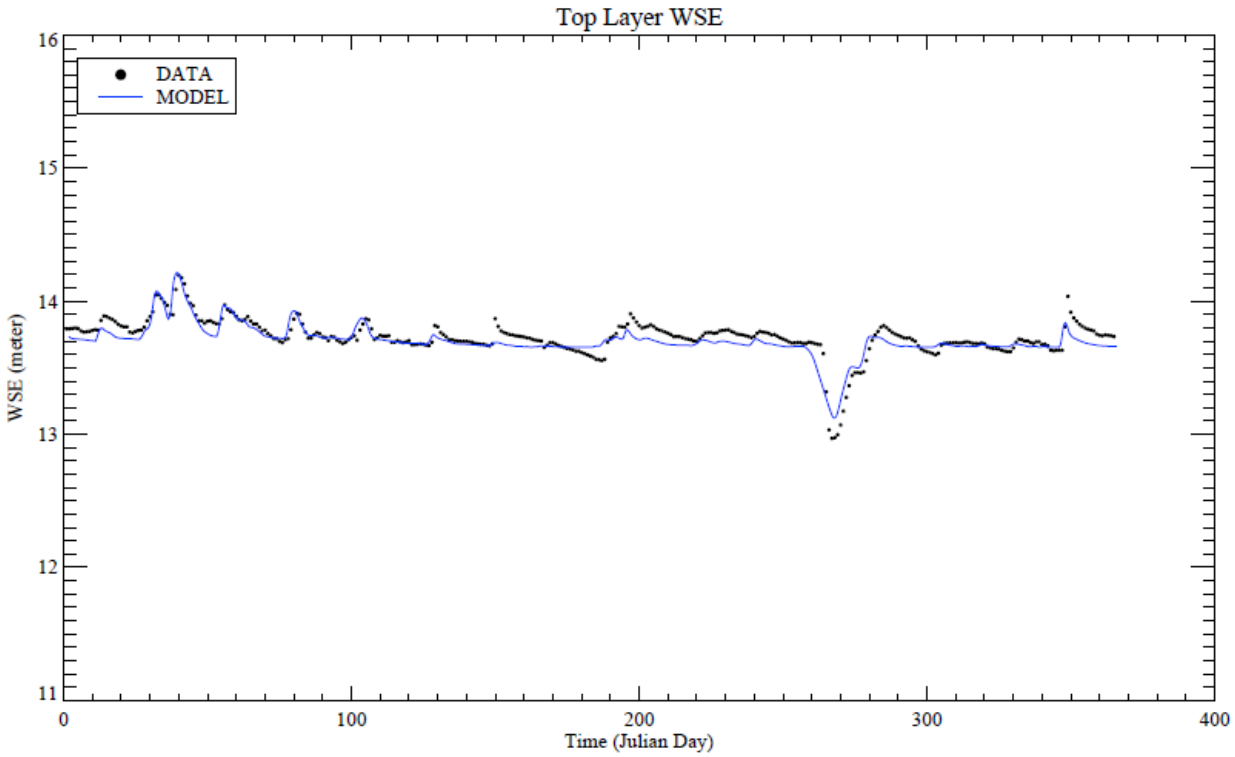

Figure 7.2 Model-predicted and measured water surface elevations for 2005

Figure 7.3 shows the results of the temperature calibration for 2005 at SWQM stations 11212, 11211, 11208 and 11204. In the graphs within the figure, temperature measurements collected at each SWQM station are compared to the simulated temperature at the corresponding grid cell. At all four stations, model-predicted temperatures compared well with the measured temperature showing that the EFDC model simulated mixing in the lake appropriately.

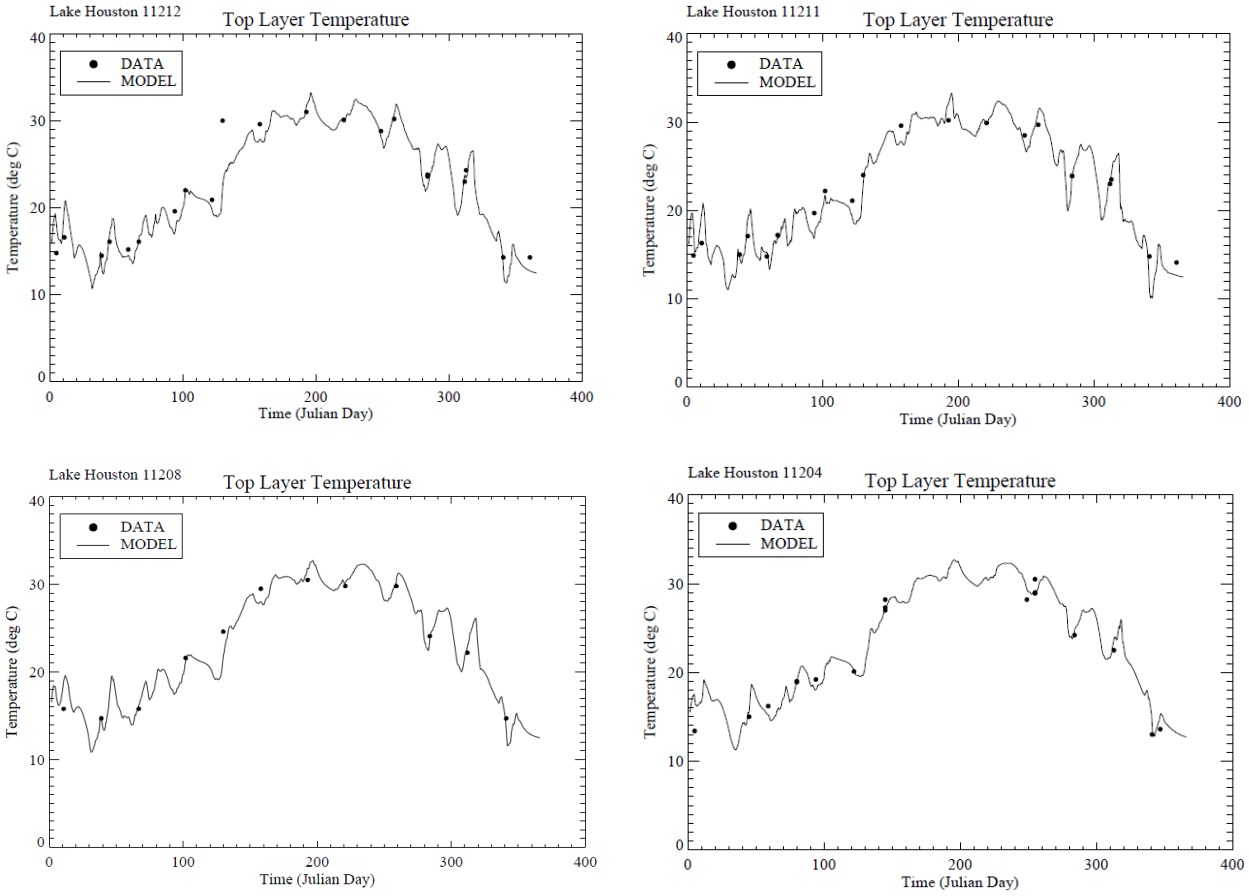

Figure 7.3 Model-predicted and measured temperatures for 2005.

A tool for visualizing the water circulation patterns in the lake was developed and applied to the 2005 calibration run. The complete set of water circulation patterns for 2005 is available in Appendix C. As an example, Figure 7.4 shows the model-predicted water velocity vectors in the top and bottom layers of the lake on 3/9/2005. It also shows the model-predicted water surface elevation of the cells with darker colors indicating higher water surface elevation and lighter colors indicating lower elevation. In the absence of velocity measurement and dye study data in the lake, these visualizations allow the qualitative comparison of the model results with external stimuli such as wind speed, inflow and diversion rates. For the 2005 calibration run, the circulation patterns predicted by EFDC respond appropriately to the external stimuli.

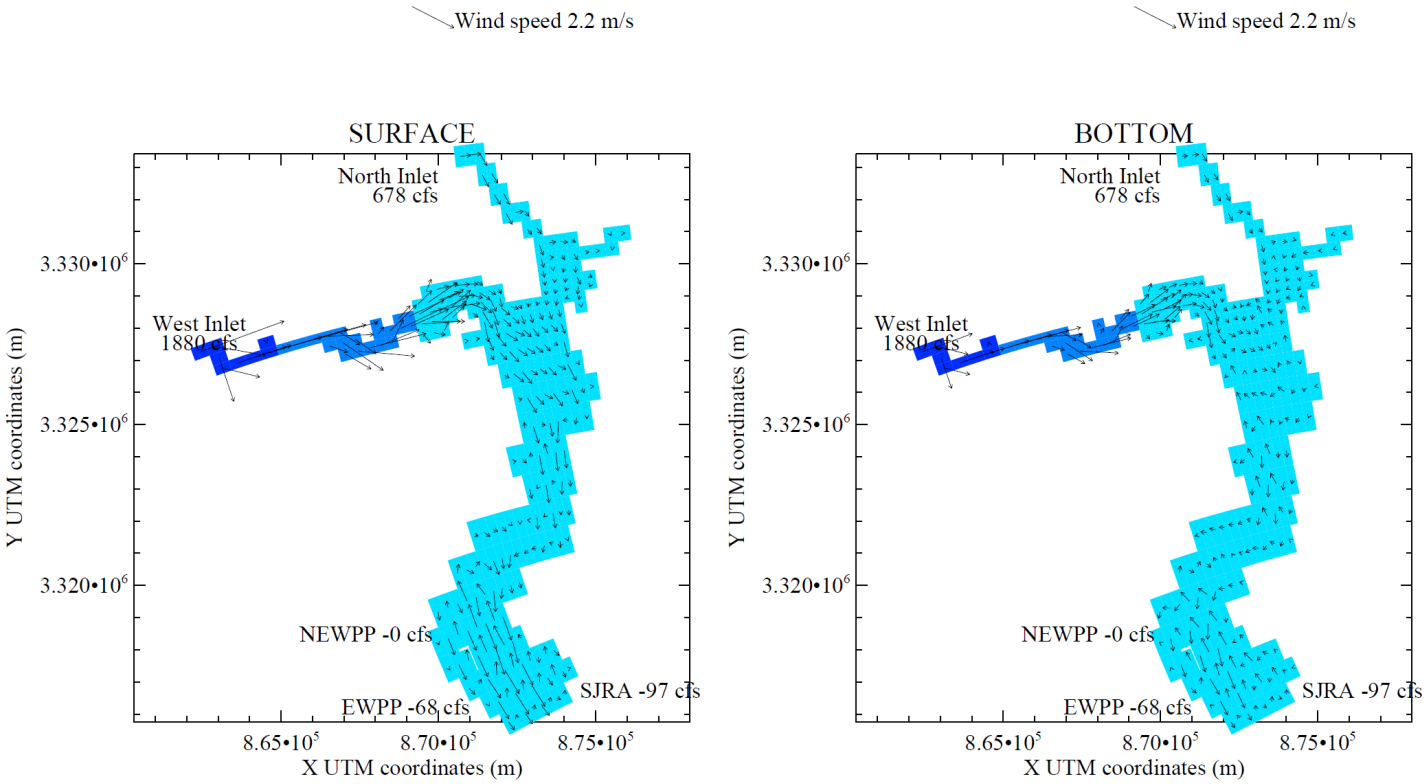

Figure 7.4 Water surface elevations and velocity vectors (at surface and bottom layers) for 3/9/2005.

7.4 VALIDATION OF EFDC MODEL

The calibrated model was validated against water surface elevation and temperature data from 2000, 2004 and 2008 to test the model's robustness under low-flow, high-flow and average-flow conditions. Figures 7.5, 7.6 and 7.7 show the validation results for water surface elevation.

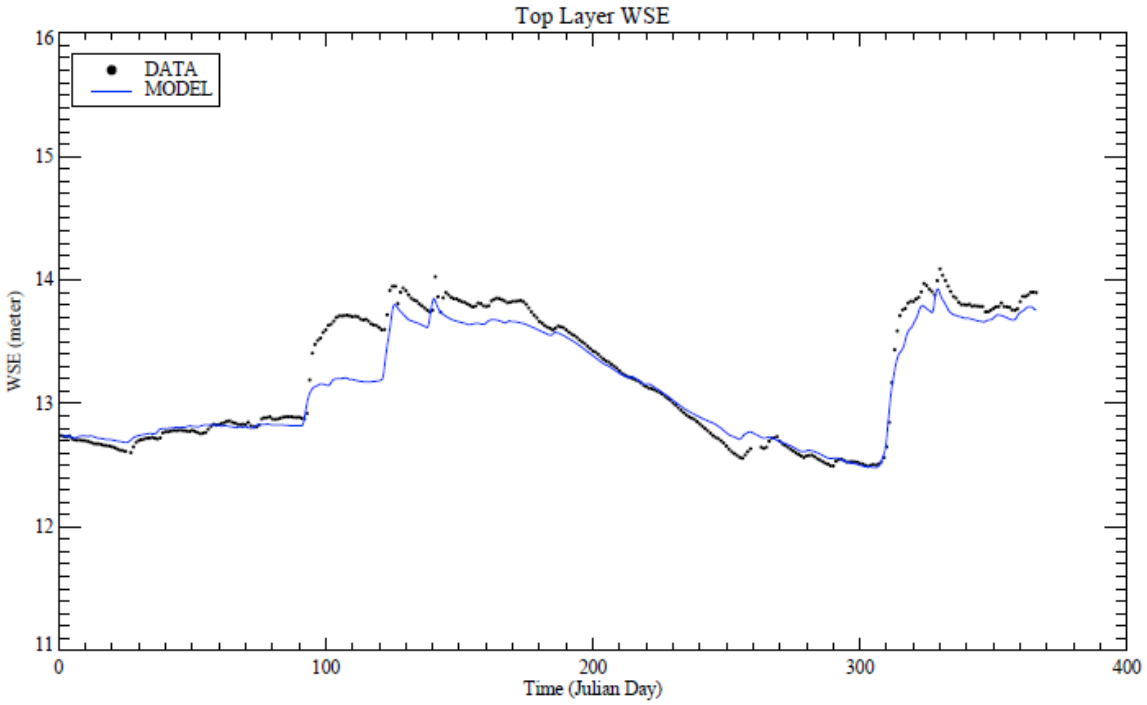

Figure 7.5 Water surface elevations predicted by hydrodynamic model for 2000.

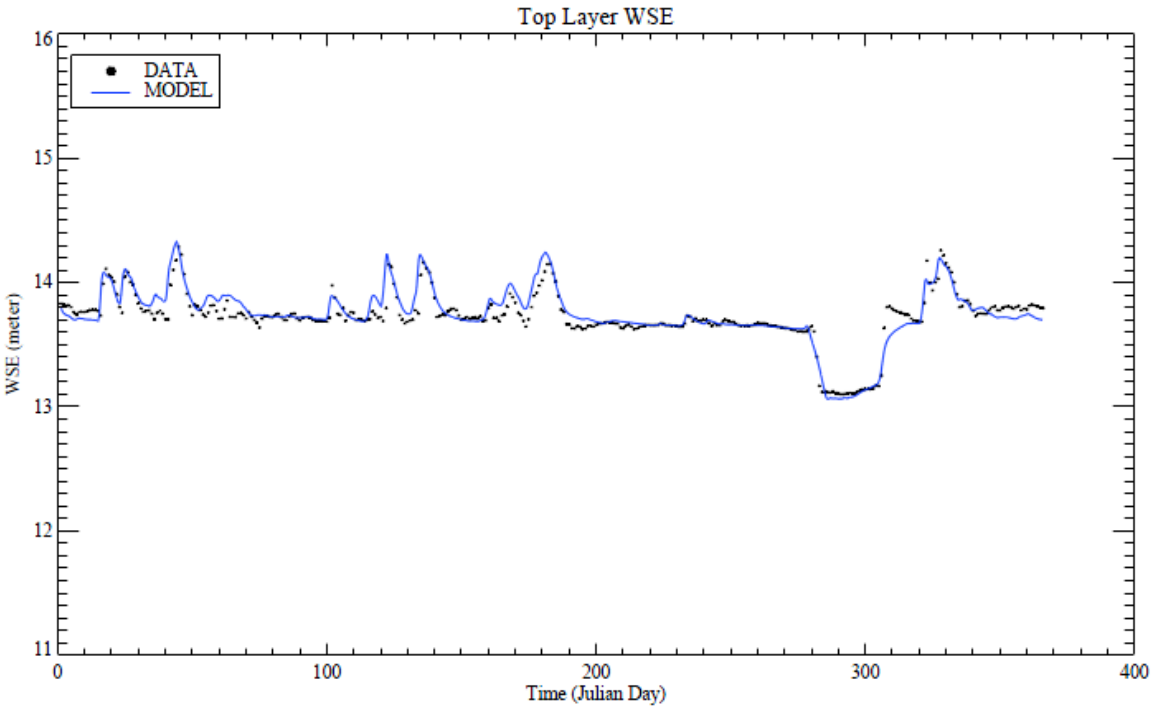

Figure 7.6 Water surface elevations predicted by hydrodynamic model for 2004.

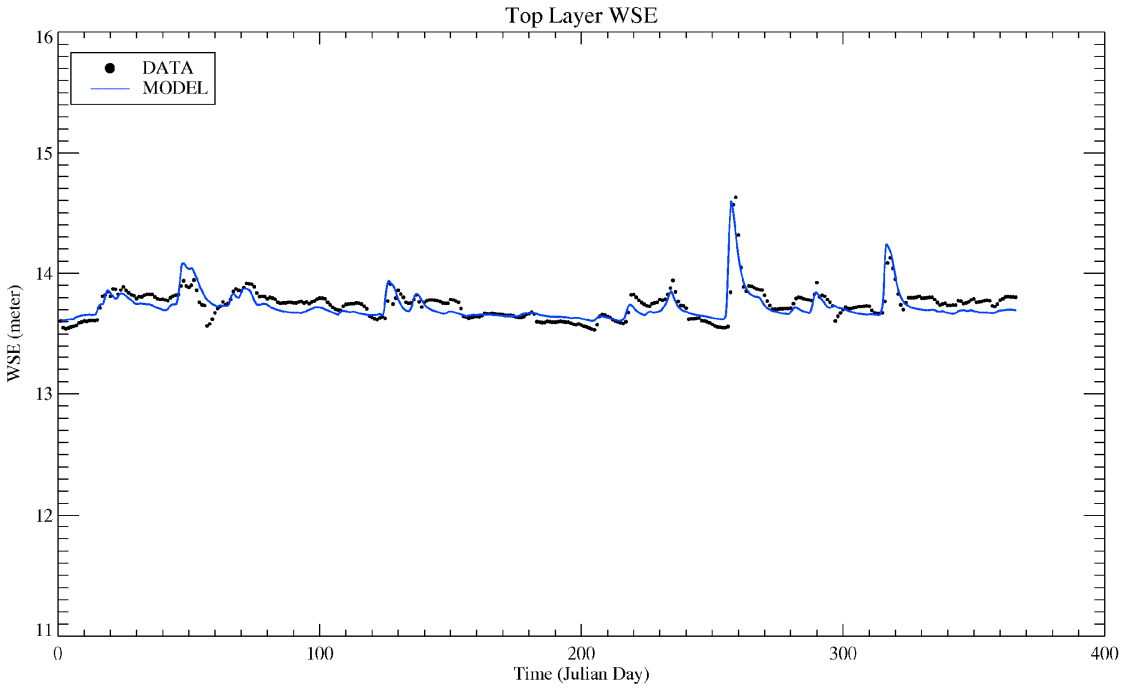

Figure 7.7 Water surface elevations predicted by hydrodynamic model for 2008.

Simulated water surface elevations for all three years matched the measured elevations very well and were within a margin of ±0.2 m (or 0.7 ft). The only exception was in 2000 between ordinal days 90 to 120 (encompassing the month of April) when the model-simulated elevations were about 0.6 m (1.9 ft) lower than the measured elevations. This difference may be caused by dam release flows. Unfortunately, dam operation records from the City of Houston are only available from 2005 forward, so the cause of the discrepancy could not be verified at the writing of this report. Simulated temperatures for the three years correspond well with data measured at the four SWQM stations. Thus, validation results show that the calibrated EFDC hydrodynamic model performs well under high-flow, low-flow and average flow conditions.

Historical water movement patterns for 2000, 2004 and 2008 were estimated using the EFDC model. Visualizations of these patterns can be found in Appendix C.

8.0 HYDRAULIC/HYDRODYNAMIC ASSESSMENT

8.1 DEFINITION OF HYDRODYNAMIC SCENARIOS

The purpose of the hydrodynamic model development in this project is to evaluate:

- water movement related to the diversion of 400 MGD of Trinity River water;
- water movement related to differing water levels dictated by reservoir operations, i.e. drops in water surface elevation of 1, 2, 3 and 5 feet; and,
- water surface elevation impacts by historical inflow patterns (i.e. low-flow, high-flow and average-flow conditions).

For each of the three simulation years, 2 diversion scenarios were evaluated. Within each of diversion scenario, five water surface elevation scenarios (drop in 0, 1, 2, 3 and 5 ft elevation) were examined. This combination of conditions results in a total of 30 scenarios evaluated using the EFDC model. A summary of the scenarios is presented in Table 8.1.

Table 8.1 Summary of scenarios for EFDC hydrodynamic evalauation

Year	400 MGD Luce Bayou Diversion?	Drop in WSE (ft)				
2000 (low-flow)	Yes	0	1	2	3	5
	No	0	1	2	3	5
2004 (high-flow)	Yes	0	1	2	3	5
	No	0	1	2	3	5
2008 (normal-flow)	Yes	0	1	2	3	5
	No	0	1	2	3	5

Lake drawdowns were implemented in the model by varying the crest elevation at the spillway. Lowering the crest elevation allowed more water to pass over the top of the dam – thereby maintaining a lower water surface elevation. At 0 ft drawdown, the crest elevation was set at 44.5 ft amsl (13.56 m amsl). At 1 ft drawdown, the crest elevation was set at 43.5 ft amsl (13.26 m amsl), at 2ft drawdown, the crest elevation was lowered to 42.5 ft amsl (12.95 m) and so on and so forth.

8.1.1 Changes in model grid with drawdown

Dropping the water surface elevation causes some grid cells in shallower areas of Lake Houston to become dry. Although EFDC has methods of handling wetting and drying during a simulation, prolonged dry periods can cause the model to become numerically unstable and terminate the simulation prematurely. To alleviate this problem, grid cells that remain dry throughout the simulation were removed from the grid. For scenarios with no lake drawdown, the simulations were conducted using the original grid (Figure 6.1) containing only cells that are submerged under normal pool elevation (i.e. the bottom elevation of all cells are lower than 44.5 ft amsl. For the drawdown scenarios, cells having bottom elevations higher than the specified water surface elevation of the lake were removed from the grid. The maximum grid cell bottom elevation for each drawdown scenario are listed in Table 8.2. In areas of the model where boundary cells were removed using this process, inlet flows were applied to the new boundary cells.

Table 8.2 Summary of scenarios for EFDC hydrodynamic evalauation

Lake Drawdown (ft)	Maximum Cell Bottom Elevation (ft amsl)	Maximum Cell Bottom Elevation (m amsl)
0	44.5	13.56
1	43.5	13.26
2	42.5	12.95
3	41.5	12.65
5	39.5	12.04

Figure 8.1 illustrates how the model grid changes as the different water surface elevation drops were applied. At the maximum drawdown of 5 ft, most of the cells representing the West and North inlets have been removed from the grid. In addition, a shallow region in the north-central part of the lake has also been removed.

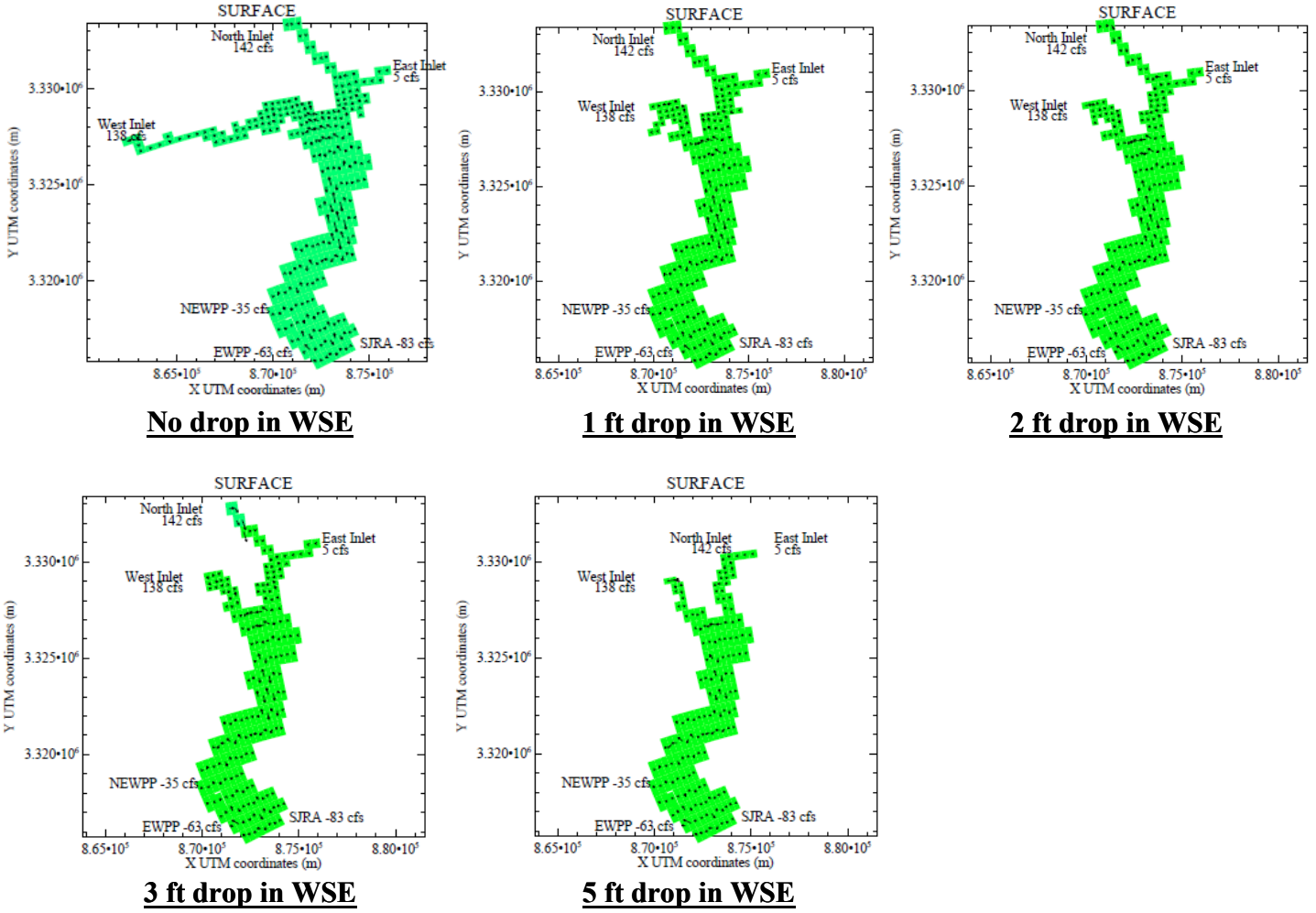

Figure 8.1 Change in Lake Houston grid for varying scenarios.

8.1.2 Results of scenario runs

Complete visualizations of the water velocities and water surface elevations predicted by EFDC under each of the scenarios are presented in Appendix D. The following section discusses the findings relevant to the objectives of this project.

8.2 WATER CIRCULATION PATTERNS IN LAKE HOUSTON

Based on the EFDC modeling results, the major circulation patterns of the lake are primarily influenced by wind and rainfall. Wind effects are dominant for most of the year when flows are at normal levels. Rainfall effects dominate during storm events. The following sections discuss the wind-driven and rainfall-driven circulation patterns.

8.2.1 Wind-driven circulation patterns

The shape and orientation of Lake Houston provide the longest fetches in the lake for the northerly and southeasterly winds (Matty, et. al., 1987) that occur most frequently along the Texas coast. Northerly winds dominate during the winter months, while southeasterly winds dominate for the rest of the year.

The wind-driven circulation pattern typically consists of fast surface currents that are pushed by the wind and slower bottom currents that sometimes run in the opposite direction. In the shallower northern part of the lake, current velocities are higher than in the southern part. A typical wind-driven circulation pattern for a southeast wind is shown in Figure 6.8, and Figure 6.9 shows a typical north wind circulation pattern.

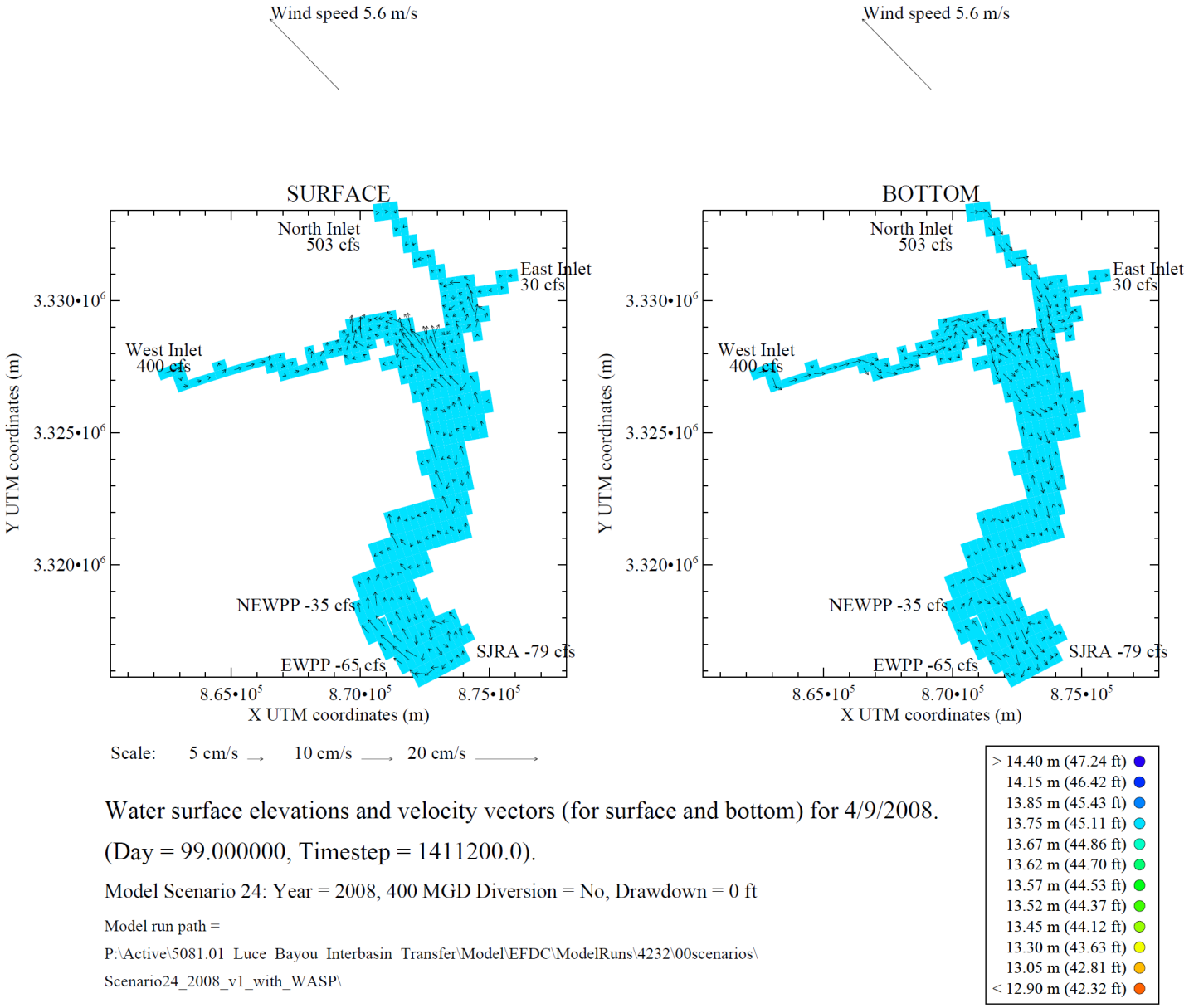

Figure 8.2. Example of a circulation pattern driven by a southeast wind (from 4/9/2008).

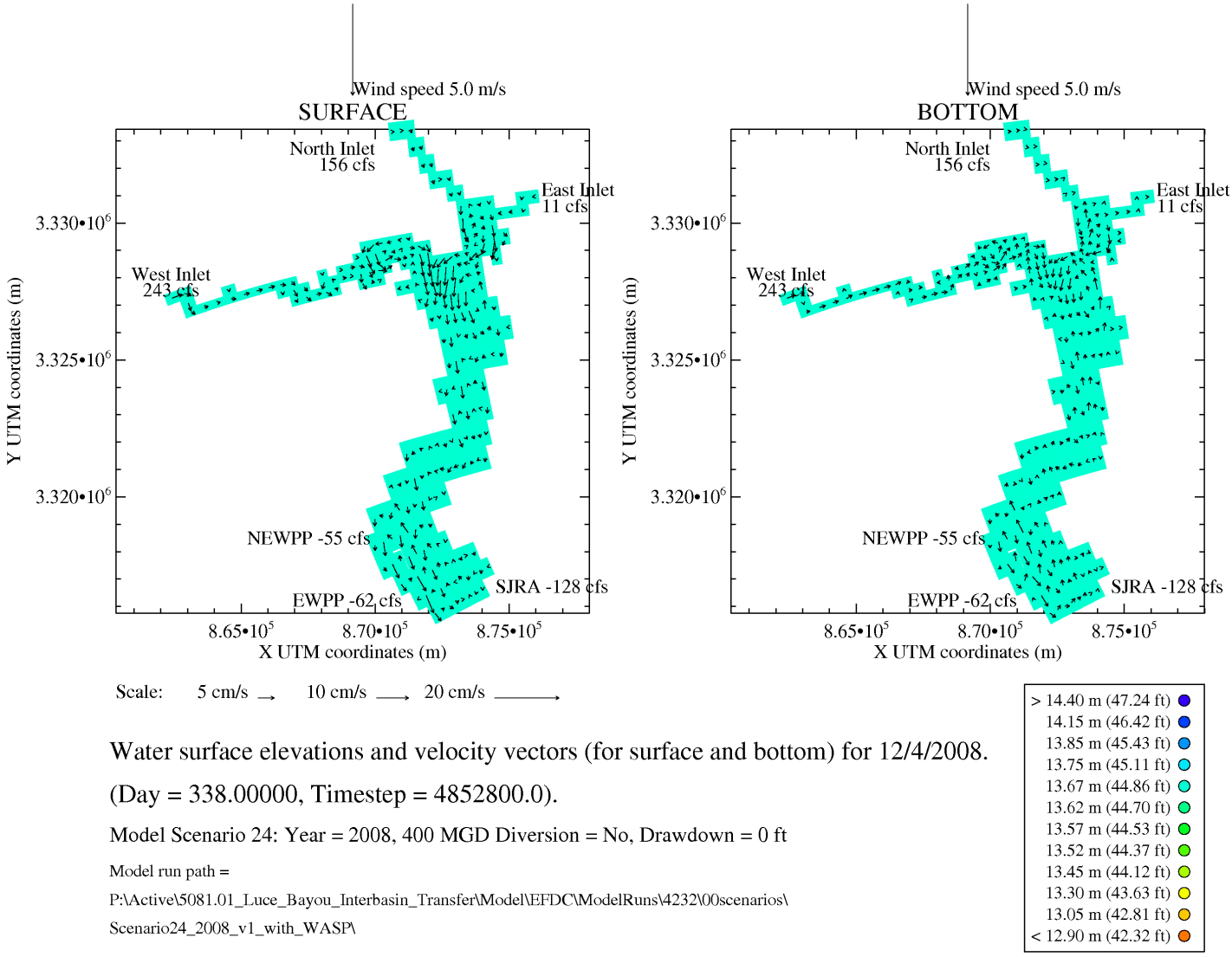

Figure 8.3 Example of a circulation pattern driven by a north wind (from 12/4/2008).

The constriction of the lake near the location of the railroad bridge (recall Figure 6.1) and the meandering of the lake downstream of the bridge create a dividing effect on the wind fetch. It is observed that high winds often cause fast currents in two separate areas in the Lake, one in the southwest near the NEWPP and EWPP plant intakes and one in the north where the three inlets converge. This observation implies that two circulation cells could exist in the Lake: one north of the bridge (North Lake) and one south of the bridge (South Lake). The presence of the two circulation cells suggests that the flows from the three inlets can potentially be well-mixed in the North Lake cell before travelling down to the South Lake cell. This observation is further investigated with a tracer simulation described later in this section.

8.2.2 Rainfall-driven water circulation patterns

Storm events typically happen during the spring (March to May) and in the fall (September to October during the hurricane season). After heavy rainfall, large quantities of runoff are delivered to the tributaries and rapidly flowing waters enter the lake. During this time, the down-lake flow dominates the

pattern of circulation and wind effects are less pronounced. Figure 8.4 shows a typical circulation pattern that is caused by a high flow event (May 8, 2008).

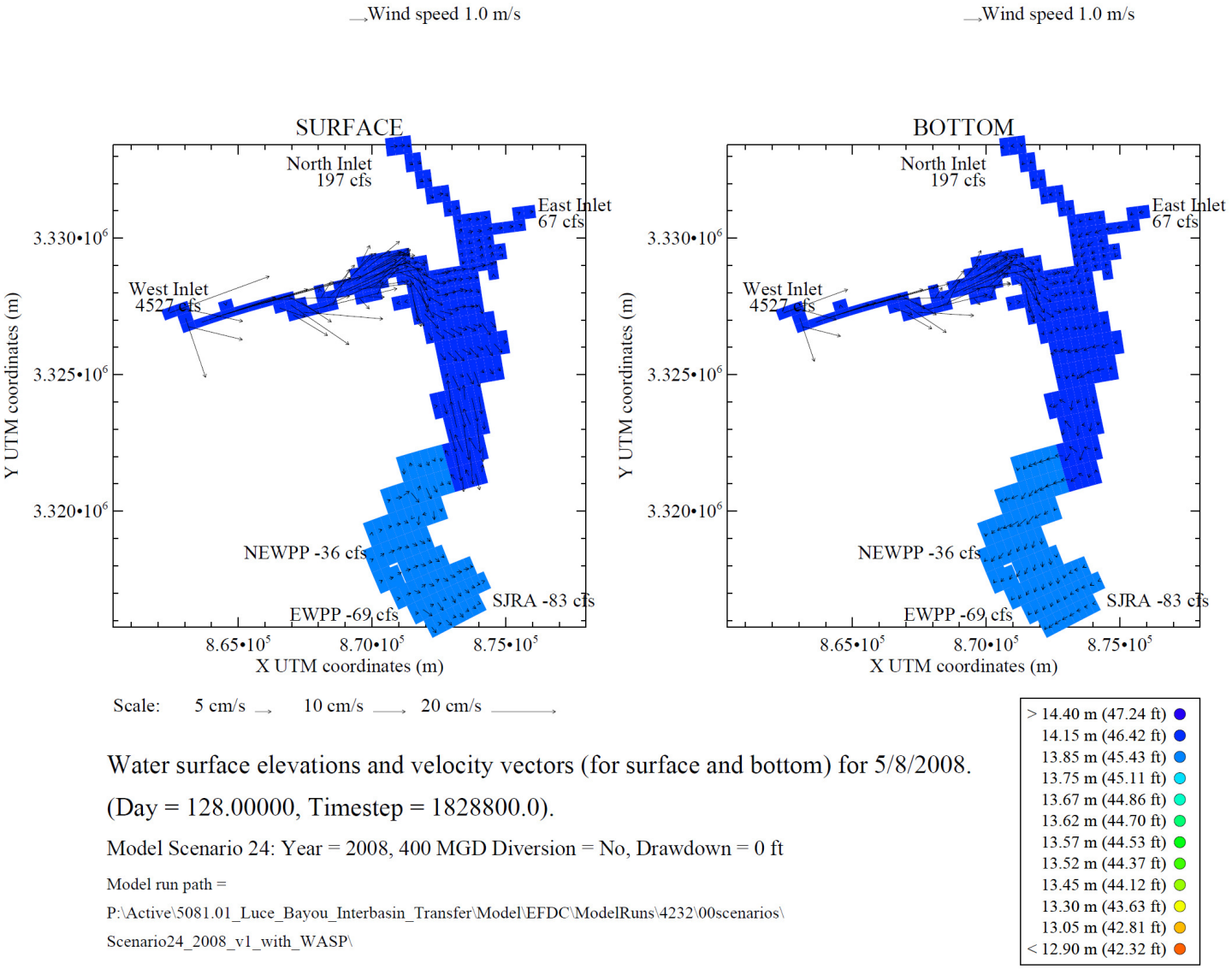

Figure 8.4 Example of a rainfall-driven circulation pattern (May 8, 2008).

Flows during rainfall events are primarily contributed by the west inlet. This effect, coupled with the shallow and narrow dimensions of the channel, causes the western arm of the lake to experience high flow velocities (ranging from 0.2 m/s to several meters per second). The increased quantity of water flowing into the reservoir causes the lake level to rise during the passage of the storm event. Historically, fluctuations of greater than 1 m have been observed during storms (Bedient et al. 1980).

8.2.3 Tracer simulation

To evaluate mixing patterns in the lake, tracer simulations were performed using the EFDC model and flow conditions for 2008. Despite being an average flow year, the summer of 2008 was relatively dry, and an extreme high flow event occurred in mid-September associated with Hurricane Ike. For this

reason, the lake's response to different hydraulic conditions can be observed during this year. Because flows in the West Inlet tend to have higher concentrations of contaminants, the tracer simulations were designed to investigate mixing and dilution of these flows with the waters from the North and East inlets. For each scenario, the model is executed over the course of a year using conditions from 2008 with a constant dye concentration imposed on the West Inlet cell. The following six scenarios were investigated using tracer simulations:

- no Trinity diversion and no drawdown
- no Trinity diversion and 2 ft drawdown
- no Trinity diversion and 5 ft drawdown
- 400 MGD Trinity diversion and no drawdown
- 400 MGD Trinity diversion and 2 ft drawdown
- 400 MGD Trinity diversion and 5 ft drawdown.

The complete tracer simulation results can be found in Appendix E. The following sections discuss the results.

8.2.4 Effects of diversions and drawdowns on mixing

Tracer simulation results for 4/30/2008, 4/3/2008, 3/12/2008 and 9/14/2008 are presented in Figures 8.5, 8.6, 8.7 and 8.8, respectively. These days were selected because they represent low flow, normal flow, high flow and extremely high flow conditions in the lake. Each figure is composed of six diagrams laid out in two rows and three columns. Diagrams along the top row show results from scenarios with no Trinity diversion. The bottom row shows results from scenarios that included the 400 MGD Trinity diversion. The left, middle and right columns show results for 0 ft, 2 ft and 5 ft drawdown. The simulated tracer concentrations range from 0 (blue) to 50 mg/L (red). Water velocities are depicted by arrows with longer arrows indicating higher velocities.

Figure 8.5 shows the tracer simulation results for the six scenarios on 4/30/2008 under low-flow conditions. Flows at the west, north and east inlets were 132 cfs, 103 cfs and 6 cfs (for no diversion) and 626 (for diversion), respectively. The total flow of 241 cfs (for no diversion) corresponds to a 22nd-percentile flow. Wind blew from the southeast at 5.3 m/s creating a southeasterly wind-driven circulation pattern. Figure 8.5 shows that most of the cells along the western arm have high concentrations that are close to the imposed tracer concentration of 50 mg/L. Because of the lack of tracer input, cells along northern and eastern arms have concentrations that are close to 0 mg/L. In the north-central part of the lake where the three arms merge, a lateral concentration gradient occurs from west to east, perpendicular to the direction of flow. Concentrations are higher along the west bank than on the east bank. This lateral gradient decreases in intensity downstream. The **mixing zone** is defined as the zone between the confluence where the three arms merge and where the lateral gradient dissipates (i.e. concentrations become uniform across the lake width). In scenarios with the 400 MGD diversion, a gradient occurs along the direction of the flow. This gradient represents the front of the tracer propagation and does not represent the extent of the lateral mixing.

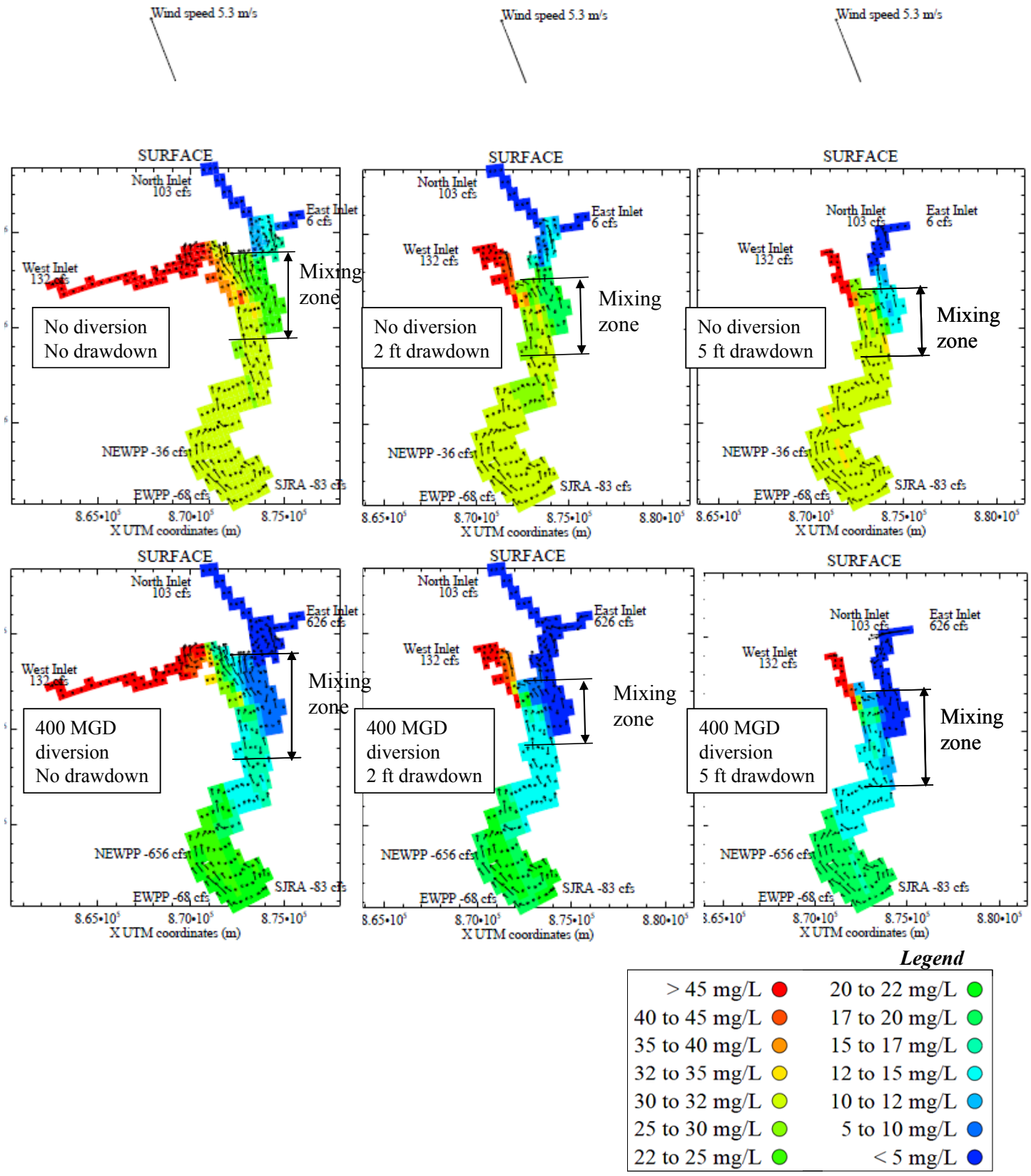

Figure 8.5 Tracer concentrations in Lake Houston on 4/30/2008 under low flow conditions.

It can be observed from the figure that for all six scenarios the mixing zone ends before or within the bend in the reservoir indicating that concentrations in the south lake are reasonably uniform. The lateral gradient is sharpest for scenarios with Trinity River diversion, because, at 626 cfs, the East inlet flow dominates flow from the other two inlets. The mixing zone tends to be longer with the diversion because water velocities are faster with the increased flow and the flows travel a longer distance before they are mixed. Drawdowns cause portions of the northern part of the lake to go dry moving the confluence of the three inlets further downstream and shifting the mixing zone towards the south.

Figure 8.6 shows the tracer simulation results for the six scenarios on 4/3/2008. Normal inflow conditions occurred on this day. Flows at the west, north and east inlets were 277 cfs, 207 cfs and 3 cfs (for no diversion) and 623 cfs (for diversion), respectively. The total flow of 487 cfs (for no diversion) corresponds to a 47^{th}-percentile flow. Wind blew from the south at 4 m/s creating a southerly wind-driven circulation pattern. Mixing zones under high-flow conditions are longer than under low flow conditions given the higher water velocities. The mixing zone for all scenarios extends to the bend of the lake.

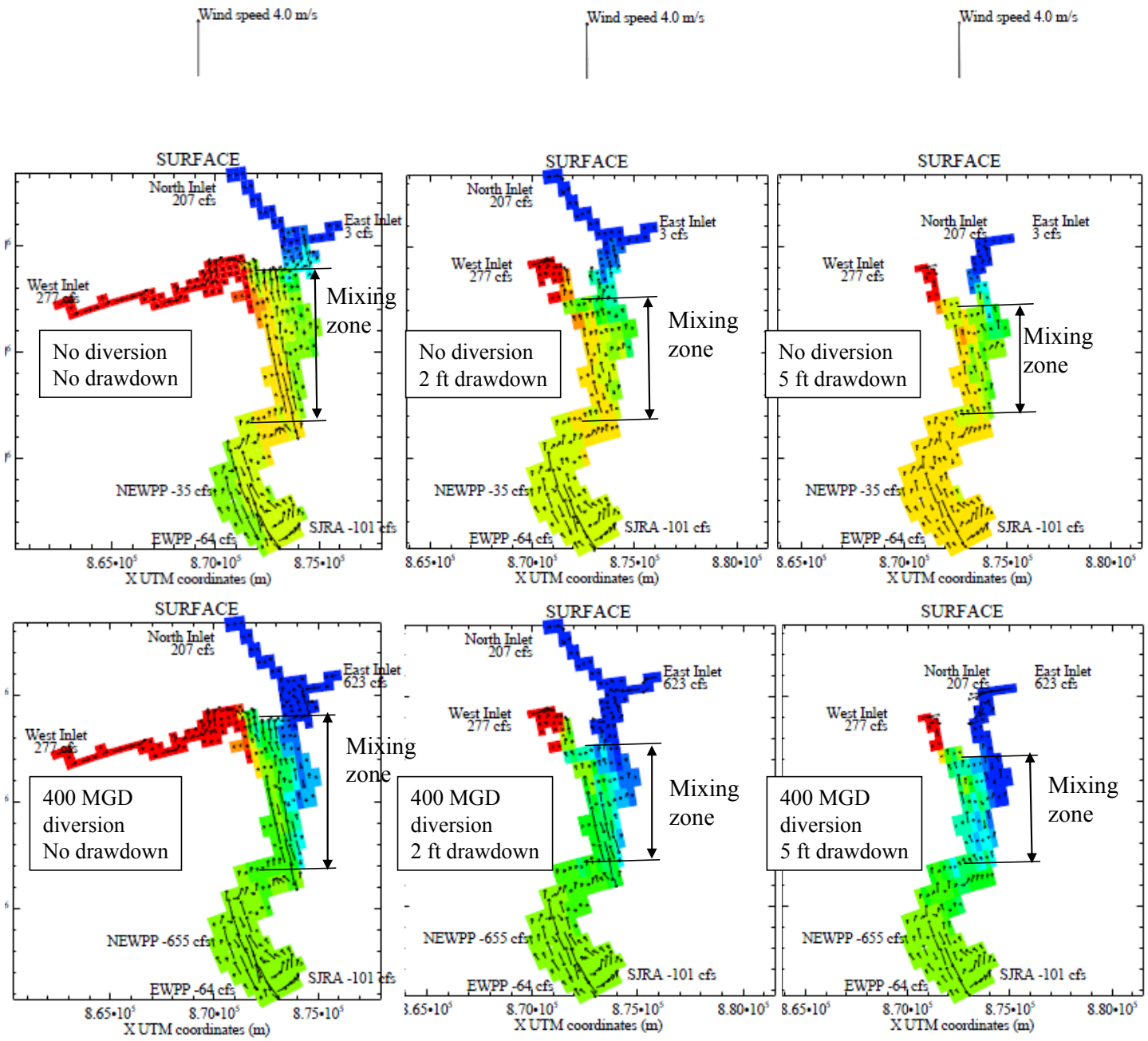

Figure 8.6 Tracer concentrations in Lake Houston on 4/3/2008 under normal-flow conditions.

Figure 8.7 shows the tracer simulation results for on 3/12/2008. High inflow conditions occurred on this day. Flows at the west, north and east inlets were 3,071 cfs, 1,268 cfs and 228 cfs (for no diversion) and 848 cfs (for diversion), respectively. The total flow of 4,567 cfs (for no diversion) corresponds to a 90th-percentile flow. Wind blew from the south at 1 m/s. High-flow conditions dominate and the lake exhibits a rainfall-driven circulation pattern. Mixing zones under high-flow conditions are longer than under normal flow conditions given the higher water velocities. As expected, the mixing zone for the scenario with 400 MGD diversion and 5 ft drawdown is the longest because the highest flow velocities occur in this scenario. The mixing zone for this scenario extends slightly past the bend and into the south part of the lake.

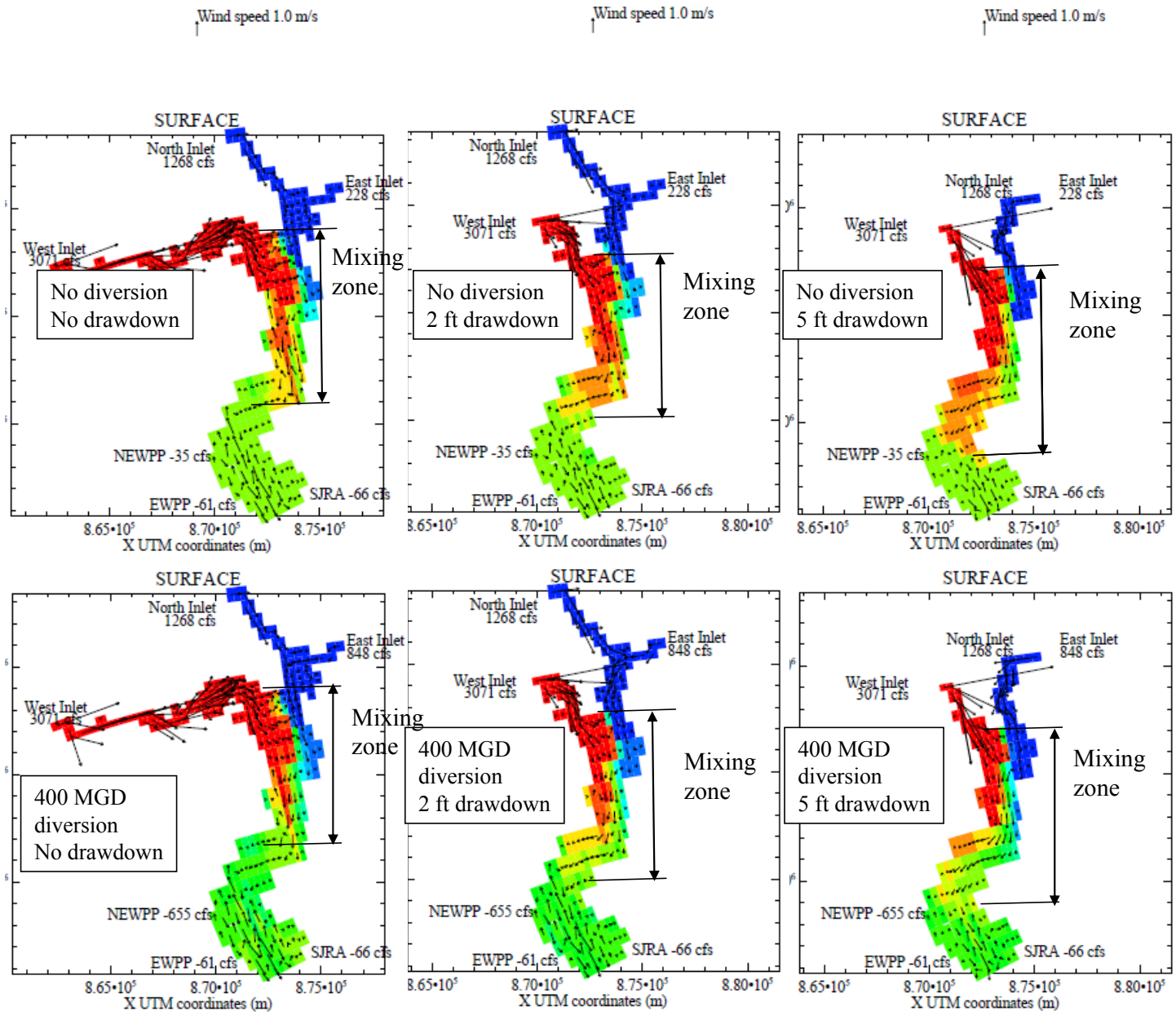

Figure 8.7 Tracer concentrations in Lake Houston on 3/12/2008 under high-flow conditions.

Figure 8.8 shows the tracer simulation results for the six scenarios on 9/14/2008 immediately after the dissipation of Hurricane Ike on 9/13/2008 when storm runoff was pouring into the Lake. Flows at the west, north and east inlets are 26,906 cfs, 13,519 cfs and 16,282 cfs (for no diversion) and 16,902 cfs(for diversion), respectively. The total flow of 56,707 cfs (for no diversion) corresponds to a 99.9th percentile flow. Wind blows from the north at 4 m/s. High-flow conditions dominate and the lake exhibits a rainfall-driven circulation pattern. The mixing zones for all scenarios now extend all the way down to the dam because of extremely high water velocities.

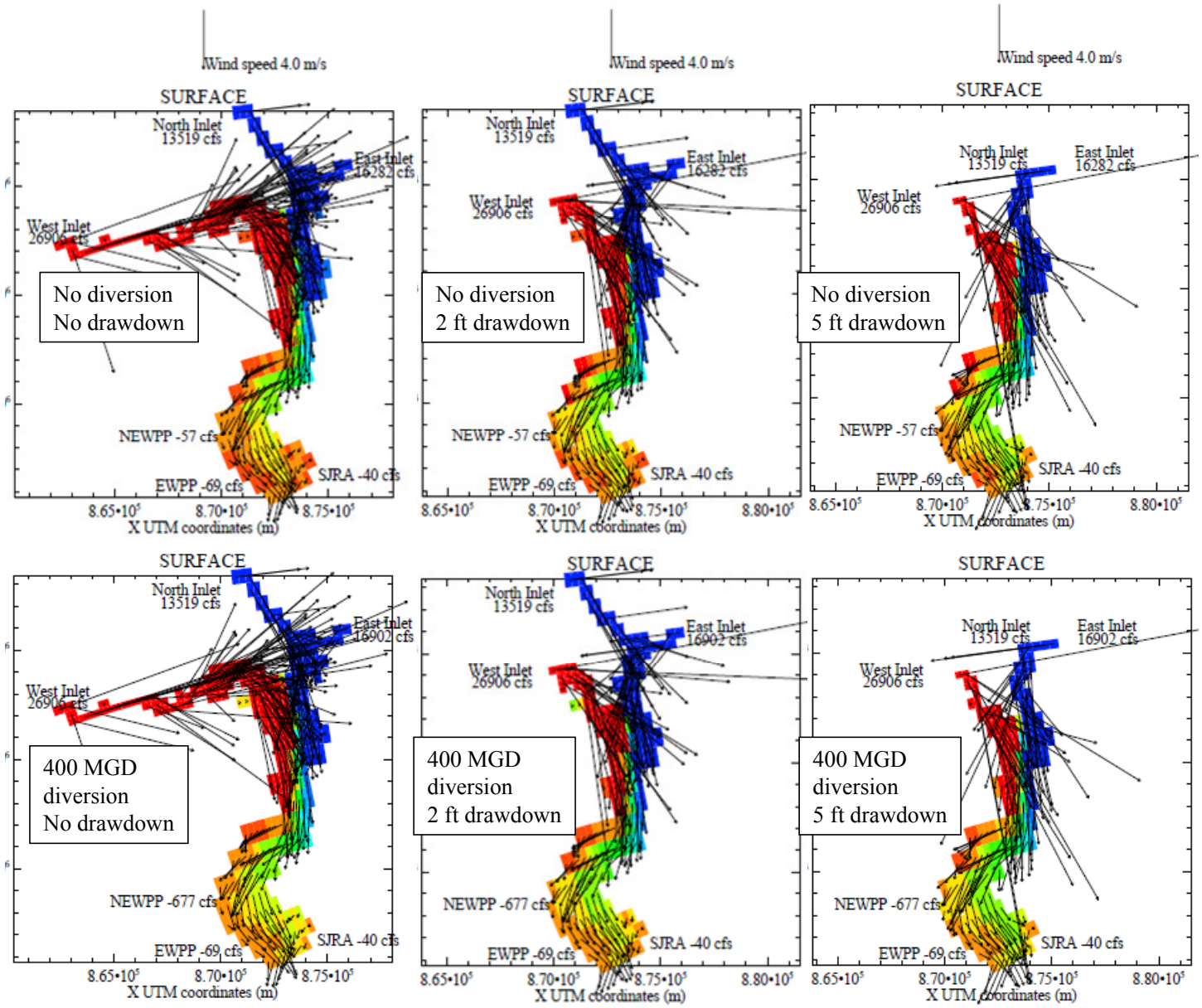

Figure 8.8 Tracer concentrations in Lake Houston on 9/14/2008 (immediately after Hurricane Ike) under extremely high flow condition.

8.3 EVALUATION OF LOCATION OF NEWPP INTAKE IN RELATION TO LAKE FLOW REGIME

The results of the tracer simulations were used to evaluate the location of the NEWPP intake in relation to the lake flow regime. The NEWPP intake is located on the west bank of the South Lake just downstream of the bend of the lake (recall Figure 7.1). The tracer simulations demonstrate that West, North and East Inlet flows are well-mixed before reaching the NEWPP intake for all flow conditions simulated except the extremely high flow conditions. High flows greater than about the 90th-percentile extend the mixing zone beyond the bend in the lake and into the South Lake. As a result, flows from the West Inlet are not well-mixed along the west bank under very high flow conditions. Water quality can be adversely affected because West Inlet flows comprise runoff from the San Jacinto River Basin.

Well-mixed conditions at the NEWPP intake location also occurred for scenarios that included the 400 MGD diversion with East Inlet flow. For this reason, the water quality at the NEWPP intake will likely benefit from the introduction of Trinity River water through Luce Bayou. However, if the Trinity River water is not brought to Lake Houston (during heavy rain periods in the San Jacinto Watershed) there may still be times when the treatment of NEWPP is impacted due to the high flow runoff events.

Drawdowns may adversely affect water quality in two ways. First, dilution of contaminant concentrations is reduced because of the smaller volume of water. Second, as shallower northern parts of the lake become dry, the confluence of the inlets is shifted downstream moving the mixing zone closer to the NEWPP intake. As a result, the NEWPP intake may receive more incompletely mixed water that is influenced by West Inlet flows.

9.0 WATER QUALITY ASSESSMENT

9.1 DEVELOPMENT OF WATER QUALITY MODEL FOR LAKE HOUSTON

Version 7.3 of EPA's WASP model (http://www.epa.gov/athens/wwqtsc/html/wasp.html) was used to simulate water quality in Lake Houston. The eutrophication module within WASP is selected to simulate nutrient fate and transport. The same model grid as developed for the EFDC model was used for WASP to allow flows estimated by EFDC to be used directly as input for WASP.

9.2 WASP INPUT DATA

The input data for the WASP model are identified in Table 9.1. Input data are time-varying properties that either describe or affect the simulated nutrient loads that enter Lake Houston. Table 9.1 shows the units and the source of information for quantifying input data. Parameters estimated from available field data as described in Section 4 are identified by the source code 'F.' Parameters calculated through deterministic or empirical formulae are identified with the code 'C.' Further information on how values were derived for these parameters is provided below.

Table 9.1 WASP model inputs

WASP Model Inputs	Units	Source
Temperature	°C	F
Solar radiation	Langleys/day	F
Light extinction function	1/meter	C
Fraction daylight	unitless	F
Wind speed	m/sec	F
Ammonia concentration	mg-N/L	F
Nitrate concentration	mg-N/L	F
Dissolved organic nitrogen concentration	mg-N/L	F
Inorganic phosphate concentration	mg-P/L	F
Dissolved organic phosphorus concentration	mg-P/L	F
Ultimate carbonaceous biological oxygen demand (CBOD)	mg-O_2/L	C
Dissolved oxygen concentration	mg/L	F
Detrital carbon concentration	mg-C/L	C
Detrital nitrogen concentration	mg-N/L	C
Detrital phosphorus concentration	mg-P/L	C
Phytoplankton Chla concentration	ug/L	F

Light extinction function

Sunlight is a major factor controlling eutrophication of lakes and reservoirs because it provides the energy for photosynthesis. The light extinction coefficient, solar radiation and day length determine the amount of light available for the aquatic vegetation. Solar radiation and day light length were obtained from the meteorological data sources mentioned in Section 3 (Table 3.4). Light extinction is an important parameter that quantifies the extent of light penetration into the water column affecting photosynthesis and respiration processes of algae. The light extinction coefficient in WASP accounts for the following four components that inhibit light penetration into the water column. These are:

- Background light extinction due to ligands, color, etc.
- Algal self shading,
- Solids light extinction,

- Dissolved organic carbon light extinction.

Algal self-shading, solids light extinction, and dissolved organic carbon light extinction are calculated internally by WASP during simulation, leaving background light extinction as the only input. For the Lake Houston model, the background light extinction is calculated using secchi depth measurements that are collected at several of the SWQM lake stations. The formula for calculating the light extinction function from secchi depth is given in Equation 9.1:

$$\text{Light Extinction Coefficient} = \frac{1.1}{Secchi\ Depth^{0.73}} \qquad \text{Equation 9.1}$$

Detrital nutrient concentrations

Detrital carbon, nitrogen and phosphorus concentrations are calculated as fractions of the total suspended solids concentration using equations from the literature (GBM & Associates, 2006) shown in Equations 9.2 to 9.4.

Detrital Carbon:

Det-C (mg/L) = 0.05 x TSS (mg/L)

Equation 9.2

Detrital Nitrogen:

Det-N (mg/L) = 0.15 x Det-C (mg/L)

Equation 9.3

Detrital Phosphorus:

Det-P (mg/L) = 0.022 x Det-C (mg/L)

Equation 9.4

Ultimate carbonaceous oxygen demand (CBOD)

The ultimate carbonaceous oxygen demand (CBOD) is calculated from the BOD_5 using equation 9.5:

CBOD (mg/L) = 2.3 x BOD_5 (mg/L)

Equation 9.5

9.2.1 Oxygen reaeration functions

By default, the eutrophication module in WASP calculates flow-induced reaeration based on the Covar method. This method calculates reaeration as a function of velocity and depth by one of three commonly used formulas - Owens, Churchill, or O'Connor- Dobbins (Covar, 1976)

9.3 CALIBRATION OF WASP MODEL

9.3.1 Calibration parameters

The calibration parameters for the WASP model are identified in Tables 9.2 and 9.3. These parameters are internal constants that affect the equations that model nutrient cycling and eutrophication. Examples are sediment oxygen demand, BOD decay rate, nitrification rate and phytoplankton growth rate. The values are obtained from the literature because site-specific data are not available. The range of literature

values is listed for each parameter. The final parameter value used is listed on the table. For parameters with no established ranges (e.g. atmospheric deposition of nitrate), the WASP model of the Cedar Creek Reservoir in North Texas (EC, 2007) was used as a reference, and parameter values from that model were applied to the Lake Houston model and adjusted during calibration.

Table 9.2 WASP Model Parameters (Part 1)

Parameter	Units	Common range of literature values	Selected Value
Atmospheric Deposition of Nitrate	mg-m^2/day	0.826 (from Cedar Creek WASP model)	0.826
Atmospheric Deposition of Ammonia	mg-m^2/day	1 (from Cedar Creek WASP model)	1
Atmospheric Deposition of Orthophosphate	mg-m^2/day	0.092 (from Cedar Creek WASP model)	0.092
Atmospheric Deposition of BOD	mg-m^2/day	0 (from Cedar Creek WASP model)	0
Atmospheric Deposition of Organic Nitrogen	mg-m^2/day	1.396 (from Cedar Creek WASP model)	1.396
Atmospheric Deposition of Organic Phosphorus	mg-m^2/day	0.06 (from Cedar Creek WASP model)	0.06
Nitrification Rate @ 20º C	day $^{-1}$	0.001 – 0.2	0.2
Nitrification Temp Coeff.	NA	1.02 – 1.08	1.04
Half Saturation: Nitrification Oxygen Limit	mg O_2/L	0.5 – 2.0	1
Denitrification Rate @ 20º C	day $^{-1}$	0 – 0.09	0.09
Denitrification Temp Coeff.	NA	1.02 – 1.09	1.06
Half Saturation: Denitrification Oxygen Limit	mg O_2/L	0 – 2.0	2
Phytoplankton Growth Rate @ 20º C	day $^{-1}$	1.0 – 3.0	1.25
Phytoplankton Growth Temp Coeff.	NA	0 – 1.07	1.06
Phytoplankton Light Formulation Switch (1 = DiToro)	NA	NA	1 = DiToro
Phytoplankton Self Shading Extinction	NA	0 – 0.02	0
Phytoplankton Carbon:Chlorophyll Ratio	mg carbon/mg chla	0 – 200	50
Phytoplankton Optimal Light Saturation	Ly/day	0 – 350	200
Phytoplankton Half Saturation Constant: Nitrogen	mg-N/L	0.01 – 0.06	0.0485
Phytoplankton Half Saturation Constant: Phosphorus	PO_4-P/L	0.0005 – 0.05	0.007
Phytoplankton Endogenous Respiration Rate @ 20º C	day $^{-1}$	0 – 0.5	0.06
Phytoplankton Respiration Temperature Coefficient	NA	1.0 – 1.08	1.045
Phytoplankton Death Rate Non-Zooplankton Predation	day $^{-1}$	0 – 0.25	0.06
Phytoplankton Decay Rate in Sediments @ 20º C	day $^{-1}$	0 – 0.02	0.02
Phytoplankton Decay Rate Temp Coeff.	NA	1.0 – 1.08	1.08
Phytoplankton Phosphorus::Carbon Ratio	mg P/mg C	0 – 0.24	0.022
Phytoplankton Nitrogen::Carbon Ratio	mg N/mg C	0 – 0.43	0.15

Table 9.3 WASP Model Parameters (Part 2)

Parameter	Units	Common range of literature values	Selected Value
BOD Decay Rate @ 20º C	day $^{-1}$	0.05 – 0.4	0.1
BOD Decay Rate Temp Correction	NA	1.0 – 1.07	1.04
BOD Decay Rate in Sediments @ 20º C	day $^{-1}$	0.0004 – 1.0	1
BOD Decay Rate in Sediments Temp Coeff.	NA	1.0 – 1.08	1.08
BOD Half Saturation Oxygen Limit	NA	0.5 – 1.0	1
Sediment Oxygen Demand	g/m^2-day	1.5 (from USGS CE-QUAL W2 model for Lake Houston)	1.5
Oxygen:Carbon Stoichiometeric Ratio	mg O_2/mg C	0 – 2.67	2.67
Reaeration Rate Constant @ 20º C	day $^{-1}$	0.5 – 3.0	1
Reaeration Rate Option (sums Wind and Hydraulic Ka)	NA	0 – 1.0	NA
Dissolved Organic N Mineralization Rate @ 20º C	day $^{-1}$	0.003 – 0.2	0.01
Dissolved Organic N Mineralization Temp Coeff.	NA	1.0 – 1.08	1.045
Organic N Decay in Sediments @ 20º C	day $^{-1}$	0.0004 – 0.01	0
Organic N Decay in Sediments Temp Coeff.	NA	1.0 – 1.08	1.045
Fraction of Phytoplankton Death Recycled to ON	NA	0 – 1.0	1
Dissolved Organic P Mineralization Rate @ 20º C	day $^{-1}$	0 – 0.22	0.01
Dissolved Organic P Mineralization Temp Coeff.	NA	1.0 – 1.08	1.045
Organic P Decay in Sediments @ 20º C	day $^{-1}$	0.0004 – 0.01	0
Organic P Decay in Sediments Temp Coeff.	NA	1.0 – 1.08	1.08
Fraction of Phytoplankton Death Recycled to OP	NA	0 – 1.0	1
Benthic Ammonia Flux	mg/m^2-day	8 – 92	13.5
Benthic Phosphate Flux	mg/m^2-day	0 – 50	9.5

9.3.2 Calibration results

The WASP model was calibrated by adjusting model parameters to improve the fit of the results to the data acquired from USGS and TCEQ stations within Lake Houston. The calibration sequence followed that recommended in the WASP7 course training materials (EPA WWQMTSC 2009) and is described below.

1. Calibration of dissolved oxygen and ultimate carbonaceous biological oxygen demand (CBOD)

Dissolved oxygen (DO) and ultimate carbonaceous biological oxygen demand (CBOD) values were calibrated to ensure that basic oxygen mechanisms are properly described. Figures 9.1, 9.2, and 9.3 show the calibration results for 2000, 2004 and 2008, respectively. Each figure is a set of four plots showing the model results and the DO data collected in the northwestern part of the lake (SWQM 11211), northeastern part of the lake (SWQM 11212), middle part of the lake (SWQM 11208 or USGS 295826095082200 – abbreviated as USGS200) and southern part of the lake (SWQM 11204 or USGS 295435095082201 – abbreviated as USGS201). Data collected at USGS200 and USGS201 are used to compare 2008 simulation results because data are not yet available for SWQM 11204 and 11208 at the writing of this report. Observed data are compared to model output from the corresponding grid cell. On these plots, crosses represent the dissolved oxygen data. Different colors of the crosses represent different depths where the data were collected (see legend below). Note that most of the data are

measured at 0.3 m (classified as DO@0m) while the simulated values are for lower depths. For the top model segment, the middle depth is typically at 1 m. For the bottom model segment, the middle depth is typically at 2 m to 3 m. The black line represents model results from the top model segment and the red dashed line represents results from the bottom model segment of the cell. The extents of the top and bottom segments are described on the upper right corner of each plot. The extents vary by cell because EFDC does not allow the user to assign absolute depths to the segments. Instead, the user specifies fractions by which the water column is partitioned. In the Lake Houston model, the upper half of the water column is assigned to the top segment and the lower half is assigned to the bottom segment, regardless of the total height of the water column. As an example, the cell depth at SWQM 11211 is 3.6 m. Therefore the top segment of the model at SWQM 11211 extends from the surface (0 m) to 1.8 m below the surface while the bottom segment extends from 1.8 m to 3.6 m below the surface. Simulated values at this cell would represent depths of 0.9 m for the top segment and 2.7 m for the bottom segment.

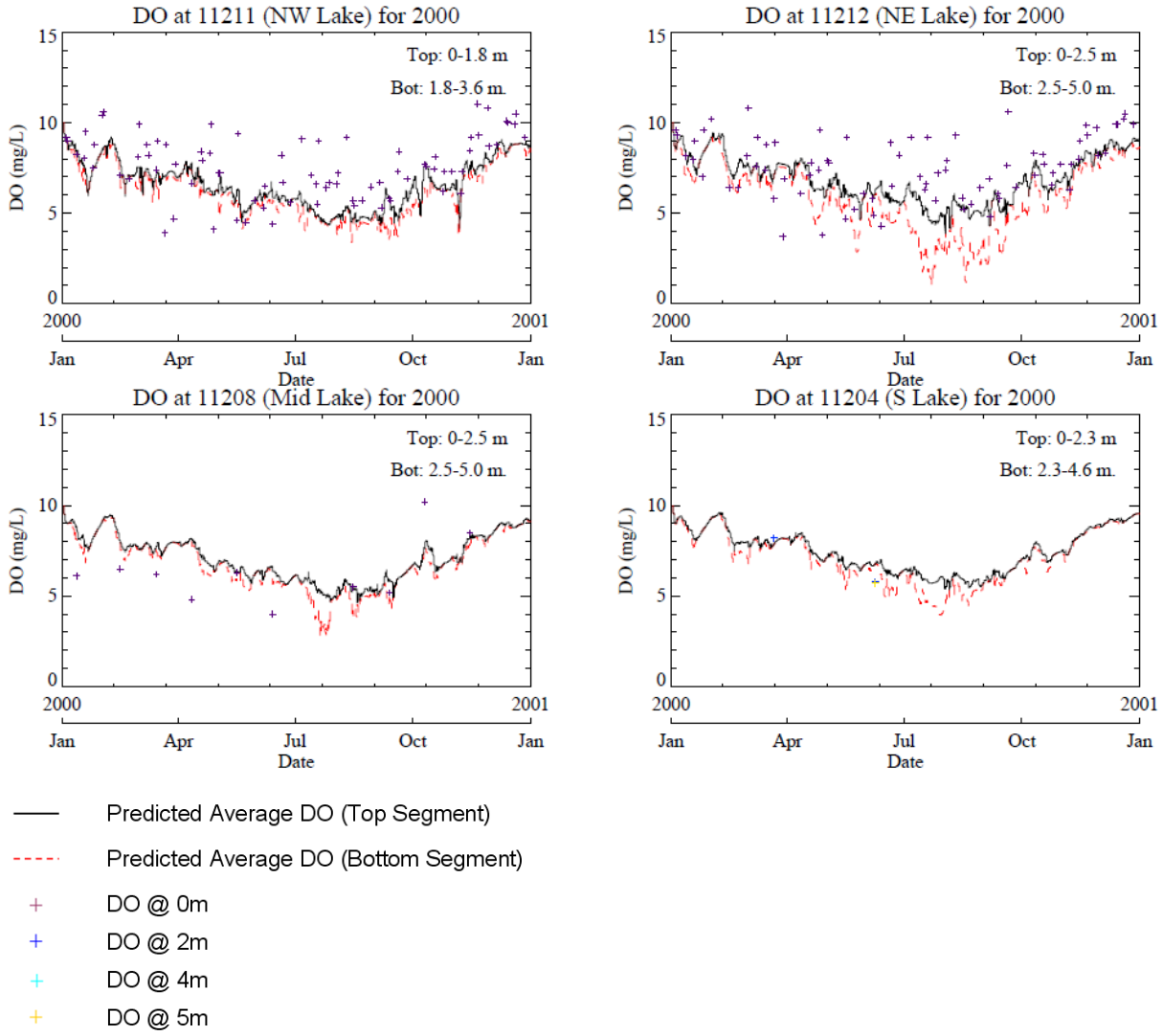

Figure 9.1 Predicted and observed dissolved oxygen for 2000 (low-flow).

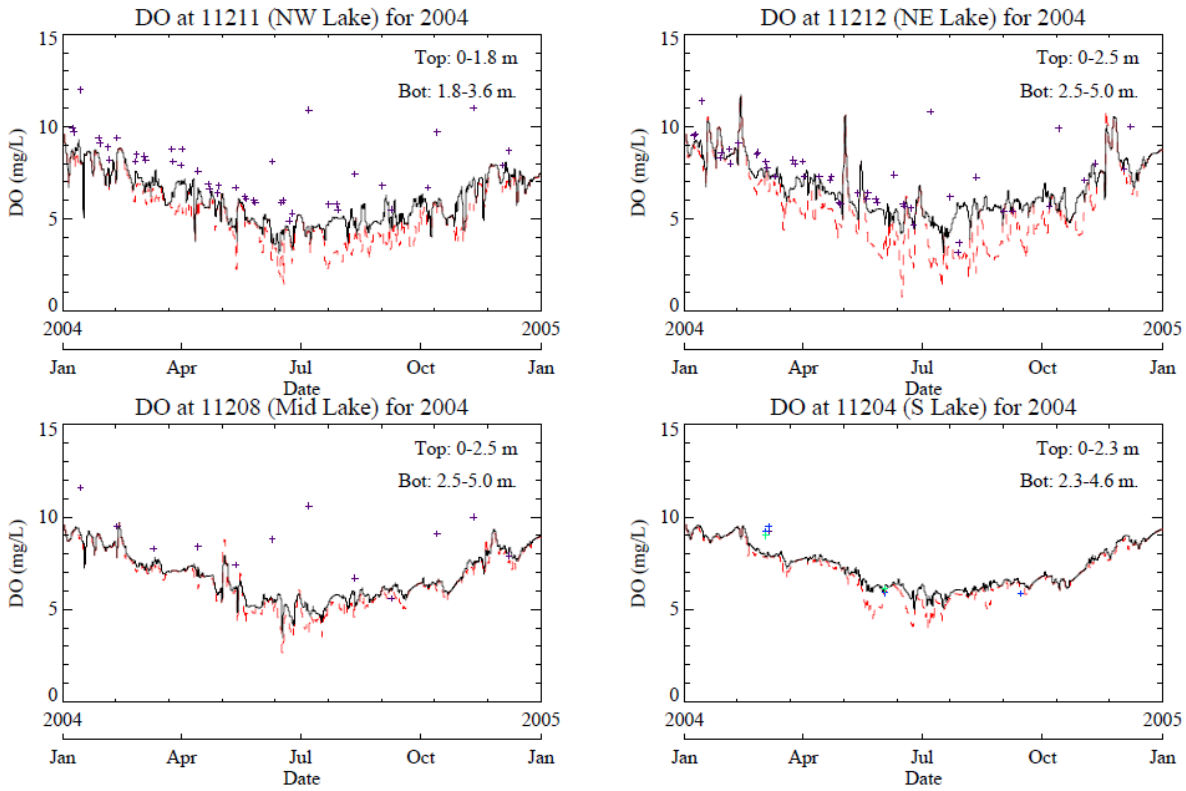

Figure 9.2 Predicted and observed dissolved oxygen for 2004 (high-flow).

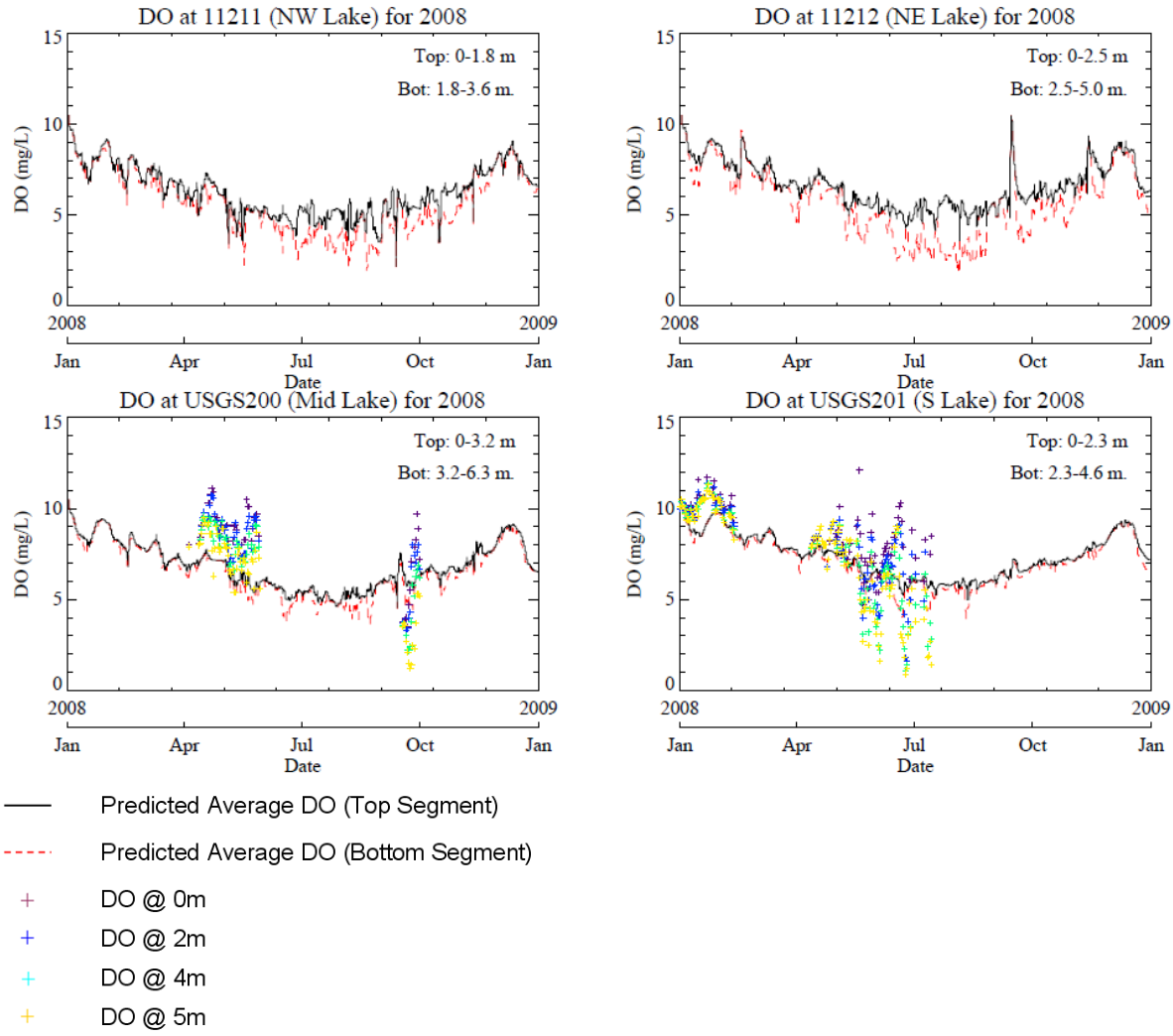

Figure 9.3 Predicted and observed dissolved oxygen for 2008 (normal-flow).

Figures 9.4, 9.5, and 9.6 show the calibration results for 2000, 2004 and 2008 respectively for CBOD. In general, CBOD data in the lake are very limited and all data were collected in the year 2000. CBOD levels in the lake are very low, and most samples collected are below the detection limit (9 mg/L). Detection limit of CBOD (ultimate) = Detection limit for BOD_5 x 2 = 4 mg/L x 2.3 = 9 mg/L). In the graph, non-detect samples are plotted at half the detection limit.

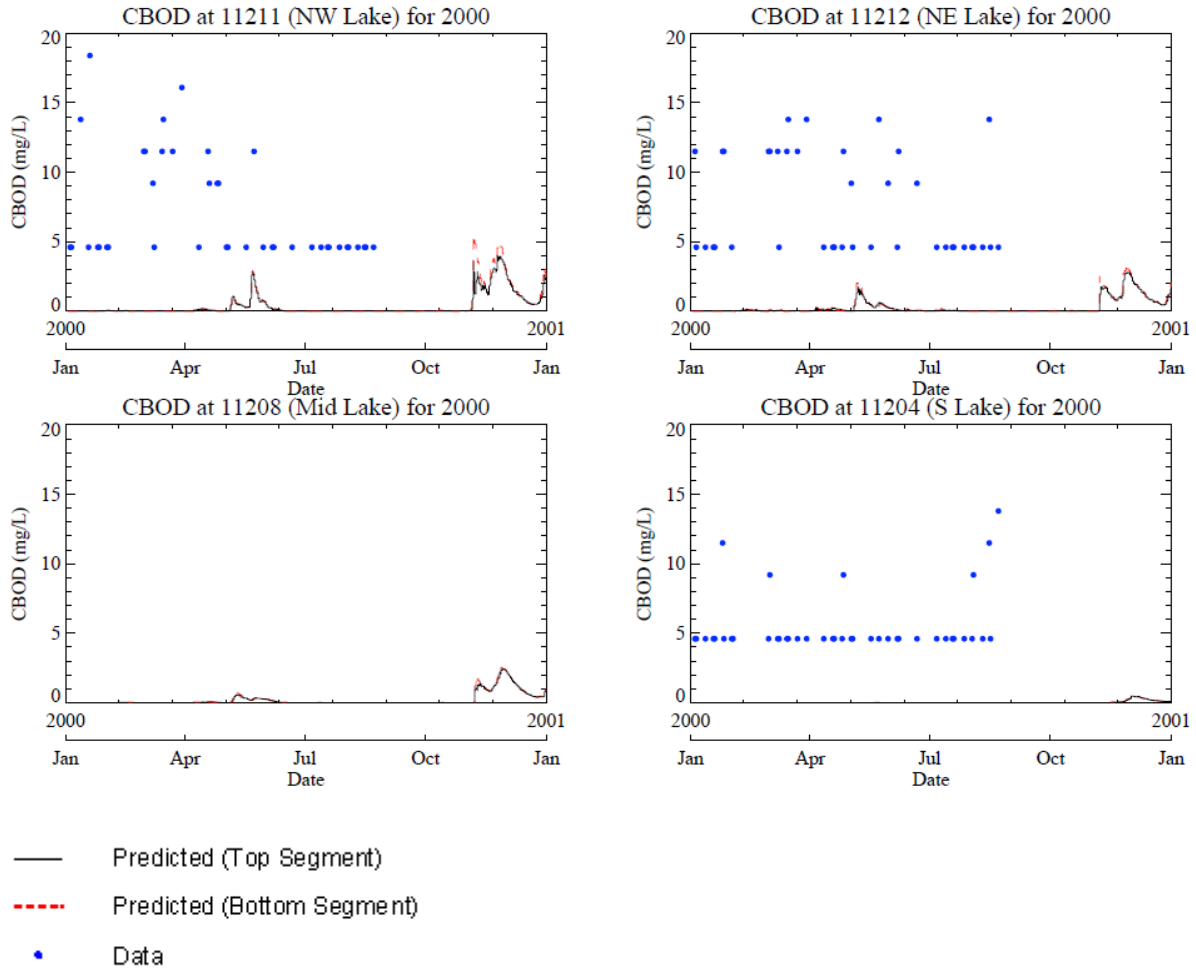

Figure 9.4 Predicted and observed ultimate carbonaceous biological oxygen demand for 2000 (low-flow).

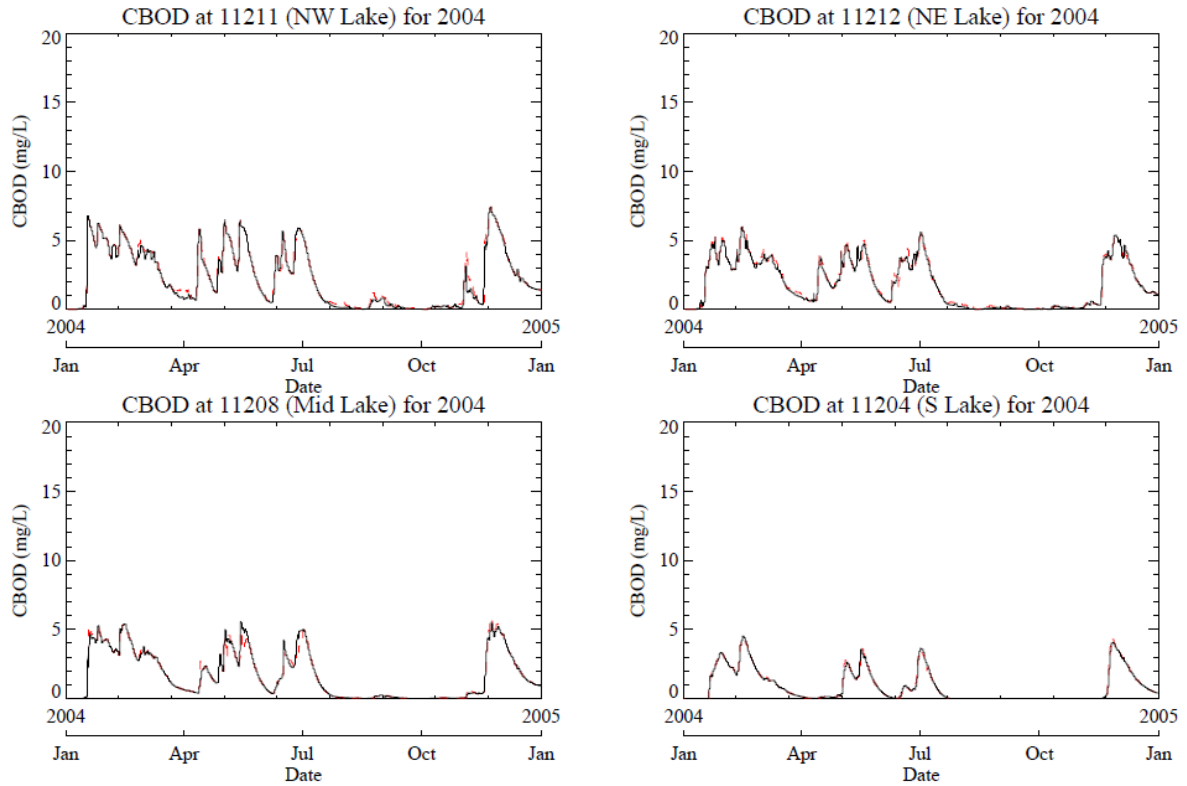

Figure 9.5 Predicted and observed ultimate carbonaceous biological oxygen demand for 2004 (high-flow).

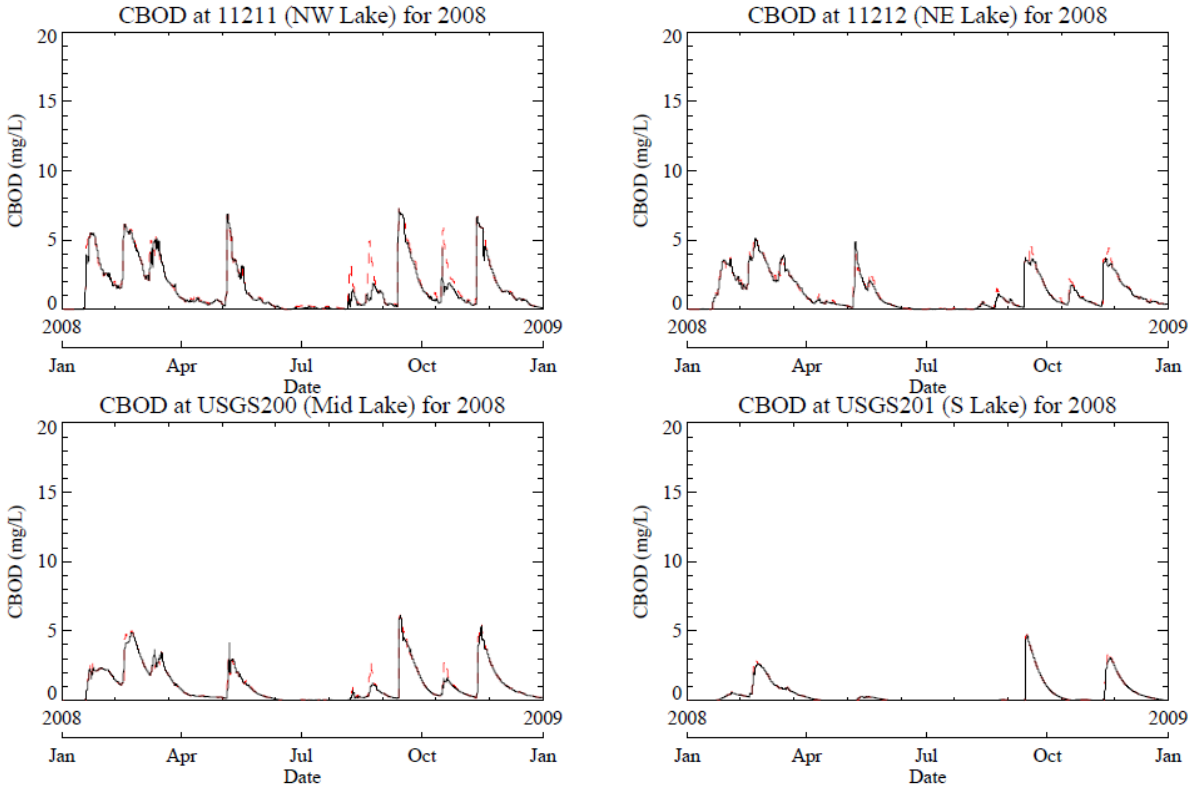

Figure 9.6 Predicted and observed ultimate carbonaceous biological oxygen demand for 2008 (normal-flow).

Trends in the data

Over 95% of DO data collected by SWQM stations are measured at a depth of 0.3 m with the maximum depth at 4.57 m. For these surface data, DO in the lake follows a strong seasonal pattern with high DO in the winter and low DO in the summer indicating that temperature and aeration are the primary drivers of surface DO trends. Deep water samples are rare in the database; however, USGS collected continuous DO data at depths of 0 m, 2 m, 4 m and 5 m at several locations in the lake from October 2007 to September 2008. In the graphs for 2008 in Figure 9.3, the DO data collected at USGS stations are plotted with the simulated values. It can be observed that measured DO concentrations decrease with depth – even to the extent of reaching hypoxic levels (i.e., < 2 mg/L). The observed vertical gradient in DO highlights the influence of sediment oxygen demand (SOD). Because of low CBOD levels, the influence of CBOD on DO is not likely significant.

Performance of the model

In comparing model to data, it is necessary to note that the top and bottom model segments each represent 50% of the total water column. Therefore, the depth intervals represented can be quite large. Because of vertical averaging, simulated values are less extreme than the data which represent concentrations at specific depths. In general, simulated DO concentrations are reasonable and follow the observed seasonal trend in the data.

The SOD rate of 1.5 g/m^2/day from USGS's Lake Houston model (USGS, 2000) was used to account for the vertical DO gradient. The model generally produces similar DO concentrations for the top and bottom segments. DO stratification is significant only during periods of low flow, when residence times are longer and SOD can exert more influence.

Simulated BOD levels are generally low in agreement with measurements in the lake. Although simulated BOD levels increase during high flow events, they tend to decline very quickly and have minimal impact on DO concentrations.

2. Calibration of total suspended solids

Total suspended solids (TSS) is a common water quality parameter of concern for reservoirs in Texas. Within the WASP eutrophication module, two types of mechanisms control the concentration of TSS: 1) physical mechanisms that include settling and resuspension; and 2) biological processes that include phytoplankton growth, death and dissolution of plant material. Both types of processes were included in the Lake Houston WASP model, but physical processes were assumed to dominate biological processes because of limited algal activity as a result of elevated inorganic turbidity in Lake Houston (Matty et. al., 1987; USGS, 1997). Turbidity limits the euphotic zone and affects nutrient cycling by decreasing light penetration into the water column. The average depth of Lake Houston is 12 ft (3.7 m), but the euphotic zone is only 2 ft to 6 ft deep (0.61 m to 1.85 m) deep (USGS, 1997).

Because of the dominance of physical processes, calibration of TSS parameters for the Lake Houston model first focused on adjusting parameters related to settling and resuspension of particulates, then parameters affecting the biological processes were adjusted.

The settling velocity was initially calculated using Stokes equation with an assumed particle density of 2.7 g/cm^3 and a modal particle size is 7 phi units or ~ 0.01 mm for suspended sediments based on measurements of particulate diameters in Lake Houston by Matty et. al. (1987). The Stokes settling velocity is calculated to be 9×10^{-5} m/s. The resuspension rate was initially estimated to be in the range of 0.03 to 0.36 g/cm^2/day based on sediment fluxes measured by Matty et. al. (1987). However, the model over-predicted TSS concentrations using these values. As a result, the resuspension mechanism was not discretely simulated. Instead, the settling velocity was adjusted downward to account for the net effect of

settling and resuspension. The best agreement between model simulated values and measured TSS was obtained using a settling velocity of 4×10^{-6} m/s.

The primary phytoplankton parameters adjusted during calibration included phytoplankton growth rate, respiration rate, and death rate. The calibration process involved a stepwise adjustment of these parameters, within reasonable and acceptable ranges, until the model adequately reproduced the observed TSS and chlorophyll-a (Chl-a) data. The phytoplankton growth rate of 2 day^{-1}, respiration rate of 0.06 day^{-1} and death rate of 0.08 day^{-1} were fit to WASP model during calibration and were within the range of commonly used values in the literature.

Trends in the data

Figures 9.7, 9.8 and 9.9 show the TSS data collected at four SWQM stations along with model results for the three simulation years. During high-flow periods, TSS levels increase rapidly due to increased loadings and then decline due to settling. Such phenomenon can be found in the spikes in 2004 and 2008. During low-flow periods, algal growth can increase the TSS although the magnitude and rate of increase is much lower than during high-flow periods. In the later part of 2000, when flow is low and residence time high, TSS concentrations are observed to increase slightly during the warm season and fall slightly during the cold season. This trend mirrors the growing pattern of algae.

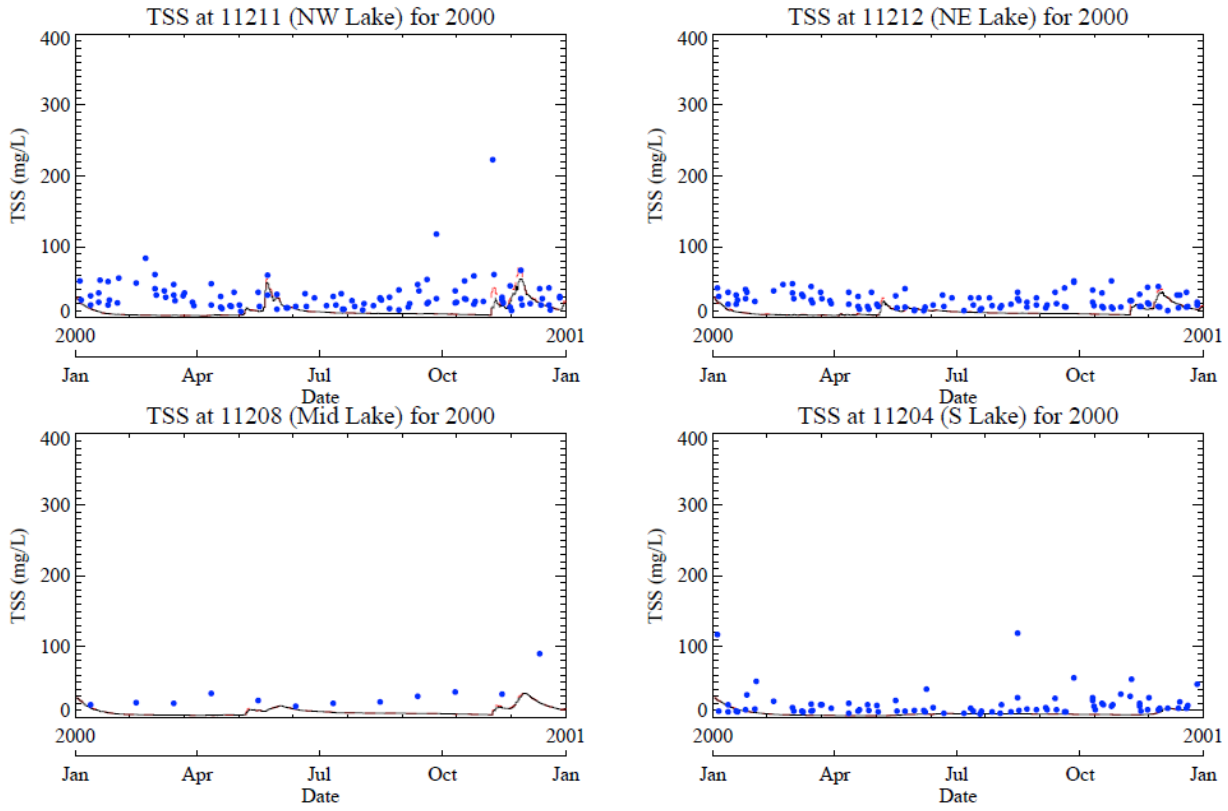

Figure 9.7 Predicted and observed Total Suspended Solids for 2000 (low-flow).

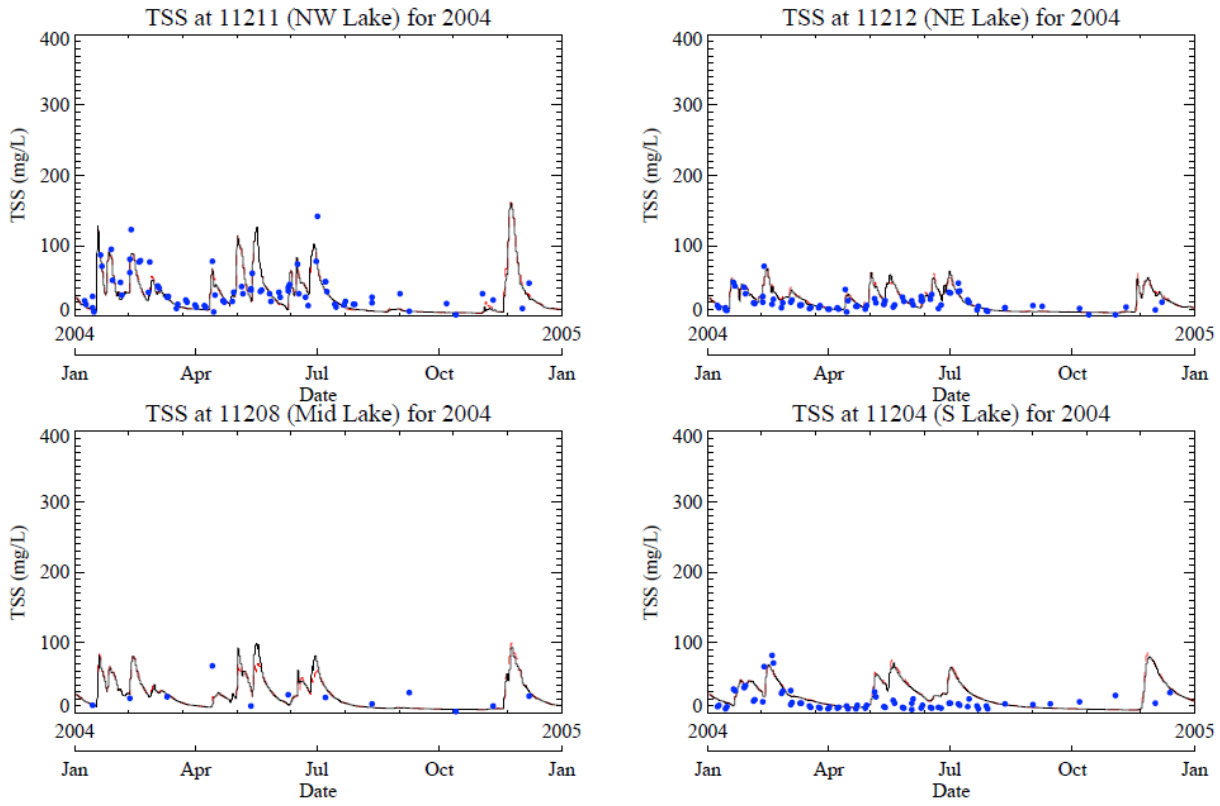

Figure 9.8 Predicted and observed Total Suspended Solids for 2004 (high-flow).

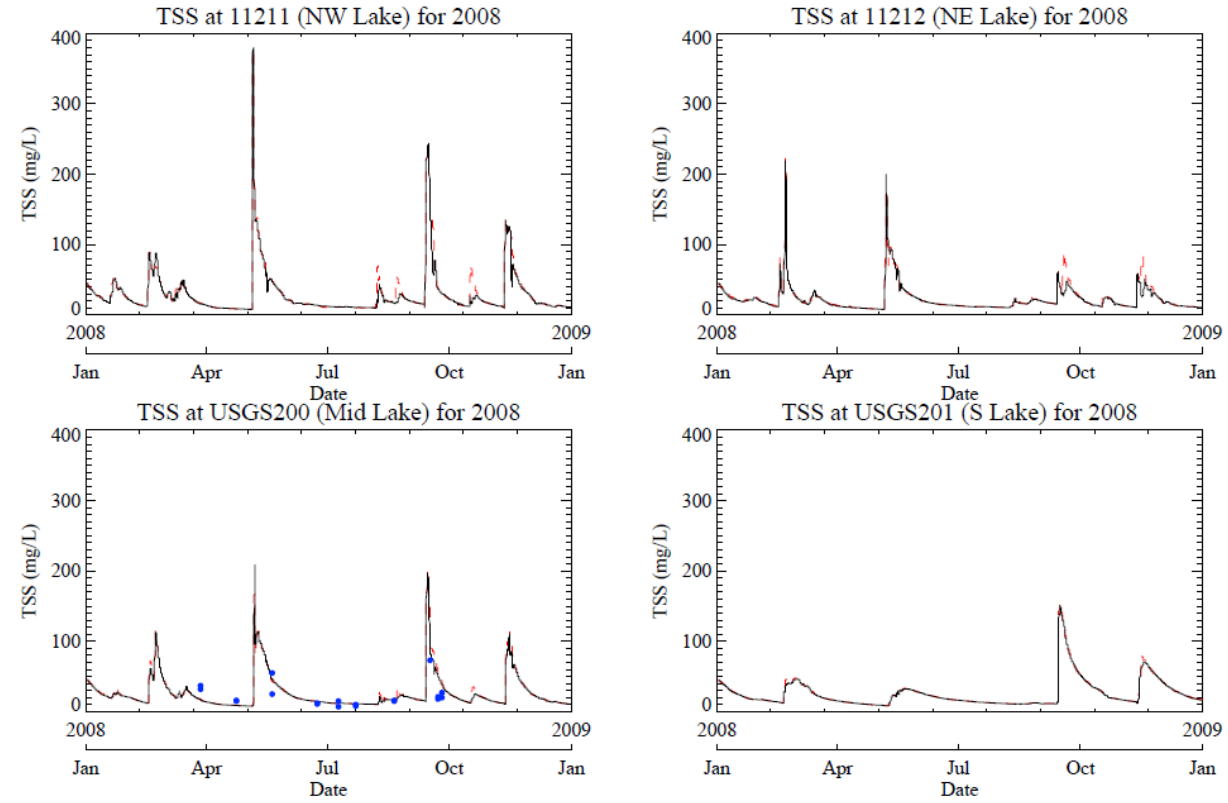

Figure 9.9 Predicted and observed Total Suspended Solids 2008 (normal-flow).

Figures 9.10, 9.11 and 9.12 plot simulated chlorophyll-a concentrations for the three simulation years with available measured data. Phytoplankton data are limited in Lake Houston. Three samples were collected in 2000, five in 2004 and none in 2008. Phytoplankton concentrations tend to be low. All samples for 2000 were non-detect, and three of the five samples for 2004 were non-detect. The only detected results from these samples were 7 ug/L (collected at 11212) and 33 ug/L (collected at 11204). Non-detects are plotted in the figure at half their detection limits.

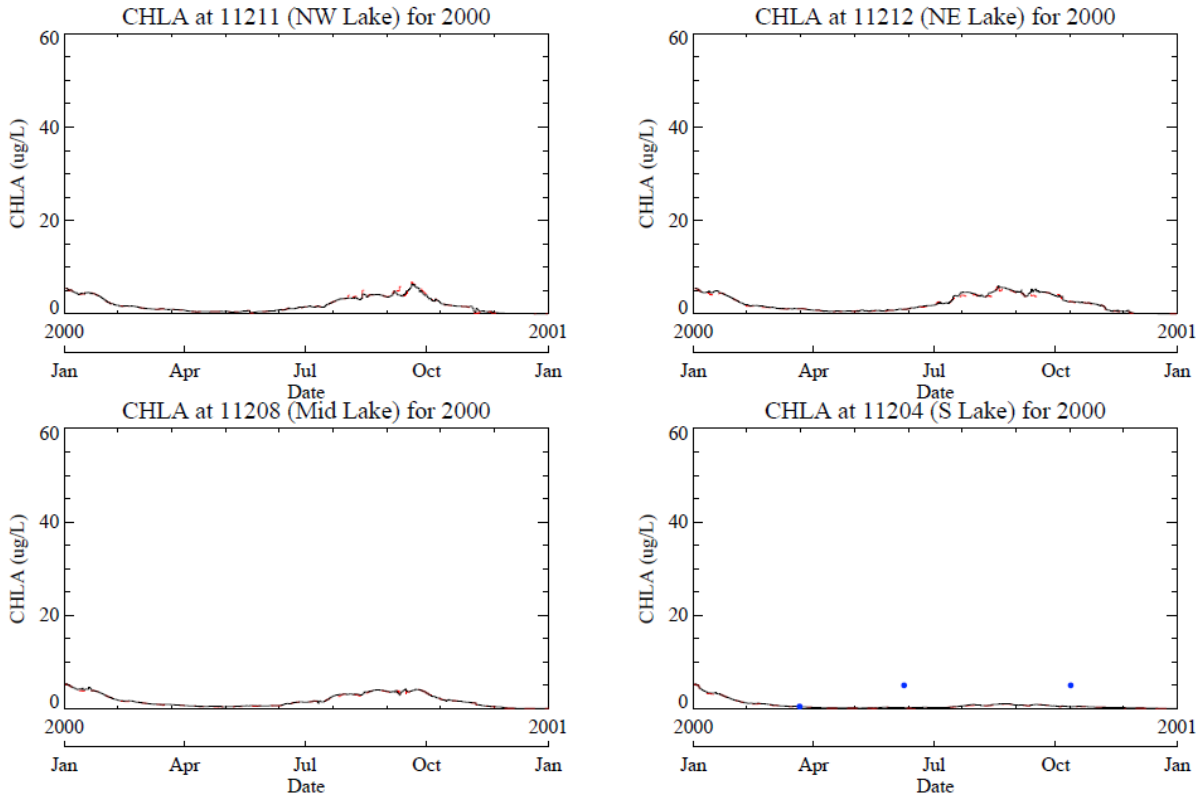

Figure 9.10 Predicted and observed chlorophyll-a for 2004 (high-flow).

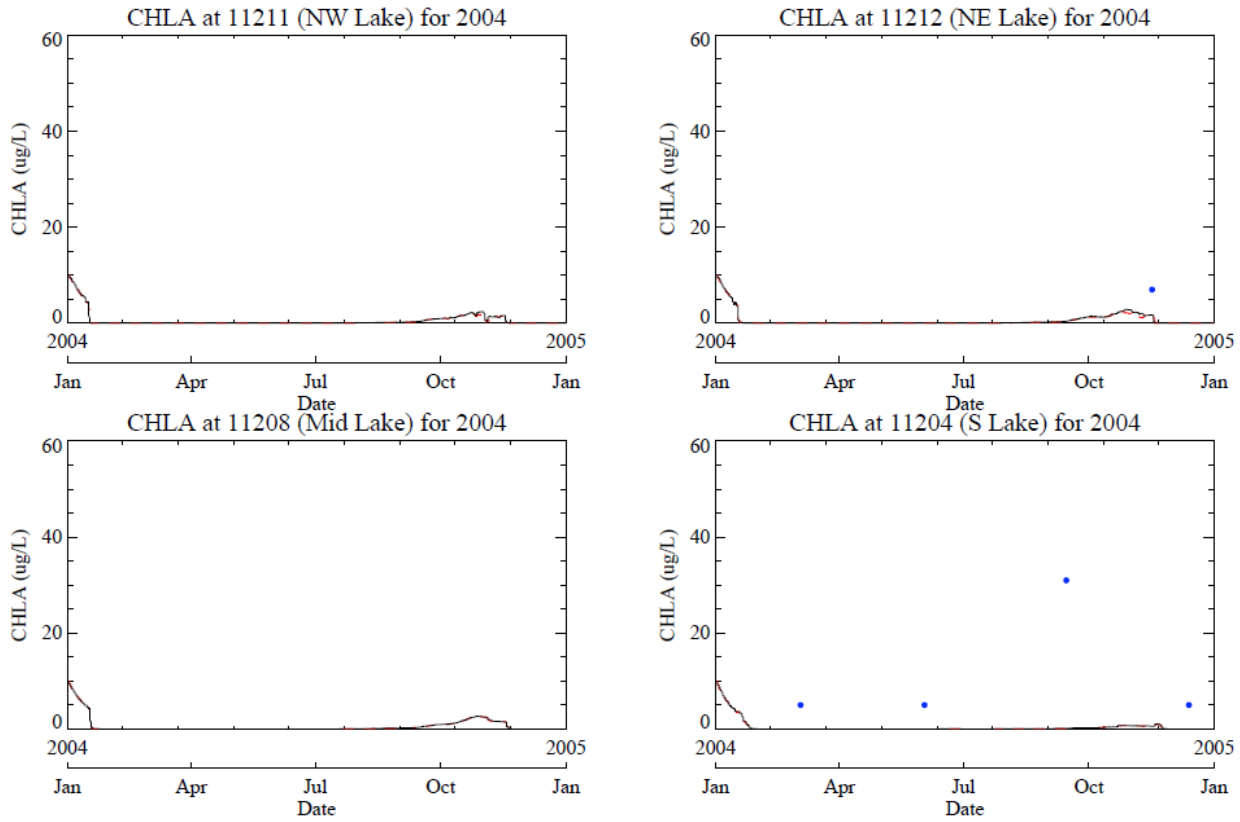

Figure 9.11 Predicted and observed chlorophyll-a for 2004 (high-flow).

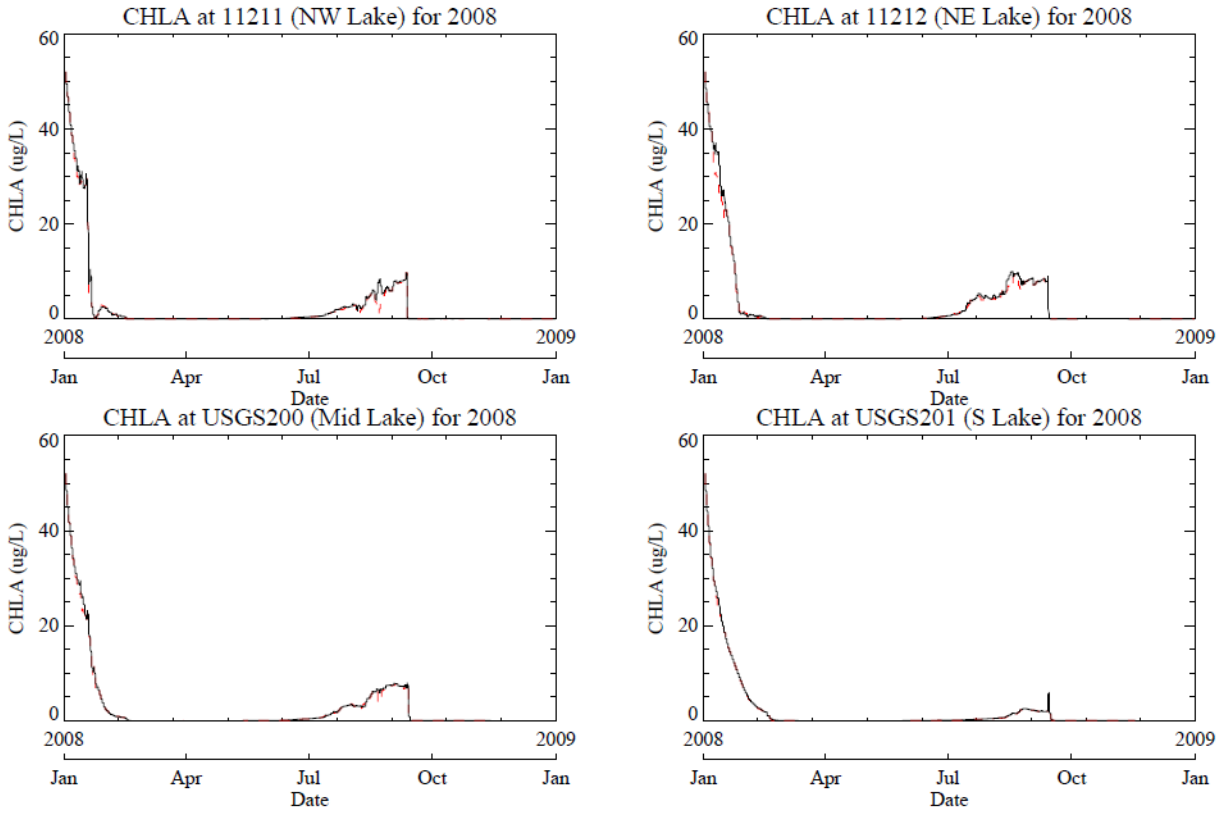

Figure 9.12 Predicted and observed chlorophyll-a for 2008 (normal-flow).

Performance of the model

For TSS, the simulated trends follow the data trends with high concentrations during high-flow periods and low concentrations during low-flow periods. Algal production of solids is insignificant compared to external loads as evidenced by the low chlorophyll-a concentrations. For low-flow, normal-flow and most high-flow periods, simulated values are within the range of the data.

These results indicate that physical mechanisms are responsible for the majority of the observed TSS variation. At extremely high-flow (such as during Hurricane Ike in September 2008), simulated values can sometimes be much greater than measured data. During the calibration, the TSS inflow concentrations described in Section 4 were reduced by 50 percent to obtain reasonable estimates of TSS in the lake. This discrepancy can be attributed to the following:

1 Limited means of characterizing upstream load.
- TSS data in the watershed are very limited. In West Fork, Peach Creek, and Luce Bayou, insufficient data are available to identify relationships between concentration and other factors, such as flows, so instead the average measured concentrations are used. A data gap exists for concentrations at high flow in these tributaries.
- LOADEST estimates TSS as a monotonic function of the streamflow. In reality, many factors can affect the TSS load carried by a stream (such as land use, channel morphology and sediment types), and the relationship can be much more complex and multi-faceted. For instance, although repeated high flows of similar magnitude occurred in 2004, TSS concentrations in the lake decreased with successive flushes. Because LOADEST estimates

the same TSS load for the same flow, it can over-estimate TSS for subsequent high-flow periods.

2. Limited means of characterizing sediment transport processes within the lake.
   Sediment transport is affected by many complex mechanisms including settling and resupension for cohesive and non-cohesive sediments. Although advanced simulation modules have been added to EFDC and WASP for simulating these mechanisms, these methods also require specialized data such as sediment critical shear stress, resuspension rates, and flocculation. These additional data can be measured by apparatus such as the sedflume (Lick, 2009).

It should be noted that during low-flow conditions (such as during 2000), the data show a persistent concentration of TSS that is higher than the model prediction. Because tributary loads and algal growth are insignificant during these conditions, a possible explanation for the source of this TSS is wind-induced resuspension in the lake. Matty et. al. (1987) noted that lake levels drop 1 to 2 m during droughts bringing the lake platform to within storm-wave base. Thus, high winds can agitate the bottom sediments and cause resuspension. Modeling wind-induced resuspension was not attempted in this study because of limited site-specific data on sediment shear stresses. Addition of wind-induced resuspension to the model is recommended for future work if data are available.

3. Calibration of nutrient species

In WASP, nutrient cycling is facilitated by microorganisms in the water as illustrated in Figure 9.13. Phytoplankton ingests inorganic nutrients (i.e., nitrate and phosphate) converting them into organic nutrients (org-N and org-P). The organic nutrients are released into the water column either through phytoplankton secretion or by dissolution of dead cell material. Dissolved organic nitrogen degrades into ammonia which is then converted to nitrate through nitrification. Dissolved organic phosphorus degrades into phosphate through mineralization. However, not all nutrients return to the nutrient cycle. Some nitrate is lost through denitrification and some phosphate is lost through adsorption to suspended solids.

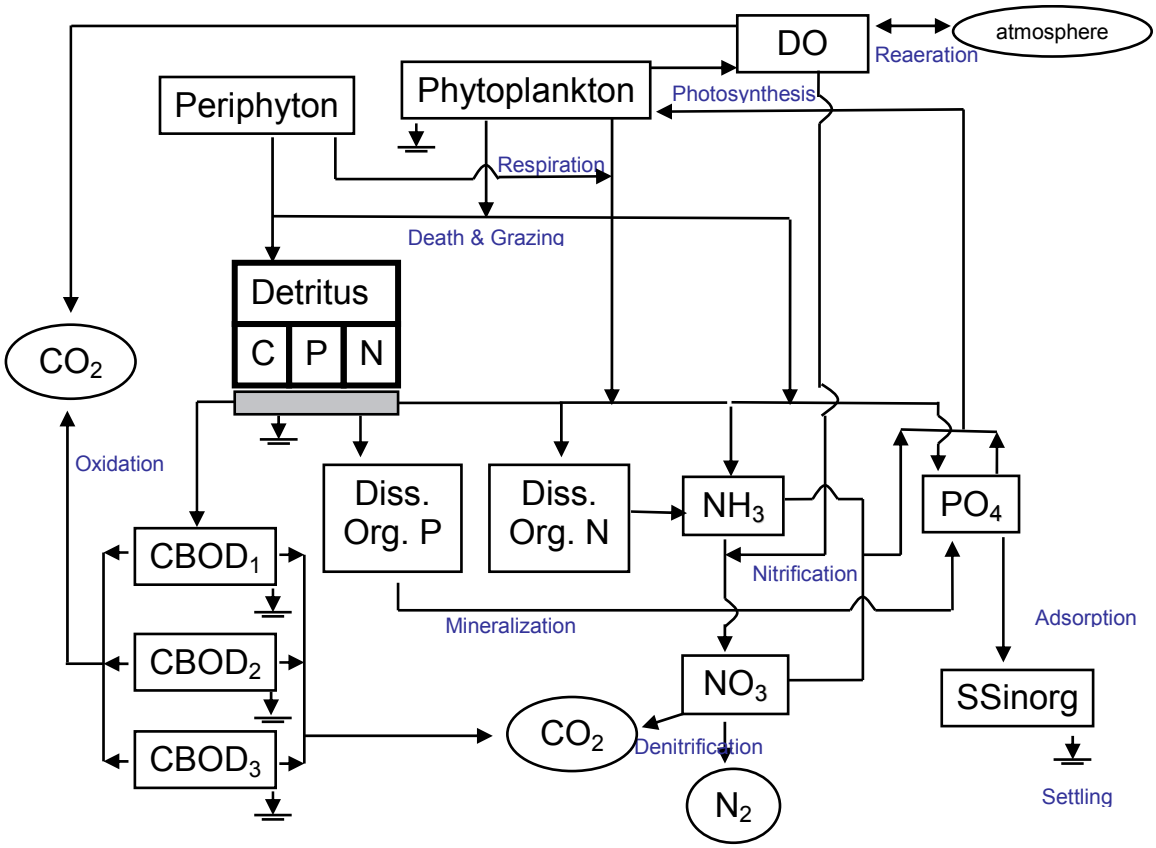

Figure 9.13. The nutrient cycle simulated by WASP's eutrophication model (EPA, 2009).

Trends in the data

Given the above nutrient cycle, dissolved organic nitrogen and organic phosphorus exhibit similar seasonal trends that are similar to that of phytoplankton. Concentrations of these nutrients increase when phytoplankton grows and decrease when the phytoplankton dies off. The inorganic nutrients are subjected to both phytoplankton processes and external loads and therefore undergo a more complicated cycle than the organics. Figures 9.14 to 9.22 show measured and simulated concentrations of inorganic nutrients (ammonia, nitrate, and phosphate). Figures 9.23 to 9.28 show the data and model outputs for the dissolved organic nutrients.

Model performance

Figure 9.14, 9.15 and 9.16 shows the simulated and observed nitrate concentrations for 2000, 2004 and 2008. The temporal trend of the simulated results follow the data well and the range of the simulated values agrees with that of the data. The availability of nitrate for phytoplankton activity was adjusted by changing the dissolved fraction. The final dissolved fraction used is 0.3. Nitrification and denitrification rates were used to fine-tune simulated nitrate concentrations. The final nitrification and denitrification rates used were 0.2 day^{-1} and 0.09 day^{-1}, respectively.

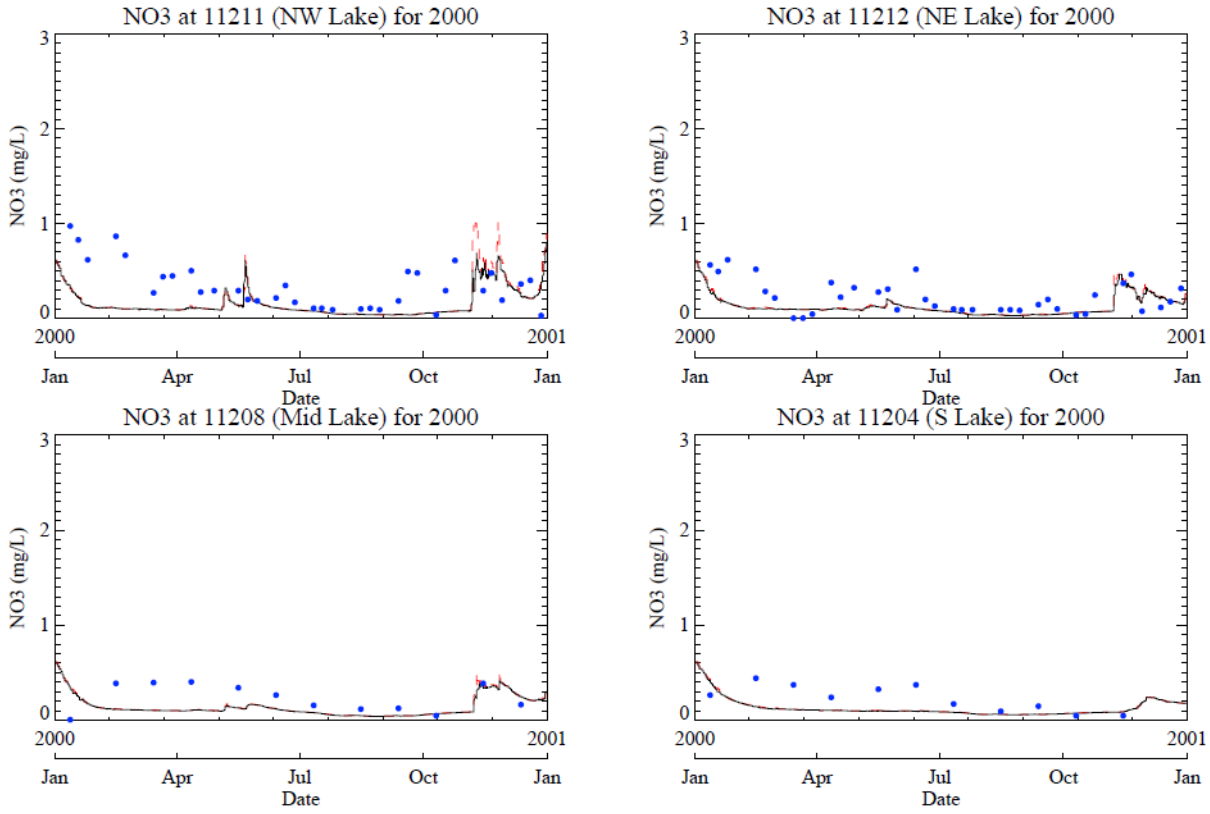

Figure 9.14 Predicted and observed nitrate for 2000 (low-flow).

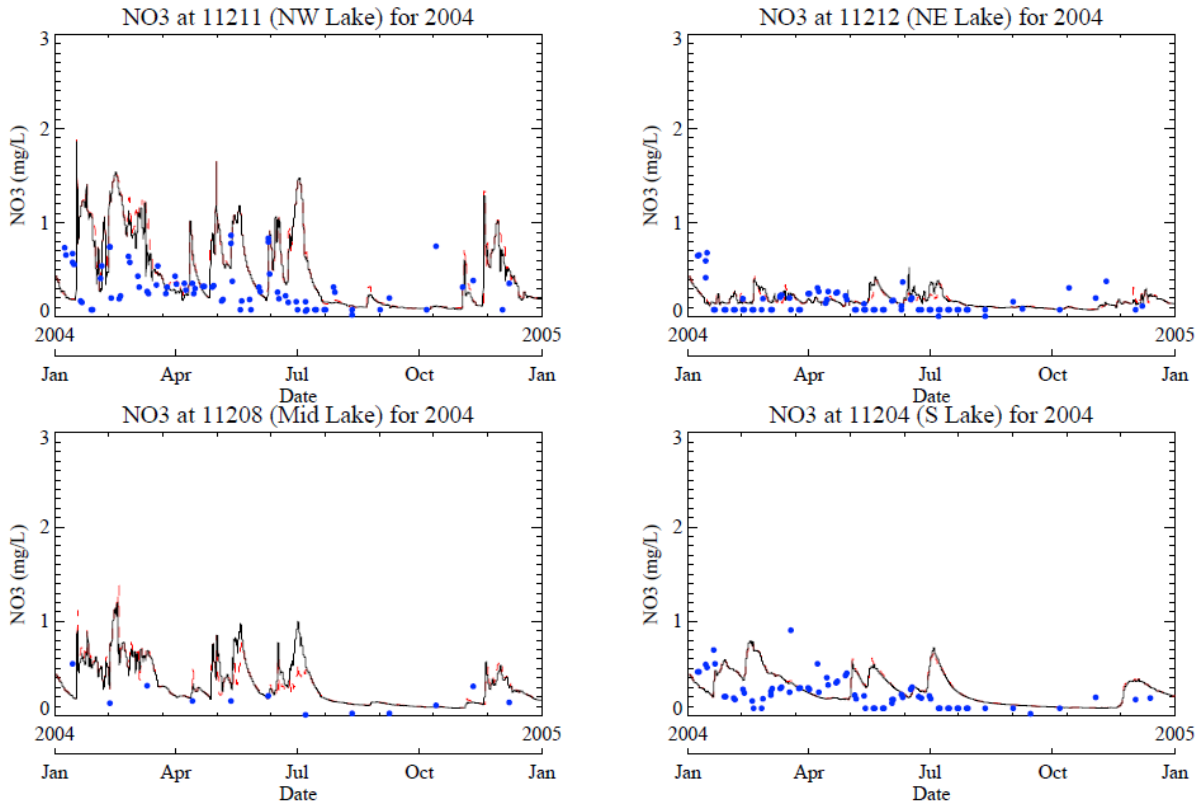

Figure 9.15 Predicted and observed nitrate for 2004 (high-flow).

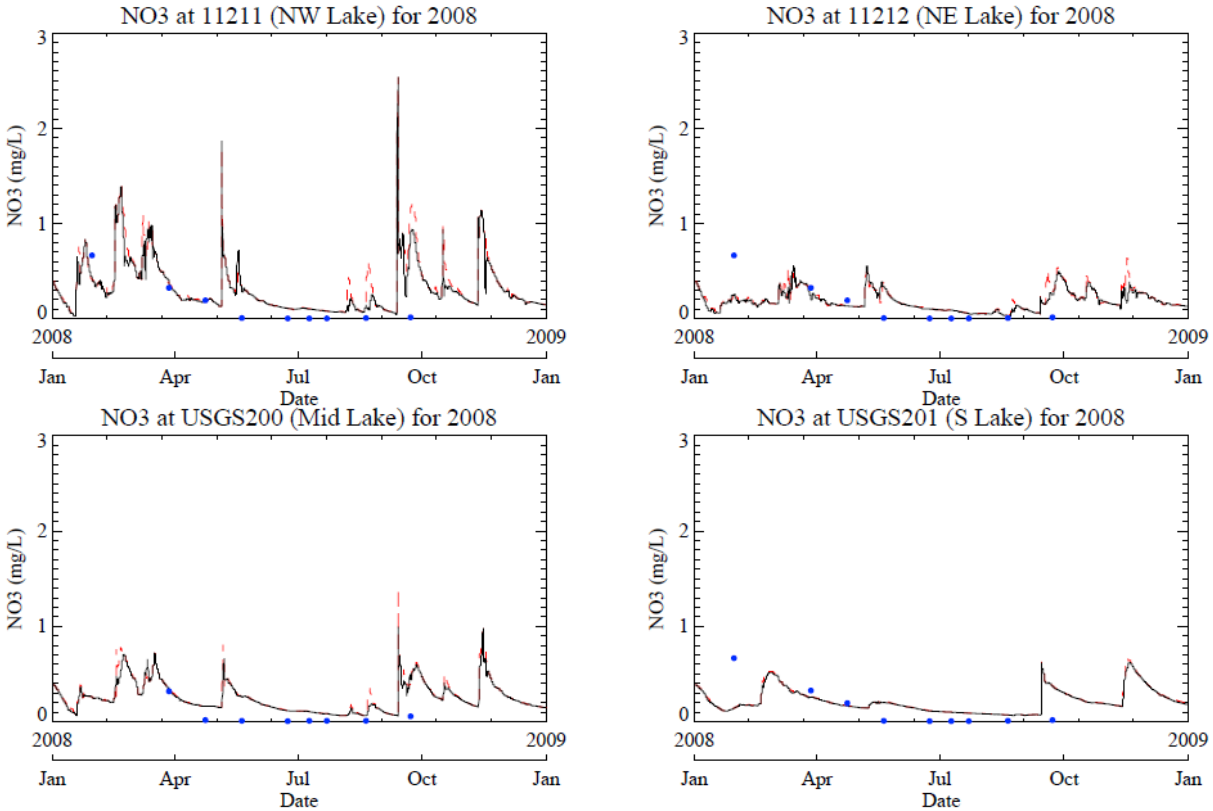

Figure 9.16 Predicted and observed nitrate for 2008 (normal-flow).

Figure 9.17, 9.18 and 9.19 shows the simulated and observed phosphate concentrations for 2000, 2004 and 2008. The simulated results follow the temporal trend of the data reasonably well and are within the range of the measured data. The availability of phosphate for phytoplankton activity was adjusted by changing the dissolved fraction. The final dissolved fraction used was 0.3. Mineralization rate was used to fine-tune the phosphate concentration. The final mineralization rate used was 0.01 day^{-1}.

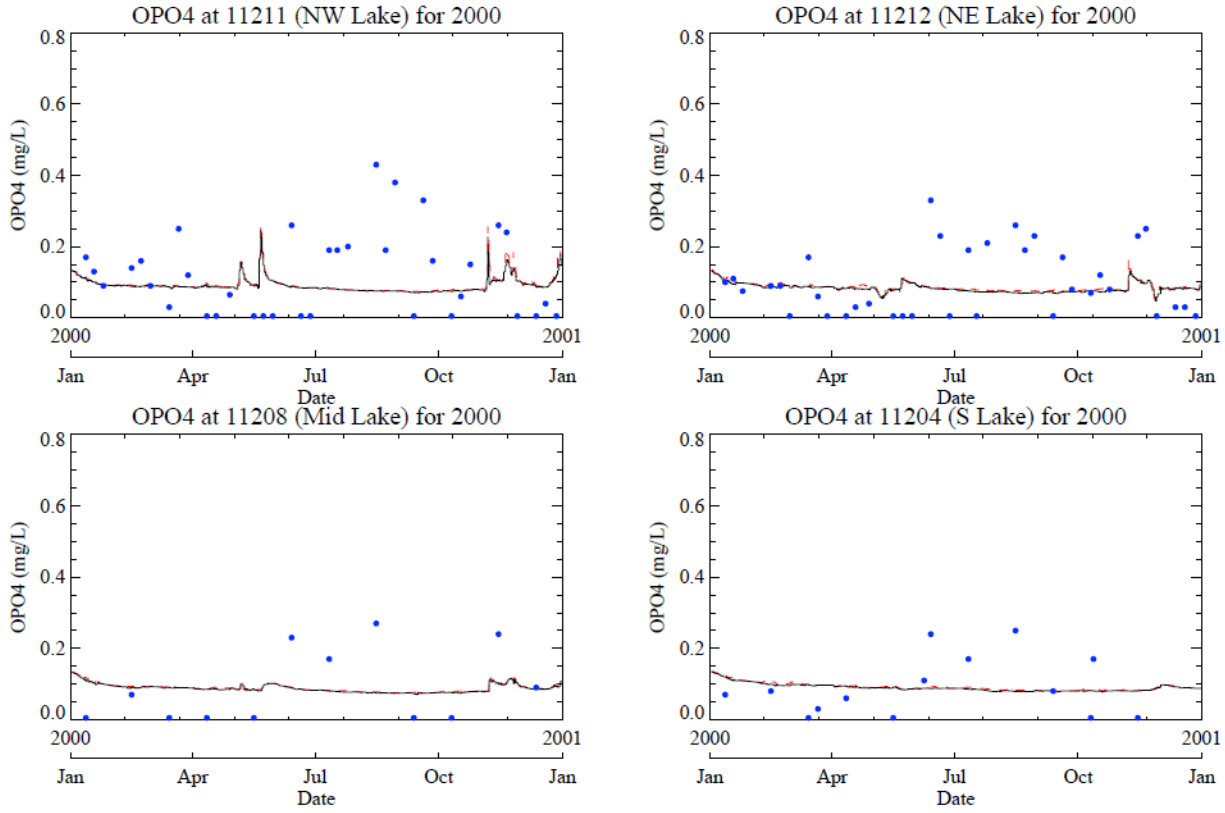

Figure 9.17 Predicted and observed phosphate for 2000 (low flow).

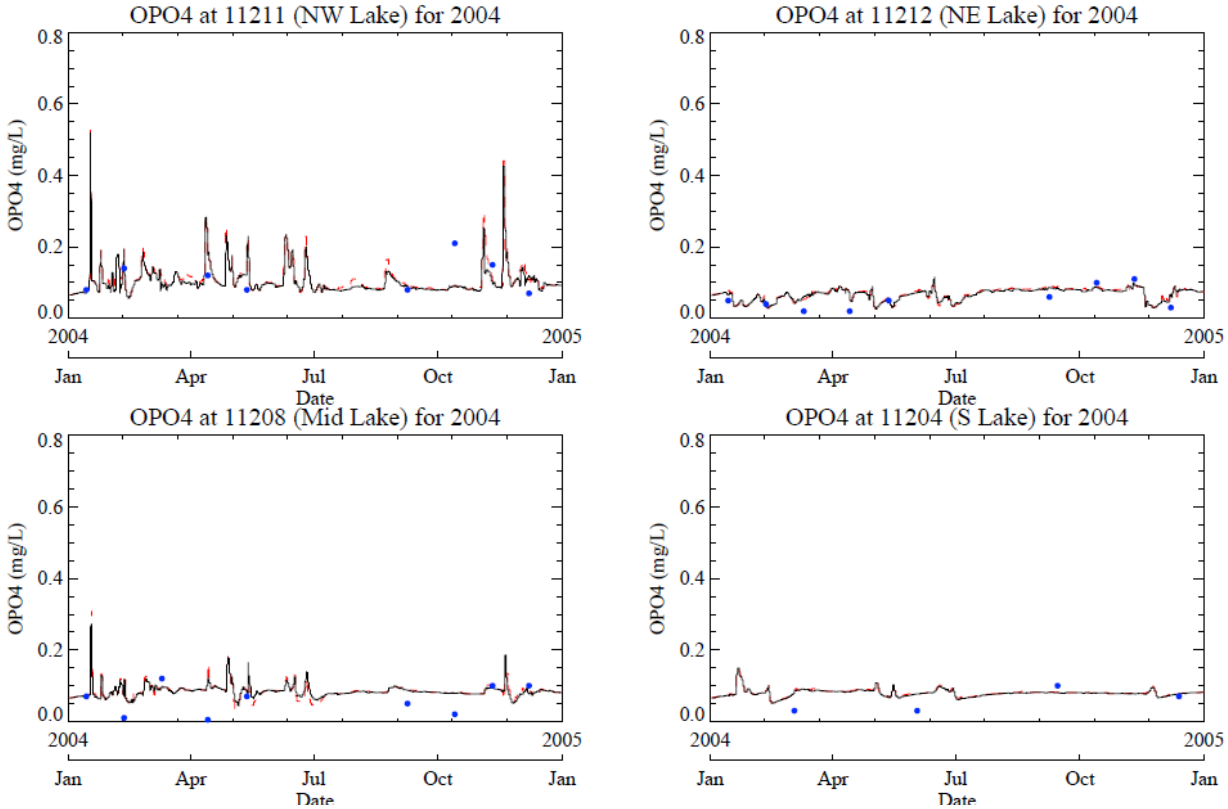

Figure 9.18 Predicted and observed phosphate for 2004 (high-flow).

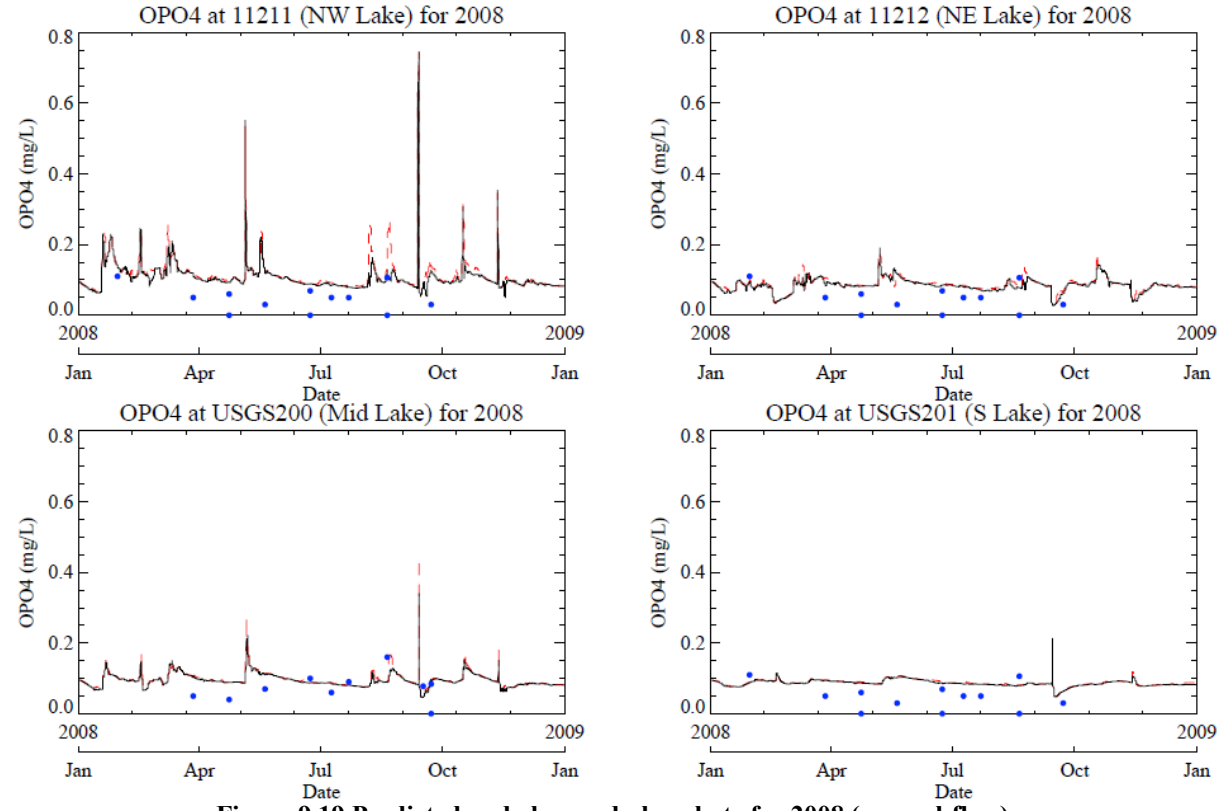

Figure 9.19 Predicted and observed phosphate for 2008 (normal-flow).

Figure 9.20, 9.21 and 9.22 show the simulated and observed ammonia concentrations for 2000, 2004 and 2008. The simulated results follow the temporal trend of the data and are within the range of data values for 2000 and 2004. Ammonia concentrations were significantly higher in the measured data in 2008 from both TCEQ and USGS stations than in 2000 and 2004. Because inflow patterns were normal in 2008, it is unclear what caused the increase in ammonia, and therefore further investigation is recommended. For 2008, simulated values are near the lower end of measured range. During calibration, the availability of ammonia for phytoplankton activity was adjusted by changing the dissolved fraction. The final dissolved fraction used was 0.7.

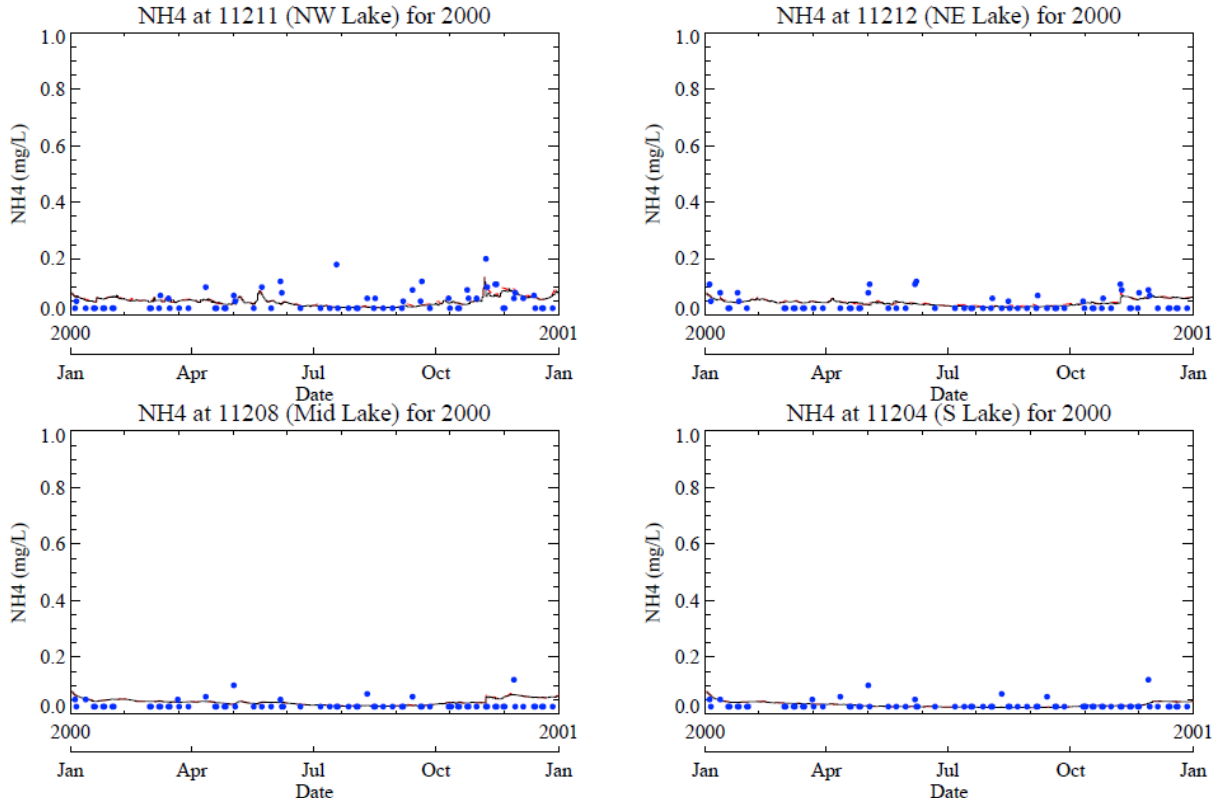

Figure 9.20 Predicted and observed ammonia concentrations for 2000 (low-flow).

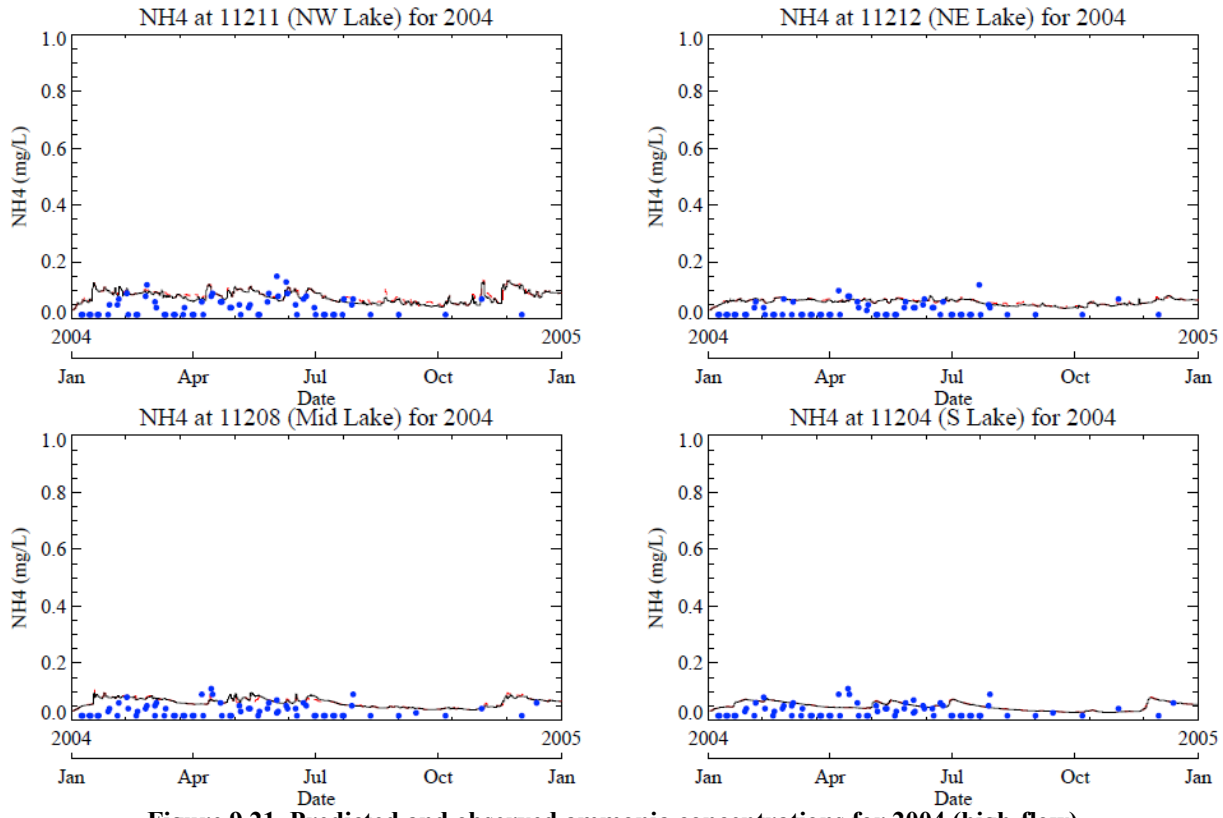

Figure 9.21 Predicted and observed ammonia concentrations for 2004 (high-flow).

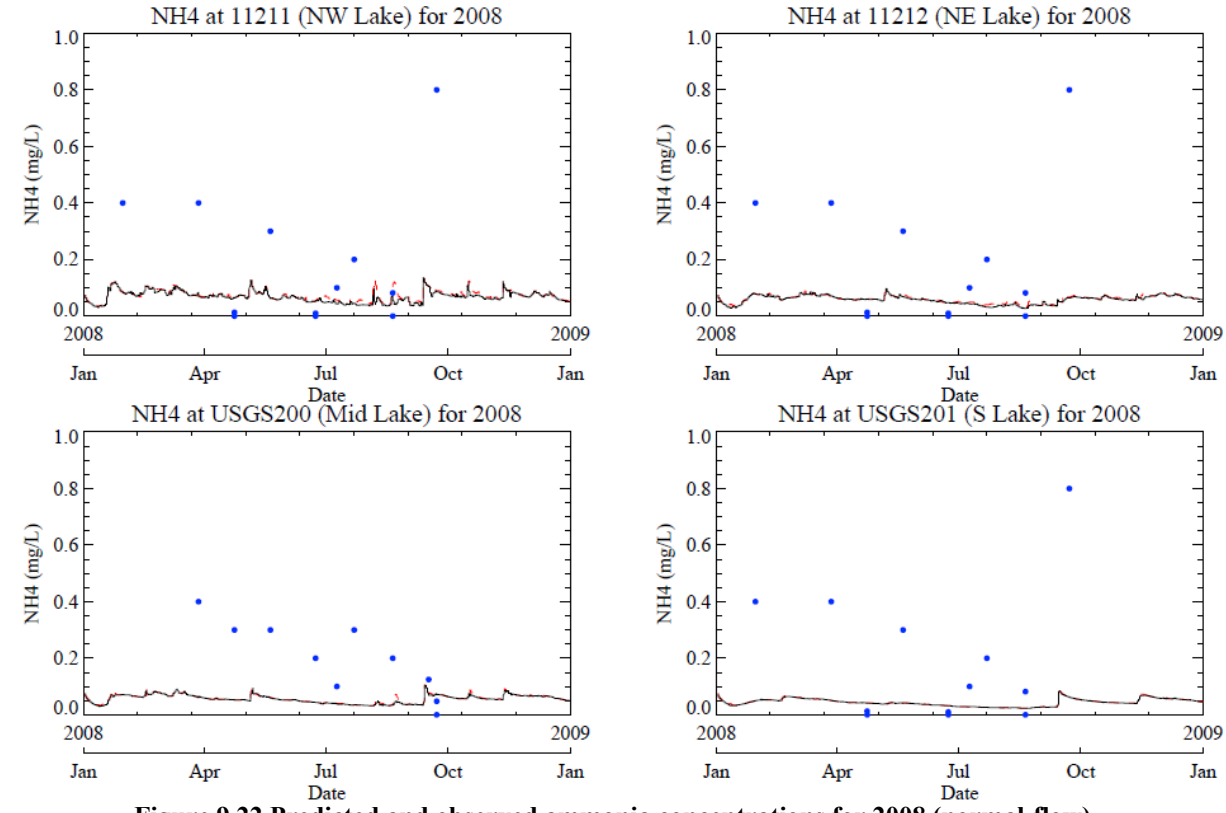

Figure 9.22 Predicted and observed ammonia concentrations for 2008 (normal-flow).

Figure 9.23, 9.24 and 9.25 show the simulated and observed dissolved organic nitrogen concentrations for 2000, 2004 and 2008. Comparison is difficult due to the scarcity of the data. Looking across all years, the simulated values are generally within an order of magnitude of the data. The final dissolved fraction used was 0.95.

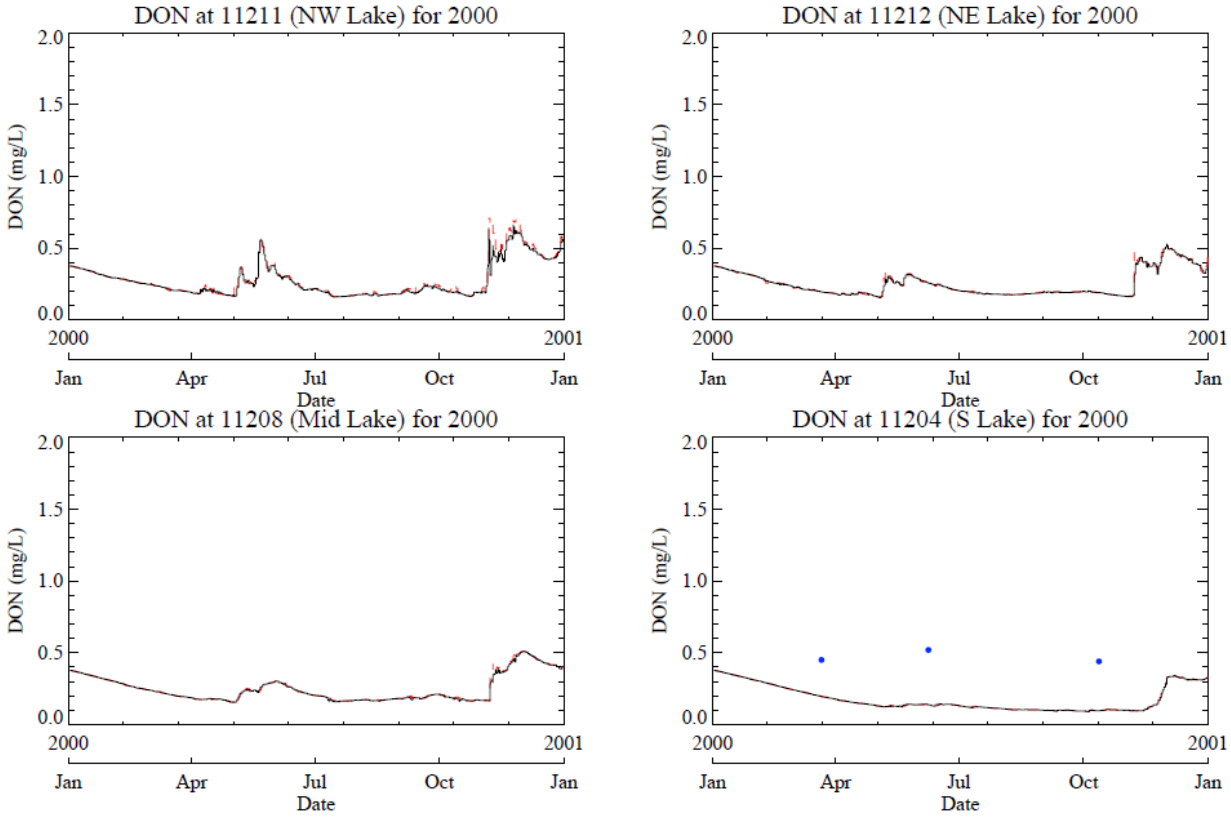

Figure 9.23 Predicted and observed dissolved organic nitrogen for 2000 (low-flow)

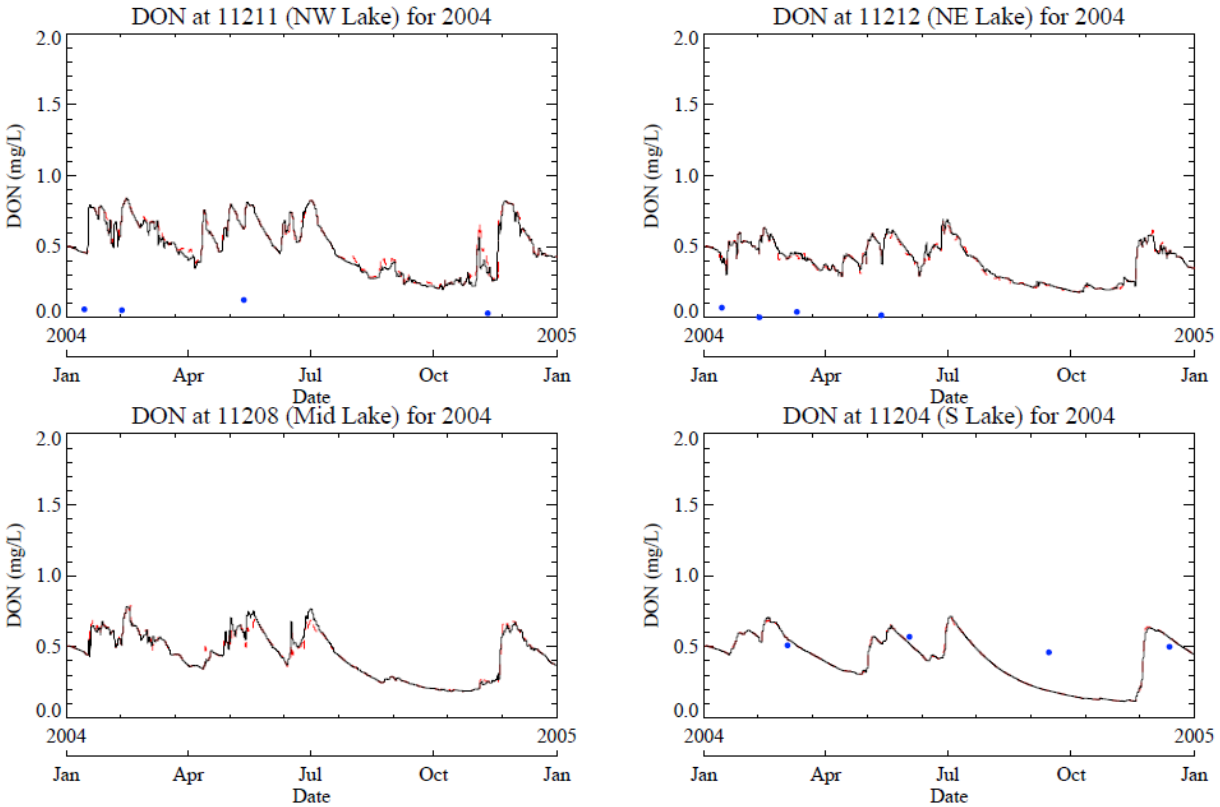

Figure 9.24 Predicted and observed dissolved organic nitrogen for 2004 (high-flow).

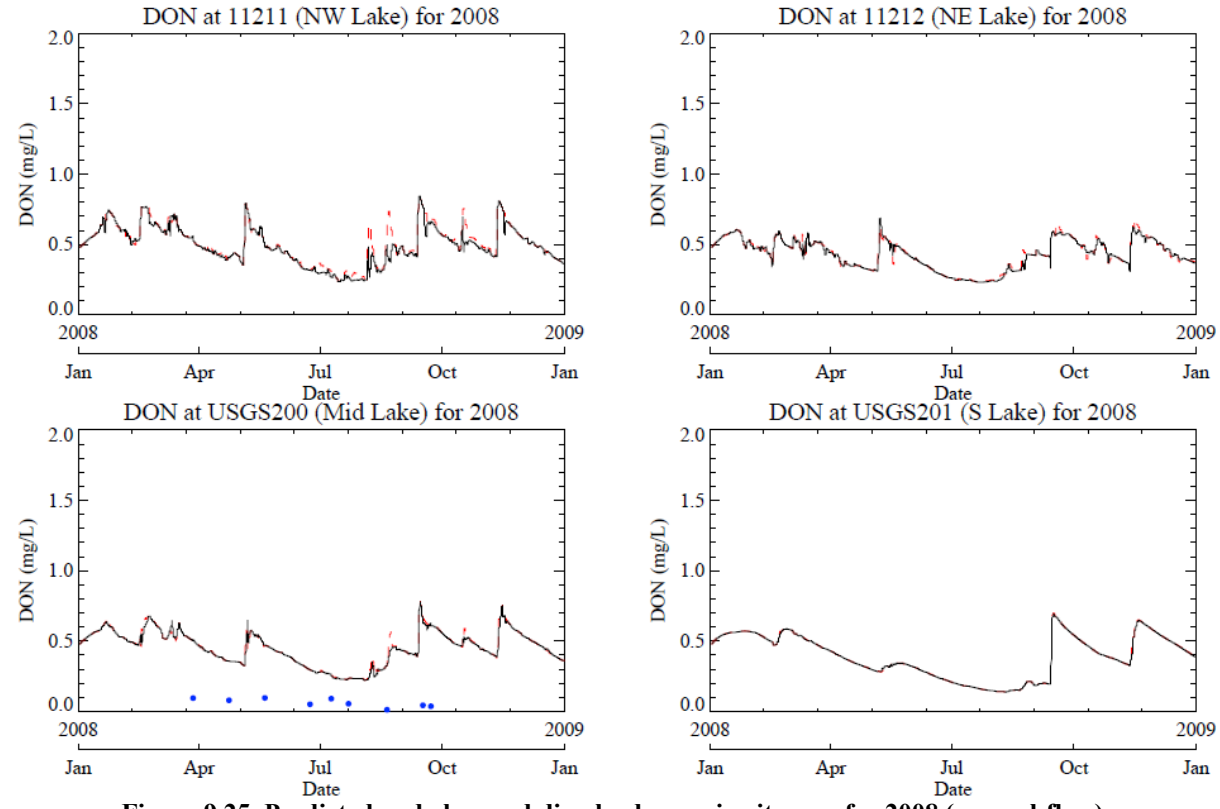

Figure 9.25 Predicted and observed dissolved organic nitrogen for 2008 (normal-flow).

Figure 9.26 shows the simulated and observed dissolved organic phosphorus concentrations for 2000, 2004 and 2008. In general, the simulated results are within the range of the data and show some adherence to the observed trends. The availability of dissolved organic phosphorus for phytoplankton activity was adjusted by changing the dissolved fraction. The final dissolved fraction used was 1.0.

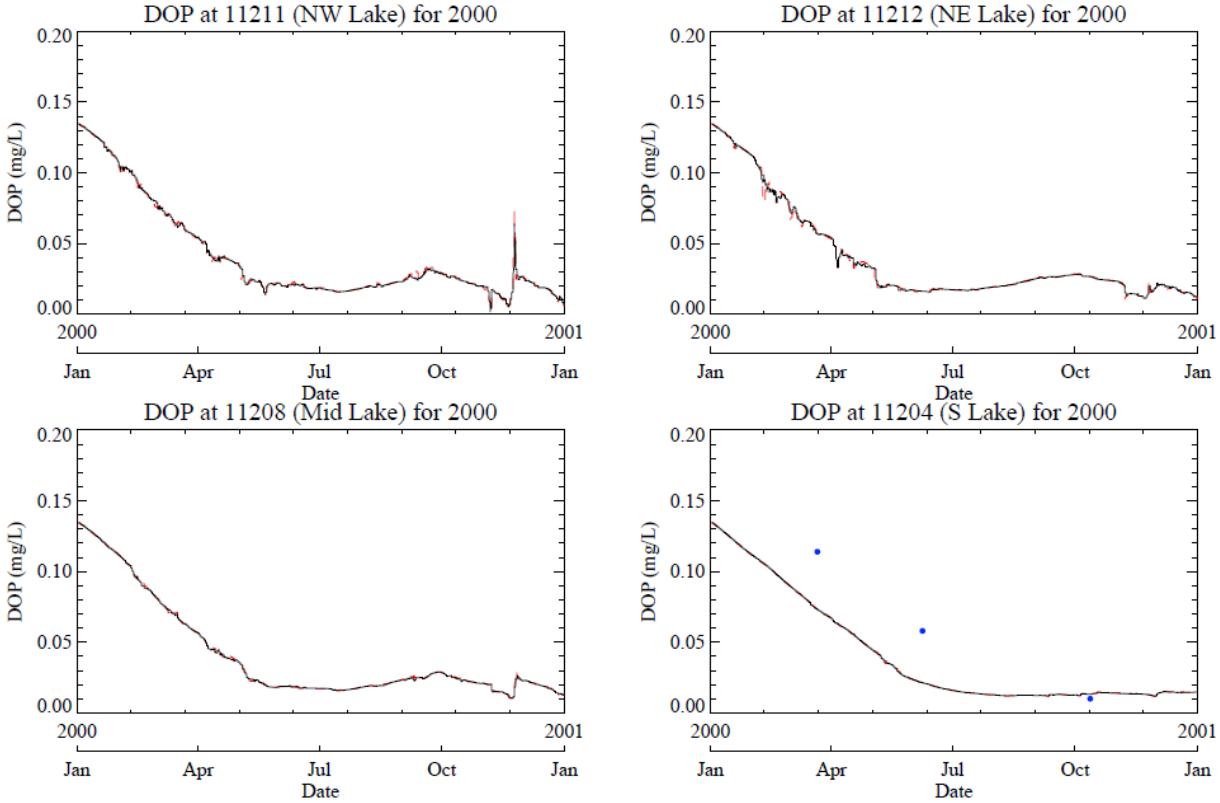

Figure 9.26 Predicted and observed dissolved organic phosphorus for 2000 (low-flow).

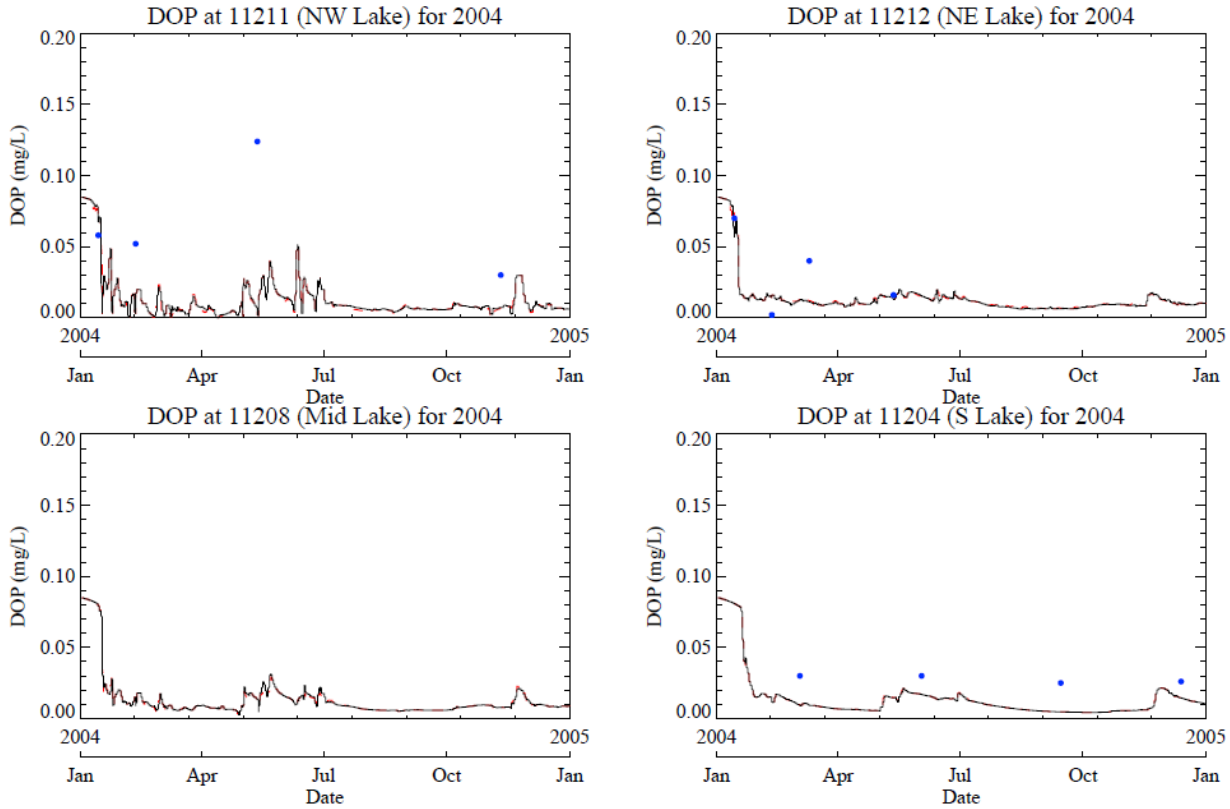

Figure 9.27 Predicted and observed dissolved organic phosphorus for 2004 (high-flow).

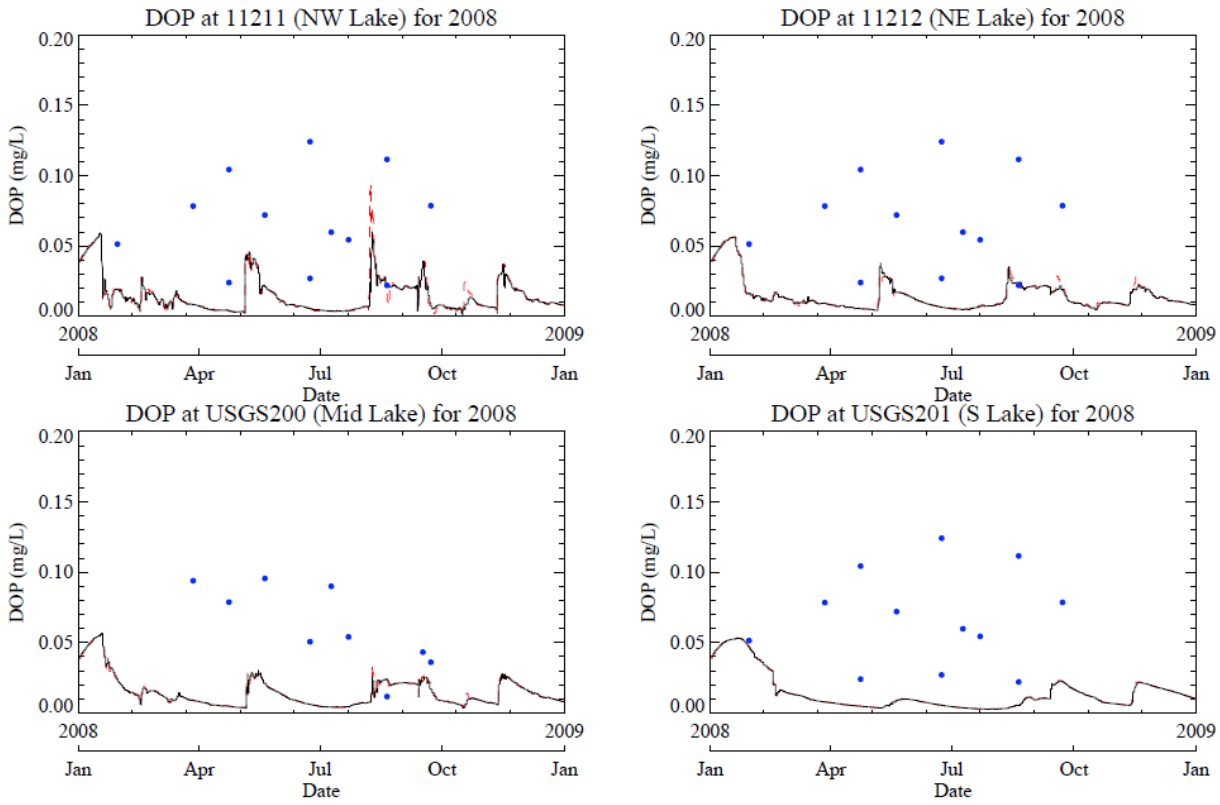

Figure 9.28 Predicted and observed dissolved organic phosphorus for 2008 (normal-flow).

9.4 CALIBRATION CONCLUSIONS

Calibration of the WASP water quality model for dissolved oxygen, total suspended solids and nutrients produced reasonable results with the model output representing most trends in the data for low-flow, high-flow and normal-flow scenarios. Based on the available data for Lake Houston and supporting watershed, the calibrated WASP model is sufficient to perform evaluations of different diversion and drawdown scenarios. Discussions of the scenarios and model results are provided in the next section.

10.0 WATER QUALITY EVALUATION SCENARIOS

Water quality scenarios were defined to evaluate impacts on eutrophication and nutrient concentrations under different combinations of diversion scenarios (with or without 400 MGD diversion) and lake drawdown scenarios (0 ft, 2 ft, and 5 ft). A total of 12 scenarios were simulated as shown in Table 10.1.

Table 10.1 Summary of scenarios for WASP water quality evaluation

Year	400 MGD Luce Bayou Diversion?	Drawdown (ft)		
2000 (low-flow)	Yes	0	2	5
	No	0		
2004 (high-flow)	Yes	0	2	5
	No	0		
2008 (normal-Flow)	Yes	0	2	5
	No	0		

10.1 RESULTS OF SCENARIO SIMULATIONS

Time series plots of each water quality parameter at the NEWPP intake location for each scenario are provided in Appendix E. An example showing simulated dissolved oxygen concentrations under average flow conditions is shown in Figure 10.1. Each figure consists of four panels, each showing the time series of a given water quality parameter at both top and bottom depths for one simulation year under one of the four evaluation scenarios (no diversion and 0ft drawdown, 400 MGD diversion and 0ft drawdown, 400 MGD diversion and 2ft drawdown and 400 MGD diversion and 5ft drawdown. A summary and comparison of the scenario results is presented in the next section.

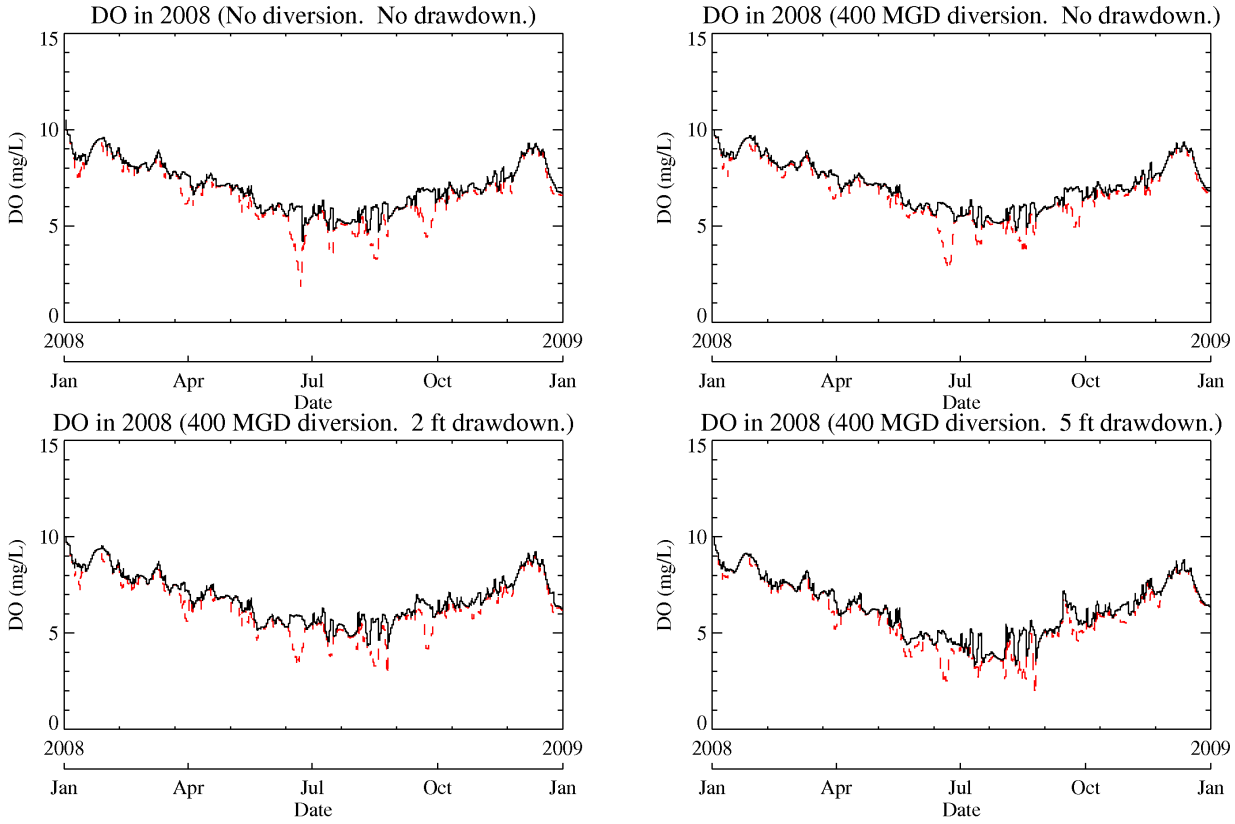

Figure 10.1 An example of scenario results in Appendix E (Dissolved oxygen concentrations at NEWPP under various scenarios for 2008).

10.2 DISCUSSION ON SCENARIO SIMULATION RESULTS

The time-averaged mean concentration at the NEWPP intake of each water quality parameter for each simulation year is presented in Table 10.2. The mean concentration is an average of the top and bottom values. CBOD, chlorophyll-a, and nutrient and concentrations near the intake are relatively unaffected by the diversion. Dissolved oxygen concentrations are improved slightly, and the change in TSS levels depends strongly on the flow conditions. Generally, the scenario with 400 MGD diversion and no drawdown offers the best water quality because of the better quality of the diverted Trinity River water. Water quality deteriorates with increasing lake drawdown because nutrient loads and benthic effects (such as sediment oxygen demand, benthic ammonia flux, and benthic phosphate flux) are exerted on smaller volumes of water. A detailed discussion of each parameter is provided in the following paragraphs.

Table 10.2 Mean concentrations of water quality parameters under different scenarios

Parameter	Flow Condition	No diversion, No drawdown	With 400 MGD diversion, No drawdown	With 400 MGD diversion, 2 ft drawdown	With 400 MGD diversion, 5 ft drawdown
DO (mg/L)	Low (2000)	6.89	**7.17**	6.80	5.80
	High (2004)	6.81	**6.89**	6.67	6.10
	Avg (2008)	6.86	**6.95**	6.67	6.10
CBOD (mg/L)	Low (2000)	**0.01**	0.04	0.19	0.27
	High (2004)	**0.75**	0.85	0.99	1.24
	Avg (2008)	**0.39**	0.44	0.59	0.84
TSS (mg/L)	Low (2000)	**5.28**	11.15	11.20	12.51
	High (2004)	22.12	**21.35**	21.95	23.03
	Avg (2008)	24.80	24.33	**19.56**	22.90
CHLA (ug/L)	Low (2000)	**0.75**	6.05	5.95	10.12
	High (2004)	0.44	**0.33**	0.42	0.48
	Avg (2008)	2.24	2.13	**2.09**	2.27
NO3 (mg/L)	Low (2000)	0.12	**0.08**	0.11	0.11
	High (2004)	**0.26**	0.27	0.29	0.31
	Avg (2008)	**0.20**	0.27	0.23	0.28
NH4 (mg/L)	Low (2000)	**0.03**	**0.03**	0.04	0.05
	High (2004)	**0.05**	**0.05**	0.06	0.06
	Avg (2008)	**0.05**	**0.05**	**0.05**	0.06
DON (mg/L)	Low (2000)	**0.17**	0.34	0.37	0.40
	High (2004)	**0.41**	0.43	0.44	0.46
	Avg (2008)	**0.38**	0.39	0.39	0.42
DOP (mg/L)	Low (2000)	0.04	**0.03**	**0.03**	**0.03**
	High (2004)	**0.01**	0.02	0.02	0.02
	Avg (2008)	**0.01**	0.02	0.02	0.02
OPO4 (mg/L)	Low (2000)	0.09	**0.07**	0.08	0.10
	High (2004)	**0.08**	**0.08**	**0.08**	0.09
	Avg (2008)	**0.09**	0.12	0.10	0.12

10.2.1 Dissolved oxygen

For all simulation years, dissolved oxygen increased with the diversion – especially for the low flow year (2000). In the 2000 simulation, the mean DO increases from 6.89 to 7.17 mg/L. The increase can be explained by the reduction in residence time in the reservoir due to more inflows. As a result sediment oxygen demand is exerted over a shorter time period.

The diversion also benefits water quality by reducing the DO stratification in the lake. Figure 10.2 shows results from two scenarios in 2000. The scenario on the left (no diversion, no drawdown) indicates the occurrence of hypoxia at the lake bottom in the month of August. The scenario on the right (400 MGD diversion, no drawdown) shows higher DO for the same period.

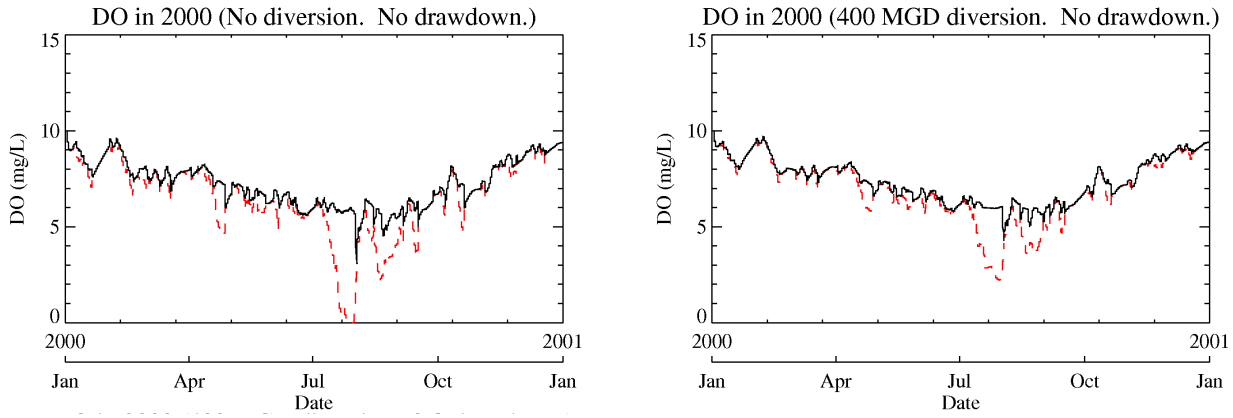

Figure 10.2 Dissolved oxygen time series in 2000 under diversion and no diversion scenarios.

For all years, increasing drawdown lowers dissolved oxygen concentrations. This effect is likely due to the exertion of sediment oxygen demand on a smaller volume of water. The average DO concentration across all the three simulation years with diversion and no drawdown is 7.0 mg/L. After the 2 ft drawdown the concentration drops to 6.7 mg/L. After the 5 ft drawdown, the concentration drops to 6.1 mg/L. On average, each additional 1 foot of drawdown causes a 0.2 mg/L drop in DO.

10.2.2 Ultimate Carbonaceous Biological Oxygen Demand

For all years and scenarios, the mean CBOD (ultimate) concentrations are below the detection limit of 9 mg/L . Because of the low levels of CBOD, the differences in concentrations from the various scenarios are not considered appreciable.

10.2.3 Total suspended solids

The TSS response of the lake to the diverted water depends on the flow condition. For high flow and normal flow years, the lower TSS concentrations in the Trinity River water have a diluting effect on the TSS from the West Inlet and North Inlet. The West Inlet and North Inlet TSS concentrations are approximately 50 mg/L and 100 mg/L, respectively (recall Figures 4.4 and 4.7) while the Trinity River concentration is approximately 25 mg/L (Figure 4.13). For 2004 the TSS concentrations drop slightly from 22.1 to 21.3 mg/L with the diversion. For 2008, the TSS concentrations drop slightly from 24.8 to 24.3 mg/L with the diversion.

On the other hand, for the low flow year (2000), TSS concentrations in the lake increase with the diversion. This is because the mean TSS concentration in the lake are low (5.3 mg/L) due to the limited contribution from the watershed. Diverting the Trinity River increases the TSS in the lake to 11.2 mg/L.

Despite the model results, it is known that wind-induced resuspension can occur when lake levels are low (Matty, et al., 1987). Because the model has limited ability in simulating this mechanism, it is likely that the lake TSS concentrations are also high during low-flow periods (recall Figure 9.7) and that the diverted Trinity River may drop the TSS concentrations slightly. However, to simulate this process in the model, additional data on sediment shear stresses and wind resuspension are needed.

Therefore, based on the analysis of the scenarios, the diverted Trinity River water decreases turbidity in the lake for most cases (i.e., normal and high-flow) although the magnitude of the difference tends to be small.

10.2.4 Chlorophyll-a (Chl-a)

The chlorophyll-a response of the lake to the diversion also depends on flow conditions. For the low flow year, chlorophyll-a concentrations increase from 0.75 µg/L to 6.1 µg/L with the diversion. This increase likely occurs because the Trinity River water carries more algal biomass (~ 15 µg/L Chl-a, see Figure 4.14) than the inflows to the West Inlet (~ 7.5 µg/L Chl-a, see Figure 4.5) and the North Inlet (~ 1.8 µg/L Chl-a, see Figure 4.8). In addition, the 400 MGD of diverted Trinity River water accounts for a high portion of the total flow into the lake during low flow conditions. Actual algal biomass imported from the Trinity River water will also depend on how the water is transported. If the water is transported in a pipeline the algal mass will decrease as opposed to an open channel transport.

For the high flow and normal flow years, simulated chlorophyll-a concentrations do not increase with the diversion. An increase in chlorophyll-a is not noticeable because the Trinity River flow accounts for a smaller portion of the total flow into the lake and because lake residence times are shorter resulting in less time available for algal growth.

Chlorophyll-a concentrations are observed to increase with larger drawdowns, possibly due to the increase in abundance of nutrients (such as nitrate) or increased detention time in the lake.

10.2.5 Nitrate

For the normal and high flow years, the diversion of the 400 MGD Trinity River causes nitrate concentrations to increase slightly. This is likely due to the decrease in residence time by the diversion. Nitrate is a substrate that is consumed by phytoplankton during cell synthesis. When residence times are short, less nitrate is consumed and nitrate concentrations remain high. When residence times are long, more nitrate is consumed and nitrate concentrations are reduced. However, for the simulation year 2000, simulated nitrate concentrations decrease with the diversion. A possible explanation for this is that in the Trinity River, nitrate is positively correlated with streamflow (recall Table 4.1). Therefore, the lower nitrate concentrations that occur during low flow may dilute nitrate concentrations in the lake. Nitrate concentrations are observed to increase with larger drawdowns.

10.2.6 Ammonia

Ammonia concentrations do not change appreciably with the diversion. This is likely because the effects of the benthic ammonia flux (13.5 $mg/m^2/d$) dominates over the ammonia loads from the tributaries. Ammonia concentrations in the lake increase slightly with larger drawdowns due to the exertion of the benthic flux on a smaller volume of water. However, the effects of the increase are not significant. For instance, for the simulation year 2000, increasing the drawdown from 0 ft to 2 ft only increases the ammonia concentration from 0.03 to 0.04 mg/L.

10.2.7 Dissolved organic nitrogen

The response of dissolved organic nitrogen concentrations to drawdowns and diversions is similar to that of chlorophyll-a possibly because DON is a by-product of cell synthesis. DON concentrations increase with the diversion and with larger drawdowns.

10.2.8 Phosphate

The response of phosphate to diversions and drawdowns is somewhat mixed. Simulated phosphate concentrations are low (< 0.1 mg/L) for all years. Although no obvious trends can be found, the mean

phosphate concentrations from the alternate scenarios tend to remain within 0.03 mg/L from the base scenario mean. The relatively small deviations in phosphate concentrations across the diversion scenarios may be due to the dominance of the benthic phosphate flux (9.5 $mg/m^2/d$) over the phosphate loads from the tributaries.

10.2.9 Dissolved organic phosphorus

Dissolved organic phosphorus concentrations in the lake tend to be low (<0.05 mg/L). In addition, the changes in deviations under the different scenarios tend to be small and not appreciable.

10.3 SUMMARY OF RESULTS FROM SCENARIO RUNS

With the exception of dissolved oxygen and chlorophyll-a, most water quality parameters do not change appreciably with the diversion. Implementing the diversion is found to be beneficial to the water quality of the lake by increasing the dissolved oxygen and reducing hypoxic events. Drawdowns deteriorate the water quality because nutrient loads and benthic effects (such as sediment oxygen demand, benthic ammonia flux, and benthic phosphate flux) are exerted on smaller volumes of water. Among the various water quality parameters, increased drawdown reduces dissolved oxygen the most.

10.4 MASS BALANCE ANALYSIS ON TREATABILITY PARAMETERS

To evaluate treatability of the lake water, a mass balance analysis was performed for alkalinity and magnesium, two parameters that impact drinking water plant operations. This section describes the analysis.

10.4.1 Mass balance analysis setup

The mass balance analysis utilizes a simple four-cell model to represent Lake Houston and the three inlets. Figure 10.1 shows a schematic of the model. Alkalinity and magnesium are modeled as conservative tracers in the model.

The volume of the lake cell is varied for different levels of drawdown. With no drawdown, the volume is 133,990 acre-ft. At 2 ft drawdown ,the volume is 113,560 acre-ft, and at 5 ft drawdown, the volume is 86,549 acre-ft. These volumes are obtained from the rating curves derived from TWDB's volumetric survey of the lake (TWDB, 2003).

The inflows at the inlets and boundary concentrations are the same as those calculated in Section 4. The East Inlet cell receives different inflows and boundary concentrations depending on the diversion scenario simulated (i.e. 0 MGD diversion vs. 400 MGD diversion). Constant volume is assumed, and the outflow from the lake is set to be equal to the sum of inflows to the lake.

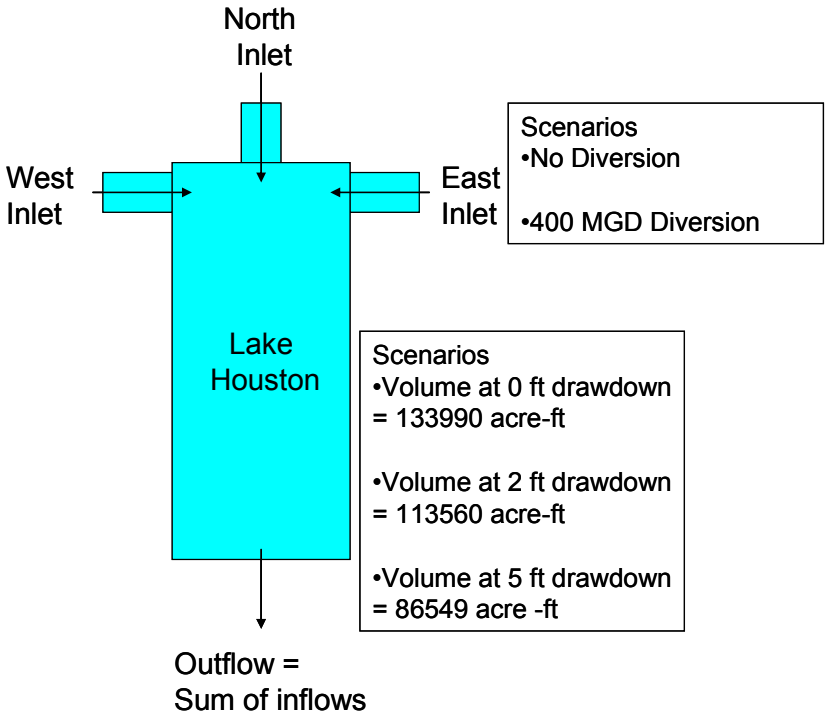

Figure 10.3 Schematic of the mass balance model for alkalinity and magnesium.

10.4.2 Mass balance analysis calibration

The entire study period from 2000 to 2009 is simulated because the simplicity of the model requires very little computation time. Figures 10.4 and 10.5 compare the model results with alkalinity and magnesium data collected by the COH (at the NEWPP intake) and by the TCEQ (at SWQM station 11204).

To calibrate the model, a multiplier was applied to the inflow concentrations to account for possible discrepancies in the estimated loads. The multiplier was adjusted to achieve the best fit between the data and model results. For alkalinity, the best results were achieved when the multiplier was set to 1.2. For magnesium, the best results were achieved when the multiplier was set to 0.75.

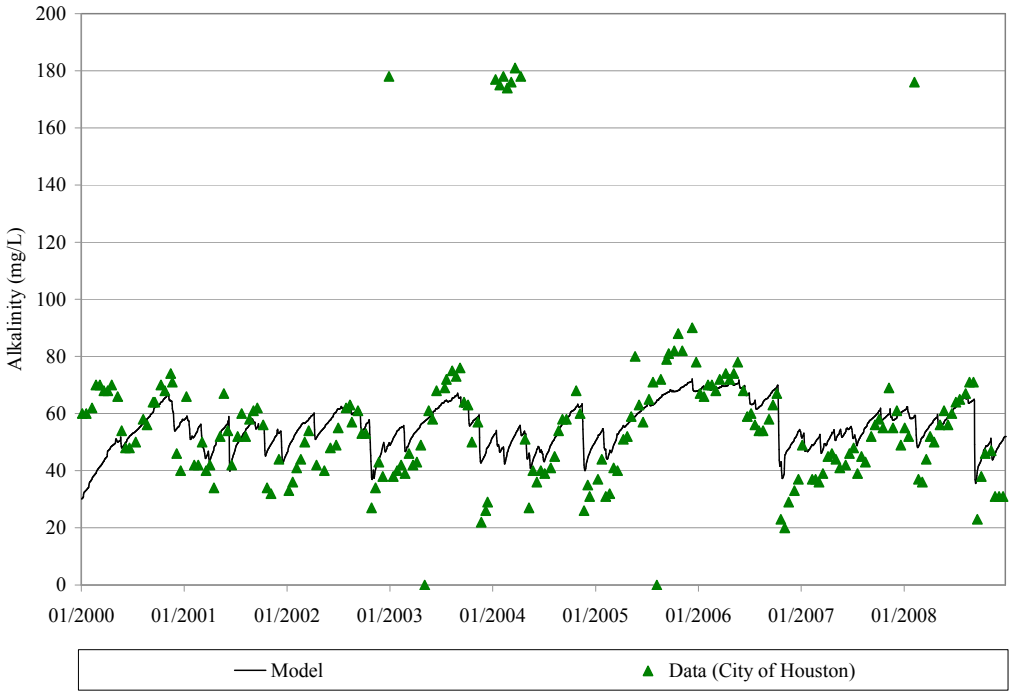

Figure 10.4 Measured and predicted alkalinity from the mass balance analysis

Simulated values from the mass balance model agree very well with the alkalinity data. The model results follow closely the temporal trend of the data. The simulated values are also within the range of the observed values.

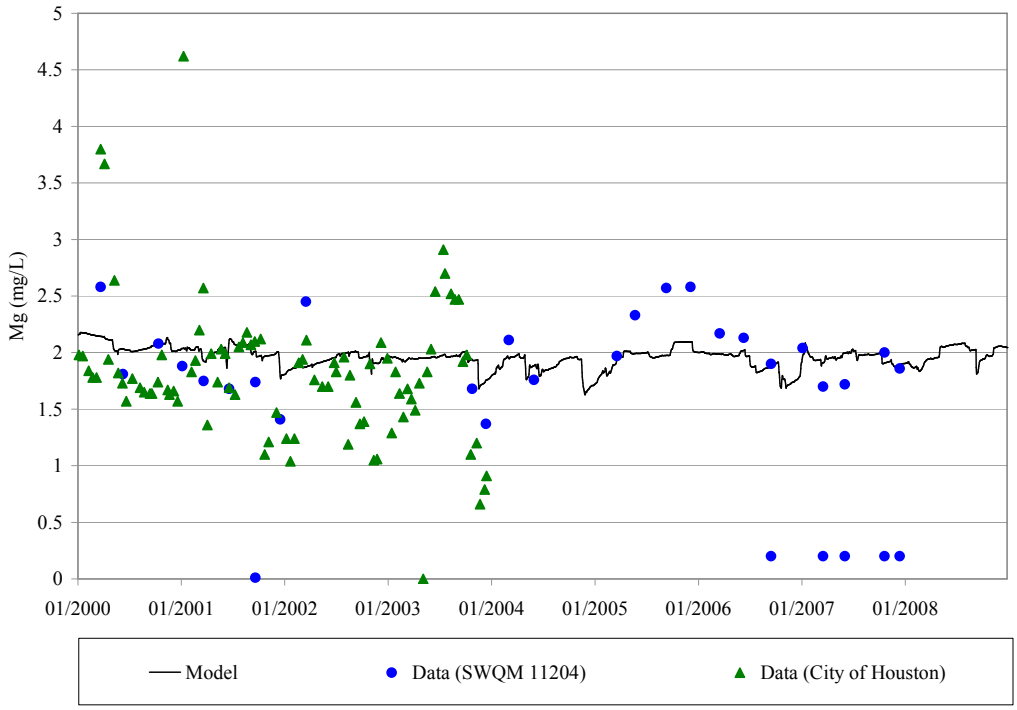

Figure 10.5 Measured and predicted magnesium from the mass balance analysis

Simulated concentrations from the mass balance model for magnesium are reasonable, but considerable scatter in the magnesium data made imitation of temporal trends difficult. Nonetheless, the graph of simulated values passes through the cloud of data and is within the range of data values.

10.4.3 Mass balance analysis scenarios

The mass balance model was run for the scenarios in Table 10.3. The results for alkalinity and magnesium are plotted in Figures 10.6 and 10.7, respectively.

Table 10.3 Mass balance analysis scenarios

Year	400 MGD Luce Bayou Diversion?	Drop in WSE (ft)		
2000-2009	Yes	0	2	5
	No	0		

Alkalinity increases with the diversion of 400 MGD of Trinity River water into Lake Houston. The average alkalinity in the lake before diversion is 55 mg/L as $CaCO_3$. The average alkalinity of the lake after diversion is 72 mg/L. The various drawdown scenarios have little effect on the alkalinity concentrations.

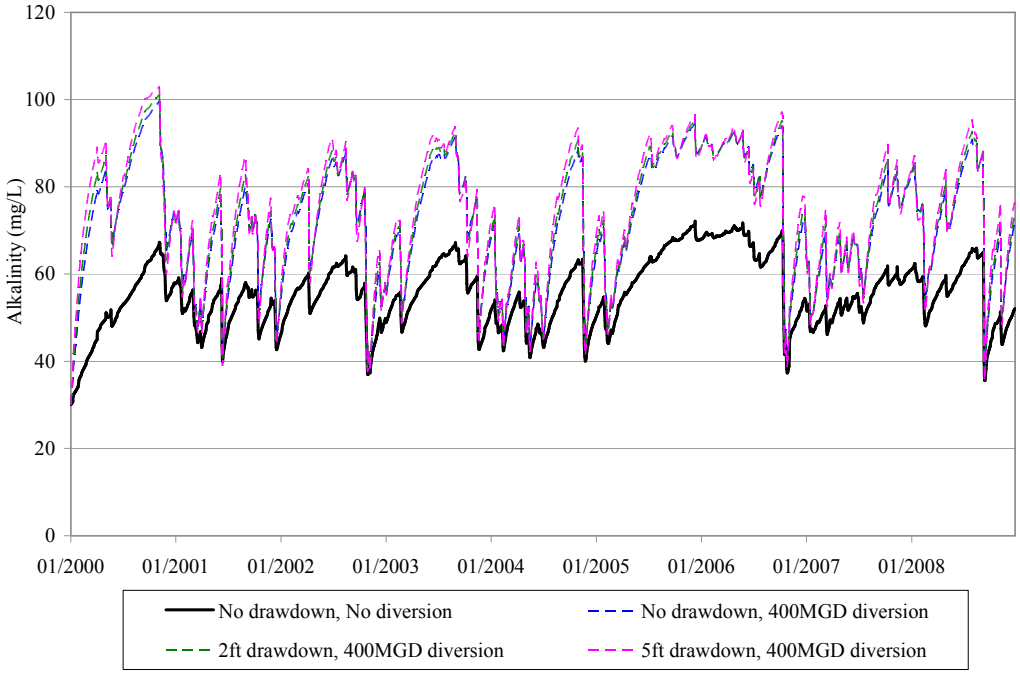

Figure 10.6 Alkalinity results from mass balance scenarios.

Magnesium concentrations increase with the diversion of 400 MGD of Trinity River water into Lake Houston. The average magnesium concentration before diversion is about 2.0 mg/L. The average magnesium concentration of the lake after diversion is 2.2 mg/L. The various drawdown scenarios have little effect on the magnesium concentrations.

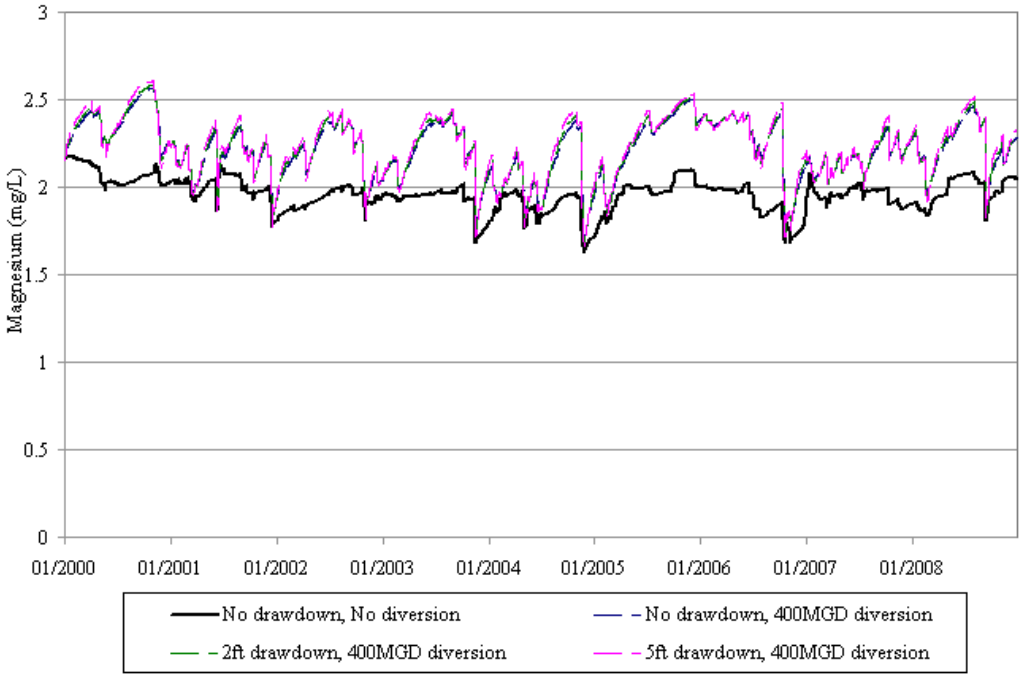

Figure 10.7 Magnesium results from mass balance scenarios.

In conclusion, alkalinity is found to increase by 31% with the diversion. Magnesium is found to increase by 10% with the diversion. For both parameters, the drawdowns have little effect on the concentrations. The increase in alkalinity by the diversion could improve the treatability of the water during high-flow periods when the watershed is producing significant inflow (assuming the diversion is constant through the high-flow periods).

11.0 CONCLUSIONS

Espey Consultants, Inc. (EC) performed an in-depth investigation on the impact of the Luce Bayou Interbasin Transfer project on water quality in Lake Houston. The study accomplished the following tasks:

1. An extensive data collection was performed to update and augment the database assembled in the 2006 study. The data collected include:
    a. streamflow and water quality data for both the lake and its tributaries;
    b. reservoir storage, stage heights, pump withdrawals and operation records; and,
    c. meteorological data such as wind, precipitation and evaporation.
2. Statistical regressions were used to analyze the relationship between water quality parameters and streamflow from the Lake Houston watershed. Rating curves were developed to estimate the time series of nutrient loads into Lake Houston from the watershed.
3. A statistical analysis of historical inflow patterns was performed. The frequencies and durations of high-flow, low-flow and normal-flow conditions and their impacts on lake water surface elevations were evaluated. Three separate years were selected to represent high-flow, low-flow and normal-flow years for model simulation.
4. A hydrodynamic model for Lake Houston was developed and calibrated. The model estimates water circulation and mixing by taking into account the physical forces caused by inflows, outflows, wind, precipitation and evaporation.
5. A tracer simulation was performed using the hydrodynamic model to evaluate the mixing of tributary inflows in the lake under different flow conditions. The location of the NEWPP intake was evaluated based on the predicted mixing patterns.
6. A water quality model was developed and calibrated to the low-flow, high-flow and normal flow years. This model links to the hydrodynamic model and use the water circulation patterns to evaluate the fate and transport of water quality parameters.
7. The hydrodynamic and water quality models are used to evaluate impacts on water circulation and water quality under the following contamination scenarios:
    - Diversion of 400 MGD of Trinity River.
    - Historical high, average and low-flow conditions in the San Jacinto Basin.
    - Drops in water surface elevations caused by operations at the Lake Houston dam.
8. A mass balance analysis was performed to evaluate the impact of the diverted Trinity River water on parameters that are related to plant operations (i.e. alkalinity and magnesium).

11.1 PROJECTED IMPACTS OF LUCE BAYOU PROJECT ON INTAKE WATER QUALITY

Based on the evaluation of mixing conditions, it is projected that for approximately 90% of the inflows to Lake Houston, water diverted from the Trinity River through Luce Bayou will mix completely with flows from the San Jacinto Basin before reaching the NEWPP intake. Thus, some improvement in water quality over current conditions is expected. During high inflows, the mixing zone may extend past the NEWPP intake potentially causing the plant to receive incompletely mixed flows. Such flows would most likely consist of rainfall runoff from the western portion of the San Jacinto watershed.

Based on the water quality simulation, it was found that the imported Trinity River water would improve dissolved oxygen concentrations in the lake more than other water quality parameters. Implementing the diversion increases the dissolved oxygen in the lower model layer and reduces the occurrence of hypoxic events. For most other nutrient parameters, concentrations are not found to change appreciably with the diversion.

Drawdowns on lake levels are found to have a deteriorating effect on the water quality because nutrient loads and benthic effects (such as sediment oxygen demand, benthic ammonia flux, and benthic

phosphate flux) are exerted on smaller volumes of water. Among the various water quality parameters, drawdowns have the greatest impact on dissolved oxygen. For all flow conditions simulated, each additional 1 foot of drawdown caused an average 0.2 mg/L drop in DO.

To evaluate the treatability of the mixed water, a mass balance analysis was performed for alkalinity and magnesium. Alkalinity was found to increase by 31% with the diversion. Magnesium was found to increase by 10% with the diversion. The increase in alkalinity by the diversion could improve the treatability of the water during high-flow periods when the watershed is producing significant inflow (assuming the diversion is constant through the high-flow periods).

11.2 RECOMMENDATIONS FOR FUTURE MODELING

The following recommendations are identified for the improving the Lake Houston model for future modeling efforts:

1. Finer vertical resolution of the model grid would allow better characterization of the vertical profile of the lake and permit identification of any stratification of water quality parameters. However, increasing the grid resolution would also significantly increase the computation time required.
2. A physical-based watershed model can be implemented to determine nutrient and sediment loads into the lake. Some of the water quality parameters, such as TSS, exhibit non-linear and non-monotonic relationships with streamflow. Mechanistic watershed models, such as Texas A&M University's Soil and Water Assessment Tool (SWAT), can account for processes such as river channel degradation (SWAT, 2005) thereby providing more accurate estimates of total suspended solids in inflows. With better characterization of the upstream loads, water quality conditions in the lake can be more accurately simulated.
3. A more sophisticated sediment transport module can be used to simulate the complex sediment transport processes in the lake. Examples of such modules are the SEDZLJ component in EFDC and the toxicant module in WASP. This study identified that wind-driven resuspension may be a significant source of total suspended solids in the lake – especially during low-flow periods when lake levels are low. Use of a sediment transport model would help determine the spatial and temporal behavior of TSS. To support this type of modeling, site-specific data on resuspension and cohesive and non-cohesive sediment settling would be needed. Collection of these data would require the collection of sediment cores and the use of apparatus such as the sedflume (Lick, 2008) to measure gross erosion rates of sediments and the variation of the erosion rate with depth below the sediment-water interface.

12.0 REFERENCES

1 Baca, Ernesto, Bedient, P.B., and Olsen, R.J., 1982, *Urban impacts of water supply reservoir*, American Society of Civil Engineers, Journal of the Environmental Engineering Division, v. 108, no. 1, p. 73–87.

2 City of Houston, 2009, e-mail communication with Lisa Lattu of the Department of Public Works and Engineering.

3 Covar, A.P. 1976. *Selecting the Proper Reaeration Coefficient for Use in Water Quality Models*. Presented at the U.S. EPA Conference on Environmental Simulation Modeling, April 19-22, 1976. Cincinnati, Ohio.

4 Espey Consultants, Inc, 2007, *Cedar Creek WASP Model Development and Calibration Results*, Technical memo submitted to Tarrant Regional Water District.

5 GBM and Associates, 2006, *Interim Report Ouachita River and Felsenthal System Water Quality Modeling - Calibrated model outputs[QUAL2K, WASP, AQUATOX],* prepared for Joint Pipeline Group, El Dorado, AR 71730.

6 Hamrick, J. M., 1992, *A Three-Dimensional Environmental Fluid Dynamics Computer Code: Theoretical and Computational Aspects*. The College of William and Mary, Virginia Institute of Marine Science. Special Report 317, 63 pp.

7 Lee and Rast, 1997, *Light Attenuation in a shallow, turbid reservoir, Lake Houston, Texas,* USGS Water-Resources Investigations Report 97-4064.

8 Lick, W., 2008, *Sediment and Contaminant Transport in Surface Waters*, CRC Press, Taylor and Francis Publishing, 400 pp.

9 Matty, Jane M., John B. Anderson, and Robert B. Dunbar, 1987, *Suspended Sediment Transport, Sedimentation, and Resuspension in Lake Houston, Texas: Implications for Water Quality*. Environ Geol Water Sci Vol. 10, No.3, 175

10 T. Viraraghavan, 1976, Correlation of BOD, COD and Soluble Organic Carbon, Journal of the Water Pollution Control Federation, Vol. 48, No. 9, Annual Conference Issue (Sep., 1976), pp. 2213-2214. Stable URL: http://www.jstor.org/stable/25040005

11 SWAT, 2005. *Soil and Water Assessment Tool.* Texas A&M University, College Station, Texas and USDA Agricultural Research Service: Grassland, Soil and Water Research Laboratory, Temple, Texas. Available at: http://swatmodel.tamu.edu/documentation

12 Texas Water Development Board, 2003, *Volumetric survey of Lake Houston*.

13 United States Environmental Protection Agency, Watershed/Water Quality Technical Support Center, 2009. WASP 7.x Workshop Training materials, http://www.epa.gov/athens/wwqtsc/html/wasp.html.

14 United States Geological Survey 1997, *Light attenuation in a shallow, turbid reservoir, Lake Houston, Texas*, Water-Resources Investigations Report 97-4064.

15 United States Geological Survey, 2000, *Estimated effects on water quality of Lake Houston from interbasin transfer of water from the Trinity River, Texas*, Water-Resources Investigations Report 00-4802.

P:\Active\5081.01_Luce_Bayou_Interbasin_Transfer\Documents\Reports\Final_Report\Luce_Bayou_Project_WQ_Study_DRAFT.doc

Appendix A Relationships between stream flow and concentration for tributaries of Lake Houston

Plots of flow versus concentration of all the Lake Houston tributaries and Trinity River can be found in the following files in the accompanying file attachments.

Appendix_A\Flow_conc_charts_Caney_Creek.pdf
Appendix_A\Flow_conc_charts_Cypress_Creek.pdf
Appendix_A\Flow_conc_charts_East_Fork_San_Jacinto.pdf
Appendix_A\Flow_conc_charts_Luce_Bayou.pdf
Appendix_A\Flow_conc_charts_Peach_Creek.pdf
Appendix_A\Flow_conc_charts_Spring_Creek.pdf
Appendix_A\Flow_conc_charts_Trinity_River.pdf
Appendix_A\Flow_conc_charts_West_Fork_San_Jacinto.pdf

Appendix **B** Time series of water quality parameters for tributaries of Lake Houston

Plots of time series of water quality parameters of all the Lake Houston tributaries and Trinity River can be found in the following files in the accompanying file attachments.

Appendix_B\Caney_Creek_TimeSeries.pdf
Appendix_B\Cypress_Creek_TimeSeries.pdf
Appendix_B\East_Fork_San_Jacinto_TimeSeries.pdf
Appendix_B\Luce_Bayou_TimeSeries.pdf
Appendix_B\Peach_Creek_TimeSeries.pdf
Appendix_B\Spring_Creek_TimeSeries.pdf
Appendix_B\Trinity_River_TimeSeries.pdf
Appendix_B\West_Fork_San_Jacinto_TimeSeries.pdf

Appendix **C** Water circulation patterns predicted by EFDC for diversion and drawdown scenarios.

Plots of time series of water circulation patterns predicted by EFDC for diversion and drawdown scenarios can be found in the following files in the accompanying file attachments.

Appendix_C\Vel_vectors_2000_No_diversion_No_drawdown.pdf
Appendix_C\Vel_vectors_2000_No_diversion_1ft_drawdown.pdf
Appendix_C\Vel_vectors_2000_No_diversion_2ft_drawdown.pdf
Appendix_C\Vel_vectors_2000_No_diversion_3ft_drawdown.pdf
Appendix_C\Vel_vectors_2000_No_diversion_5ft_drawdown.pdf
Appendix_C\Vel_vectors_2000_400_MGD_diversion_No_drawdown.pdf
Appendix_C\Vel_vectors_2000_400_MGD_diversion_1ft_drawdown.pdf
Appendix_C\Vel_vectors_2000_400_MGD_diversion_2ft_drawdown.pdf
Appendix_C\Vel_vectors_2000_400_MGD_diversion_3ft_drawdown.pdf
Appendix_C\Vel_vectors_2000_400_MGD_diversion_5ft_drawdown.pdf
Appendix_C\Vel_vectors_2004_No_diversion_No_drawdown.pdf
Appendix_C\Vel_vectors_2004_No_diversion_1ft_drawdown.pdf
Appendix_C\Vel_vectors_2004_No_diversion_2ft_drawdown.pdf
Appendix_C\Vel_vectors_2004_No_diversion_3ft_drawdown.pdf
Appendix_C\Vel_vectors_2004_No_diversion_5ft_drawdown.pdf
Appendix_C\Vel_vectors_2004_400_MGD_diversion_No_drawdown.pdf
Appendix_C\Vel_vectors_2004_400_MGD_diversion_1ft_drawdown.pdf
Appendix_C\Vel_vectors_2004_400_MGD_diversion_2ft_drawdown.pdf
Appendix_C\Vel_vectors_2004_400_MGD_diversion_3ft_drawdown.pdf
Appendix_C\Vel_vectors_2004_400_MGD_diversion_5ft_drawdown.pdf
Appendix_C\Vel_vectors_2008_No_diversion_No_drawdown.pdf
Appendix_C\Vel_vectors_2008_No_diversion_1ft_drawdown.pdf
Appendix_C\Vel_vectors_2008_No_diversion_2ft_drawdown.pdf
Appendix_C\Vel_vectors_2008_No_diversion_3ft_drawdown.pdf
Appendix_C\Vel_vectors_2008_No_diversion_5ft_drawdown.pdf
Appendix_C\Vel_vectors_2008_400_MGD_diversion_No_drawdown.pdf
Appendix_C\Vel_vectors_2008_400_MGD_diversion_1ft_drawdown.pdf
Appendix_C\Vel_vectors_2008_400_MGD_diversion_2ft_drawdown.pdf
Appendix_C\Vel_vectors_2008_400_MGD_diversion_3ft_drawdown.pdf
Appendix_C\Vel_vectors_2008_400_MGD_diversion_5ft_drawdown.pdf

Appendix **D** Tracer simulation results for Lake Houston

Tracer simulation results for Lake Houston can be found in the following files in the accompanying file attachments.

Appendix_D\Tracer_2008_no_diversion_no_drawdown.pdf
Appendix_D\Tracer_2008_no_diversion_2ft_drawdown.pdf
Appendix_D\Tracer_2008_no_diversion_5ft_drawdown.pdf
Appendix_D\Tracer_2008_400MGD_diversion_no_drawdown.pdf
Appendix_D\Tracer_2008_400MGD_diversion_2ft_drawdown.pdf
Appendix_D\Tracer_2008_400MGD_diversion_5ft_drawdown.pdf

Appendix **E** Simulation results for water quality scenarios

Simulation results for water quality scenarios can be found in the following file in the accompanying file attachments.

Appendix_E\Simulations_of_water_quality_scenarios.pdf